# Hormone and Gene Feedback during Development and Regeneration in *Arabidopsis thaliana*

Thesis by

Sean Gordon

In Partial Fulfillment of the Requirements

for the Degree of

Doctor of Philosophy


California Institute of Technology

Pasadena, California

2009

(Defended April 29th, 2009)

# Acknowledgments

With much gratitude I would like to thank the many individuals that have supported me during my thesis research at Caltech.

Most of all, I would like to thank my research mentor and advisor Elliot Meyerowitz for his continuous support of this project and for the independence he has given me. His enthusiasm and positive attitude were key to my success. His ability to free his busy schedule for useful discussions was truly exemplary.

I would also like to thank my thesis committee: Raymond Deshaies, Michael Elowitz, Ellen Rothenberg and Paul Sternberg for taking interest in my research project and their invaluable comments and advice during the past four years.

I would like to thank all of great assortment of people who have come and gone from the Meyerowitz lab for the supportive lab atmosphere. In particular, I would like to acknowledge Vijay Chickarmane for his development of the computational models used throughout this thesis. I also thank him for his inspiring enthusiasm for science and life. In addition, I would like to thank Marcus Heisler, Henrik Jönsson, Patrick Sieber, Venu Reddy, Pradeep Das, Adrienne Roeder, Annick Dubois, and Carolyn Ohno for their support, intellectual discussions and assistance. I have learned a lot from each of you and your scientific excellence has inspired as well as challenged me to strive for improvement. Many great thanks to Arnavaz Garda for her excellent technical assistance and help. None of this would have happened of course had it not been for my undergraduate research advisors, especially Victoria Corbin. Professor Corbin was my first research mentor and directly contributed to my desire to undertake graduate training.

I thank my parents for their appreciation of higher education and encouragement along my long academic career. Lastly, I would like to thank Marta. She is a great experimentalist and has above all others inspired me to do better. In addition, her support and encouragement has brought greater meaning to this work.

# Abstract

Higher plants maintain continuous development throughout their life by closely regulating the process of cell differentiation (Clark, 2001; Sablowski, 2007). In plants, the balance between undifferentiated and differentiated cell fate is managed within a stem cell niche termed the meristem. Cell differentiation in the meristem is in part controlled by genetic mechanisms. For example, mutations in *CLAVATA (CLV)* genes increase the number of undifferentiated cells within shoot and floral meristems leading to supernumerary organs (Clark, 2001). In contrast, mutations in genes of the homeodomain transcription factors *WUSCHEL* (*WUS*) and *SHOOT-MERISTEMLESS* (*STM*) lead to the absence of the shoot or floral meristem or its early termination through differentiation (Laux et al., 1996; Long et al., 1996).

Cell differentiation in the meristem is also controlled by hormonal cues, which interfaces with gene function. For example, cytokinin treatment leads to phenotypes resembling *clv* mutants (Lindsay et al., 2006). Furthermore, exogenous cytokinin treatment has been shown to rescue the *stm* mutant phenotype and WUS protein has been shown to repress transcription of genes that act in the negative feedback pathway of cytokinin signaling (Leibfried et al., 2005; Yanai et al., 2005). The plant hormone auxin also plays a role in regulating differentiation. Auxin is thought to stimulate the initiation, development and differentiation of cells specified into organs (Teale et al., 2006). Disruption of auxin transport leads to a reduction in organ initiation and differentiation (Okada et al., 1991).

In this thesis we investigate spatially regulated signaling and action of auxin and cytokinin which regulate patterning of gene expression and cell differentiation. To this

end, we employed two model systems of shoot meristem initiation and development in the model plant *Arabidopsis thaliana*: shoot and floral meristem development and *de novo* shoot meristem initiation from tissue culture. Based on characterization of hormone signaling and patterning of gene expression during *de novo* shoot meristem initiation from tissue culture we propose a novel Turing-like model by which auxin and cytokinin interact to regulate patterning of cell differentiation. In this model, the activity of auxin, the activator of cell differentiation, is regulated by cytokinin, an inhibitor of cell differentiation. Computational models of these interactions lead to self organizing patterning of hormone response and cell differentiation as observed in experiments.

In our second investigation, we show that cytokinin signaling regulates the spatial patterning of the homeodomain transcription factor WUS within the shoot meristem. We demonstrate that *WUS* misregulation after cytokinin treatment is mediated by both *CLAVATA*-dependent and independent mechanisms leading to multiple feedback loops. We reveal the presence of a cytokinin perception and signaling gradient within the shoot meristem, which spatially influences size and position of the *WUS* domain.

Finally, we have begun to identify the molecular components required for cytokinin activation of *WUS* expression. Of the three characterized cytokinin receptors, only Arabidopsis Histidine Kinase 2 (AHK2) is required for *WUS* induction in the presence of cytokinin. In contrast, the AHK3 receptor is required for negative feedback on cytokinin signaling and thus *WUS*. These data reveal an unappreciated specificity in cytokinin signaling in regulating downstream targets which may be important for eliciting different cell behaviors depending on the threshold of signaling and the ratio of the three cytokinin receptors within a given cell.

# Contents

# List of Figures

# Chapter 1 Introduction

## 1.1 Genetic regulation of differentiation in the shoot and floral meristem

Higher plants are capable of long term growth and development due to a group of apical stem cells (Clark, 2001). These stem cells are maintained by local cues emanating from within the stem cell niche (Tucker and Laux, 2007). The proliferation of the apical stem cells is necessary to provide new cells for organ initiation. At the same time, as the apex of the stem cell niche moves away from these cells by continued cell division, the undifferentiated cells that are now on the flanks of the niche must be allowed to enter a specific developmental pathway, such as leaf or flower development, leading to eventual differentiation. It is the balancing of these two features that allows for the continued growth of the plant and its continuous initiation of new organs (Fletcher and Meyerowitz, 2000).

A number of mutations have been identified which alter the regulation of cell differentiation within the stem cell niche, also referred to as the meristem. Mutations in *CLAVATA* genes increase the number of undifferentiated cells within shoot and floral meristems leading to excess floral organs (Clark, 2001). In contrast, loss of the homeodomain transcription factors *WUSCHEL* (*WUS*) and *SHOOT-MERISTEMLESS* (*STM*) leads to the absence of the shoot meristem or its early termination by differentiation (Laux et al., 1996; Long et al., 1996). Interactions between these genes have also been discovered leading to the WUS/CLV circuit paradigm (Brand et al., 2000; Schoof et al., 2000). In this network, WUS expression in the center of the shoot meristem promotes undifferentiated cell fate at the meristem apex (Fletcher et al., 1999). In response, undifferentiated cells at the apex in turn express CLV3 ligand which is secreted from these cells to diffuse throughout the meristem (Clark, 2001). CLV3 ligand binds to the CLV1/CLV2 receptor complex expressed in internal cells of the meristem. CLV3 bound

receptor complex activates intracellular signaling which results in repression of *WUS* transcription. Thus *WUS* is regulated through negative feedback via the CLV pathway to control the number of undifferentiated stem cells at the shoot meristem apex.

## 1.2 Hormonal regulation of differentiation in the shoot and floral meristem

For decades the plant hormones auxin and cytokinin have been known to have important roles in regulating cell differentiation. Skoog and Miller demonstrated that a quantitative balance between the hormones auxin and cytokinin determines the types of growth and cell differentiation which will occur in culture (Skoog, 1950; Skoog and Miller, 1957). Other researchers showed that chemical inhibitors of auxin transport were sufficient to block organ initiation and differentiation (Estelle, 1998). Recently genetic and molecular analysis has stimulated a renewed interest in hormone signaling in plants and the molecular mechanisms by which hormones control cell behavior and plant physiology. Currently the core mechanisms by which auxin and cytokinin are perceived and initiate downstream signaling appear to have been identified (Muller and Sheen, 2007; Teale et al., 2006). In contrast, it remains poorly understood how auxin and cytokinin signaling exert their influence on cell behavior and plant physiology which is a topic of this thesis.

### *1.2.1 Auxin perception and signaling*

Auxin is a small molecule perceived by its intracellular binding to an F-box protein called TIR1 (Vanneste and Friml, 2009). Auxin promotes interaction between TIR1 and a family of transcriptional repressor proteins called Aux/IAAs, leading to ubiquitination and destruction of the Aux/IAAs. Destruction of the Aux/IAAs relieves the transcriptional repression of genes which Aux/IAAs formerly suppressed.

Key to auxin physiology is the import and directional export of auxin out of the cell by carrier proteins (Vanneste and Friml, 2009). While auxin can freely diffuse into cells, intracellular pH favors its charged form which cannot freely cross the plasma membrane. Thus, movement of auxin within tissues can be regulated. The disruption of this regulation by chemical inhibition of polar auxin transport suppresses organ initiation from the shoot meristem highlighting its importance in this process. Subsequently, mutants with phenotypes resembling wild type plants treated with chemical inhibitors of auxin transport were identified (compromised in ability to make differentiated lateral organs) (Okada et al., 1991). This work led to the identification of the PIN family of auxin efflux facilitators. Additional work showed that local application of exogenous auxin to these mutants could induce organ primordia (Reinhardt et al., 2003b). This indicated that local auxin maxima provide spatial information critical for initiating organ development and cell differentiation at that site. Live imaging of the green fluorescent protein (GFP) tagged auxin efflux facilitator PIN1 showed that PIN proteins are dynamically polarized at the shoot meristem periphery towards sites of organ initiation (Heisler et al., 2005). This data led to the model in which PIN proteins establish sites of organ initiation by increasing local auxin concentration through regulation of the direction of auxin efflux. Additionally, PIN1 was shown to be transcriptionally activated by auxin. The assumption that auxin influences the polarization of its own efflux leads to positive feedback of auxin on itself (Jonsson et al., 2006). Such a model is capable of generating patterns of organ initiation similar to observed experimentally.

### *1.2.2 Cytokinin perception and signaling*

First purified from autoclaved herring sperm DNA extracts, the adenine derived signaling hormone cytokinin is intimately associated with regulating cell division and

differentiation within the plant (Muller and Sheen, 2007). Unlike auxin, cytokinin is perceived by trans-membrane hybrid histidine kinases (HKs). *Arabidopsis* HKs (AHKs) signal through a hybrid two component signaling system. Receptor activation by ligand binding leads to autophosphorylation and subsequent transfer of phosphoryl groups to histidine phosphotransfer proteins (HPTs), which then transfer phosphorylation to downstream proteins called response regulators (RRs) (Hwang and Sheen, 2001). In response to phosphorlyation, B-type RRs activate transcription. In contrast, A-type ARRs negative regulate signaling by an unknown mechanism which may or may not involve competition with B-Type ARRs for phosphorylation (To and Kieber, 2008). In contrast to auxin, there is little evidence that cytokinin is directionally transported from cell to cell. Thus, local synthesis or long range transport through the plant vasculature and diffusion are thought to be important for distribution of cytokinin within the plant.

Early experiments showed that cytokinin could stimulate cell proliferation and regeneration of tobacco tissue explants in culture (Skoog, 1950). More recently, research has shown that cytokinin is important for maintenance of undifferentiated cells within the shoot stem cell niche (Tucker and Laux, 2007). In these experiments, exogenous cytokinin treatment was shown to rescue the inability of the *stm* mutant to maintain undifferentiated cells within the shoot meristem (Yanai et al., 2005). Furthermore, STM over expression was shown to activate transcription of genes controlling cytokinin synthesis. Cytokinin biology was also shown to interface with the function of the well studied homeodomain transcription factor WUS. WUS is non-cell autonomously required to promote stem cell fate in overlying cells at the shoot apex (Fletcher and Meyerowitz, 2000). Loss of function mutations in *WUS* leads stem cell loss and premature termination of shoot growth. Recent experiments have shown that WUS protein suppresses transcription of a subset of Type-A ARR genes that act in the negative feedback pathway of cytokinin signaling, thus enabling cytokinin signaling within these cells (Leibfried et al., 2005). Interestingly, overexpression of this subset of Type-A ARRs reduced WUS expression.

In the following chapters we provide evidence for the involvement of auxin and cytokinin in the patterning of genes which feedback on hormone signaling to self-assemble patterns of hormone response and gene expression. We begin in Chapter 2, studying the interaction of auxin and cytokinin in regulating *de novo* patterning of cell identity during in vitro re-establishment of the shoot stem cell niche (Gordon et al., 2007). In Chapter 3, we provide evidence that a cytokinin signaling gradient interacts with downstream genes and cytokinin signaling components to influence relative patterning of gene expression and cytokinin response within the shoot stem cell niche.

CHAPTER 2

# Pattern formation during de novo assembly of the *Arabidopsis* shoot meristem

Sean P. Gordon, Marcus G. Heisler, G. Venugopala Reddy, Carolyn Ohno, Pradeep Das and Elliot M. Meyerowitz

(A chapter published in *Development* (2007) 134, 3539-3548)

Most multi-cellular organisms have a capacity to regenerate tissue after wounding. Few, however, have the ability to regenerate an entire new body from adult tissue. A half century ago Skoog and Miller demonstrated an in vitro system for regenerating flowering plants from fragments of adult somatic tissue (Skoog, 1950; Skoog and Miller, 1957). This regeneration system uses the plant hormones auxin and cytokinin to stimulate the self assembly of new plant clones from somatic explants. The stepwise process by which new plants were regenerated is however unknown. In this study we characterize early patterning and morphogenesis during the plant regeneration process. We show that plants are regenerated through *de novo* development of the *Arabidopsis* shoot stem cell niche, termed the shoot meristem. We use fluorescent reporters of known gene and protein activities required for shoot meristem development and maintenance to characterize the mechanism of shoot meristem self-organization. We find that a small number of progenitor cells initiate development of new shoot meristems through stereotypical stages of reporter expression and activity of *CUP-SHAPED COTYLEDON 2 (CUC2)*, *WUSCHEL (WUS)*, *PIN-FORMED1* (*PIN1*), *SHOOT-MERISTEMLESS* (*STM*), *FILAMENTOUS FLOWER (FIL)*, *REVOLUTA (REV), ARABIDOPSIS THALIANA MERISTEM L1 LAYER (ATML1),* and *CLAVATA3 (CLV3)*. During normal

development the shoot meristem acts as a niche for apical stem cells which enable the indeterminate growth of above-ground tissues. Our real-time observations indicate that cytokinin triggers the first steps in reestablishing the shoot stem cell niche *in vitro* through activation of a master regulator of rib meristem fate. Within the stem cell niche, the rib meristem is necessary for promoting adjacent cells to assume stem cell fate. Our observations also lead us the novel hypothesis that a Turing-like mechanism may underlie patterning during de novo plant regeneration. We explore this hypothesis using computational modeling.

## 2.1 Introduction

Regeneration of a patterned multicellular organism from isolated pieces of adult somatic tissues is a remarkable phenomenon which occurs both in plants and animals (Morgan, 1901). The small Cnidarian, *Hydra*, for example, can self-assemble a new correctly patterned body from re-aggregated cells derived from dissociated somatic cells of adult tissue (Gierer et al., 1972). Recently, the observation that several genes critical for proper embryonic development in higher animals are expressed during de novo *Hydra* head regeneration has lead to important insights into the molecular basis of animal self-organization (Hobmayer et al., 2000). However, animal model systems for studying de novo patterning, such as *Hydra*, are not well developed for molecular analysis or genetics compared to classical model organisms with established collections of mutants, transgenic lines, and protocols (Lowenheim, 2003; Wittlieb et al., 2006).

While assembly of a complete organism from fragments of adult somatic tissue is rare among animals, many plants are capable of this type of regeneration. A half century ago Skoog and Miller demonstrated an in vitro system for regenerating flowering plants from fragments of adult somatic tissue (Skoog, 1950; Skoog and Miller, 1957). Remarkably, the identity of induced tissues in this in vitro system was shown to be driven by the ratio of two plant hormones: auxin and cytokinin. It was shown that transfer tissue explants to medium with higher levels of auxin induced development of

root regenerative tissues, whereas transfer of explants to medium with higher levels of cytokinin induced new shoot regenerative tissues, and inductive media containing both auxin and cytokinin induced a proliferation of cells termed callus.

During post-embryonic development in flowering plants such as *Arabidopsis thaliana*, all above ground organs of the plant originate from stem cells within the apical tip of the shoot meristem. The origin of the primary shoot meristem during embryogenesis can be traced back to a small group of apical precursors (West and Harada, 1993). Throughout embryogenesis the apical lineage is marked by precisely regulated expression of many genes which are required for proper patterning of the shoot meristem (Aida et al., 1997; Barton and Poethig, 1993; Laux et al., 1996; Long et al., 1996). For example, early patterning during embryogenesis is recognizable by expression of the auxin transporter, *PIN-FORMED1 (PIN1)*, required for the initiation and maintenance of auxin gradients within various tissues of the plant (Friml et al., 2003; Heisler et al., 2005). In the two-cell pro-embryo, *PIN1* expression coincides with an initial differential activation of auxin response in the apical cell. Expression of the homeodomain transcription factor *WUSCHEL (WUS)* begins at the 16-cell stage embryo in two inner apical cells and maintains a tightly restricted pattern throughout embryogenesis (Mayer et al., 1998). The dynamic expression of the redundant transcription factors *CUP-SHAPED COTYLEDON 1 and 2 (CUC1,2)* and the homeodomain transcription factor, *SHOOT MERISTEMLESS (STM),* marks a small number of apical cells at the mid-globular stage embryo and are required for meristem initiation (Aida et al., 1997; Aida et al., 1999; Long and Barton, 1998).

Although much is known about patterning of the shoot meristem during embryogenesis, there is little understanding of patterning that must occur during de novo induction of plant tissues in culture (Cary et al., 2002; Long and Barton, 1998). The cell proliferation observed during callus formation ensures that the ordered morphology of normal tissue is severely disrupted (Cary et al., 2002; White, 1939). Furthermore, new shoot meristems can be induced from root-derived explants, which differ in cell lineage, gene

expression, and tissue structure from the shoot meristem (West and Harada, 1993), thus raising the question of how root cells react to changes in environment and initiate patterned shoot tissues.

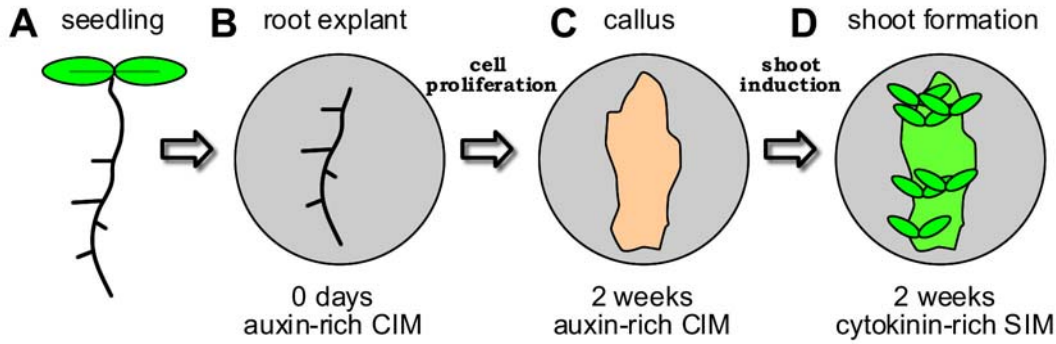


**Figure 2.1 Overview of the de novo shoot induction system.**
(A) Root explants are harvested from two week old seedlings and (B) transferred to auxin-rich CIM, which induces cell proliferation resulting in (C) callus formation. (D) Transfer of callus to cytokinin-rich SIM induces greening and induction of shoot meristems from callus often in clusters (marked by two green leaves).

Live imaging of the *Arabidopsis* meristem has been recently applied to the analysis of cell lineage and cell fate during active growth of the shoot meristem, to understand genetic control of meristem size, and to cell type specification leading to flower primordium initiation and patterning (Heisler et al., 2005; Reddy et al., 2004; Reddy and Meyerowitz, 2005). In this study we use a live imaging approach to characterize stage-specific molecular patterning events during de novo organization of the shoot meristem from callus (Figure 2.1).

## 2.2 RESULTS

### *2.2.1 Auxin/cytokinin response and gene expression during callus formation*

Our first goal was to determine a correlation between callus induction and distribution of auxin response during callus formation from root explants on auxin-rich CIM. Auxin response was visualized using the auxin responsive *DR5* element (Casimiro et al., 2001; Ulmasov et al., 1997) driving expression of tandem VENUS yellow fluorescent protein localized to the cell nucleus, *pDR5rev::3XVENUS-N7*. In non-induced root explants, the *DR5* reporter (green) marked root pericycle cells, a subset of lateral root progenitors, and the distal tip of lateral roots including columellar root cap cells (Figure 2.2A), as previously reported (Benkova et al., 2003). However, after five days incubation on CIM proliferative growth was marked by the *DR5* reporter and was initiated in the vicinity of lateral roots, root meristems and to a lesser extent, the root pericycle (Figure 2.2B). *DR5* response diminished over time and was not observed within large callus outgrowths after one week of culture (Figure 2.2C). In addition, after 2-3 days induction on CIM, a reporter for the auxin efflux carrier *PIN-FORMED 1* (*PIN1*), was induced in callus outgrowths (Figure 2.12B, green), but was later down-regulated and was not detected after ten days of induction.

We next investigated the spatial distribution of cytokinin response within root explants on CIM. The *Arabidopsis response regulator 5* gene (*ARR5)* has been shown to be transcriptionally responsive to cytokinin and its level of expression correlates with cytokinin content in various tissues (Aloni et al., 2004). We used transgenic plants bearing *ARR5* regulatory sequences driving GFP expression, *pARR5::GFP,* to dynamically monitor cytokinin response. In the non-induced root, *pARR5::GFP* activity was observed in the root stele, root meristems, and lateral root progenitor cells (Figure 2.2D, green). After eight days of induction on CIM, signal from the *ARR5* reporter was detected in the root explant vasculature and strongly marked proliferating callus cells (Figure 2.2E), and later expanded throughout callus after two weeks of induction (Figure 2.2F).

A recent study using an enhancer trap for *CUC1* demonstrated that *CUC1* upregulation is associated with callus formation on CIM (Cary et al., 2002). We determined if transcription of the partially redundant gene *CUC2* is also upregulated on CIM. Prior to

induction, a reporter consisting of *CUC2* regulatory sequences driving tandem VENUS expression localized to the cell nucleus, *pCUC2::3XVENUS-N7*, was active in a subset of cells of the root vascular cylinder and lateral root primordia founder cells (Figure 2.2G, green). After eight days of induction on CIM, the *CUC2* reporter was upregulated in small proliferating callus cells (Figure 2.2H) and was later observed throughout callus (Figure 2.2I). In contrast, *WUS*, *STM*, and *CLV3* were not expressed in callus, consistent with RT-PCR data from previous literature (Cary et al., 2002), nor did we observe *FIL* and *REV* reporter activity.

CIM contains 10-fold higher levels of the synthetic auxin 2,4-D, to the cytokinin, kinetin. We next investigated which of these hormones was responsible for callus induction and upregulation of the *CUC2* reporter. Modified CIM containing 2,4-D as the sole hormone induced callus and *CUC2* reporter expression (Figure 2.2J, green). On the same medium, the cytokinin responsive *pARR5::GFP* reporter was upregulated at sites of callus formation (Figure 2.2K). In contrast, culture of explants on CIM containing only kinetin did not lead to callus proliferation and *CUC2* reporter expression was faint and did not expand outside the vasculature of the primary root (Figure 2.2L). Expression of the auxin responsive *DR5* reporter also did not expand on this medium (data not shown).

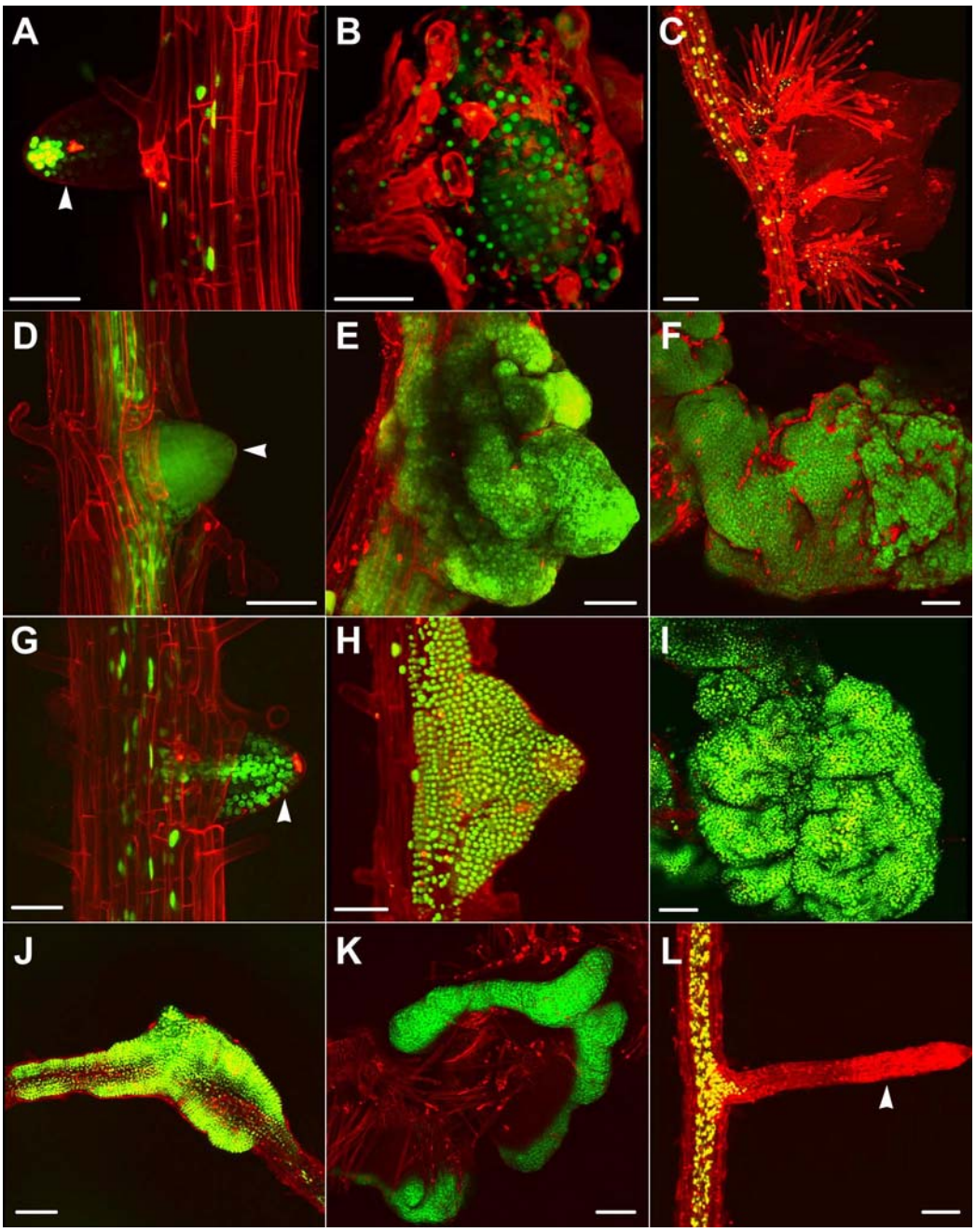


**Figure 2.2 Hormone response and gene expression during callus induction.**

All samples were stained with propidium iodide (red) to stain cell walls. (A) In wildtype roots, the auxin-responsive reporter, *pDR5rev::3XVENUS-N7* (green), is detected in a subset of cells in the root vasculature, lateral root progenitors, and columellar root cap cells. (B) Clusters of small cells marked by *pDR5rev::3XVENUS-N7* reporter (green) proliferate to form callus, five days after induction on CIM. (C) After eight days of CIM induction, the *pDR5rev::3XVENUS-N7* reporter was weakly expressed in callus. (D) Pre-

CIM cytokinin-responsive *pARR5::GFP* reporter expression (green) in the root stele, and lateral root progenitors. (E) *pARR5::GFP* reporter expression, eight days or (F) two weeks after CIM induction, was visible in proliferating callus cells. (G) Pre-CIM *pCUC2::3XVENUS-N7* reporter expression (green) in a subset of cells within the root stele and lateral root meristems. (H) *pCUC2::3XVENUS-N7* reporter expression eight days or (I) two weeks after CIM induction marked proliferating callus cells originating from sites of lateral root formation, root meristems and pericycle. (J, K) Two weeks induction on CIM without cytokinin, cell proliferation and expression of the *pCUC2::3XVENUS-N7* (J) and *pARR5::GFP* reporters (K) was observed. (L) Two weeks after induction on CIM without 2,4-D, callus was not induced and expression of the *pCUC2::3XVENUS-N7* reporter was faint and confined to the vasculature of the primary root. Scale bars: 50µm (A, B, D, E, G, H) or 100µm (C, F, I-L). Arrowheads indicate lateral roots.

Callus induction is associated with the proliferation of multipotent cell-types such as cells of the root meristems, lateral root progenitors and pericycle cells. To test the hypothesis that these cells were capable of responding to respecification cues without an intermediate culture on CIM, we cultured root explants directly on cytokinin-rich shoot inducing medium (SIM). After five weeks, an average of 3.9 ± 0.2 shoots were induced per two-centimeter root explant, compared to an average of 5.1 ± 0.3 after two weeks of culture on auxin-rich CIM followed by subsequent four weeks induction on SIM. In addition, we observed that shoots arose from proliferating cells originating from lateral root meristems labeled by the *CUC2* reporter.

### *2.2.2 Partition of cell identity and hormone response within callus*

The *CUC2* reporter was active throughout two week old root callus explants on auxin-rich CIM. Within 24-48 hours after transfer to cytokinin-rich SIM, *CUC2* reporter expression regressed within callus. After one week of culture on SIM, clusters of small dividing *CUC2* positive cells (Figure 2.3A, green) were observed in some regions of callus while absent from others. These cells developed into new shoot meristems with high frequency (Figure 2.3B-D, green). As the expression of *CUC2* is known to be post-transcriptionally regulated by the *MIR164* family of microRNAs (Baker et al., 2005; Sieber et al., 2007), we investigated the spatial distribution of CUC2 protein. The

expression of a translational CUC2-VENUS fluorescent protein fusion driven by *CUC2* upstream regulatory sequences, *pCUC2::CUC2-VENUS* was detected at low levels within shoot progenitor cells in a similar expression pattern as the *CUC2* transcriptional reporter (Figure 2.12C-E, red).

Down-regulation of the *CUC2* reporter from non-progenitor cells lead us to question if these cells had changed identity, marked by concomitant activation of other gene regulators. RT-PCR and oligonucleotide arrays have previously shown that *WUS* expression is upregulated in callus after three days induction on SIM (Cary et al., 2002). We documented the expression of a transgene containing *WUS* regulatory sequences driving GFP expression localized to the endoplasmic reticulum (ER), *pWUS::mGFP-ER*. The *WUS* reporter was upregulated after three days on SIM and its expression spread throughout large domains of callus by 5 days of induction (Figure 2.3E, green), and declined after 10 days culture. We observed that the *WUS* reporter was initially expressed in cells peripheral to shoot meristem progenitor cells but was later upregulated within the center of the phyllotatic shoot meristems (Figure 2.3F,G). We investigated the relative expression domains of *CUC2* and *WUS* activity using a *pCUC2::3XVENUS-N7; pWUS::DsRed-N7* marker line. These markers formed non-overlapping domains of activity within callus (Figure 2.3H, I). As described above, small rapidly dividing cells labeled by the *CUC2* reporter (green) gave rise shoot meristem progenitor cells while the *WUS* reporter (red) was expressed in peripheral cells which did not rapidly divide (Figure 2.12F). At later stages, the *CUC2* reporter was expressed in a radial pattern and the *WUS* marker was upregulated in the future rib zone of the developing shoot promeristem (Figure 2.3J).

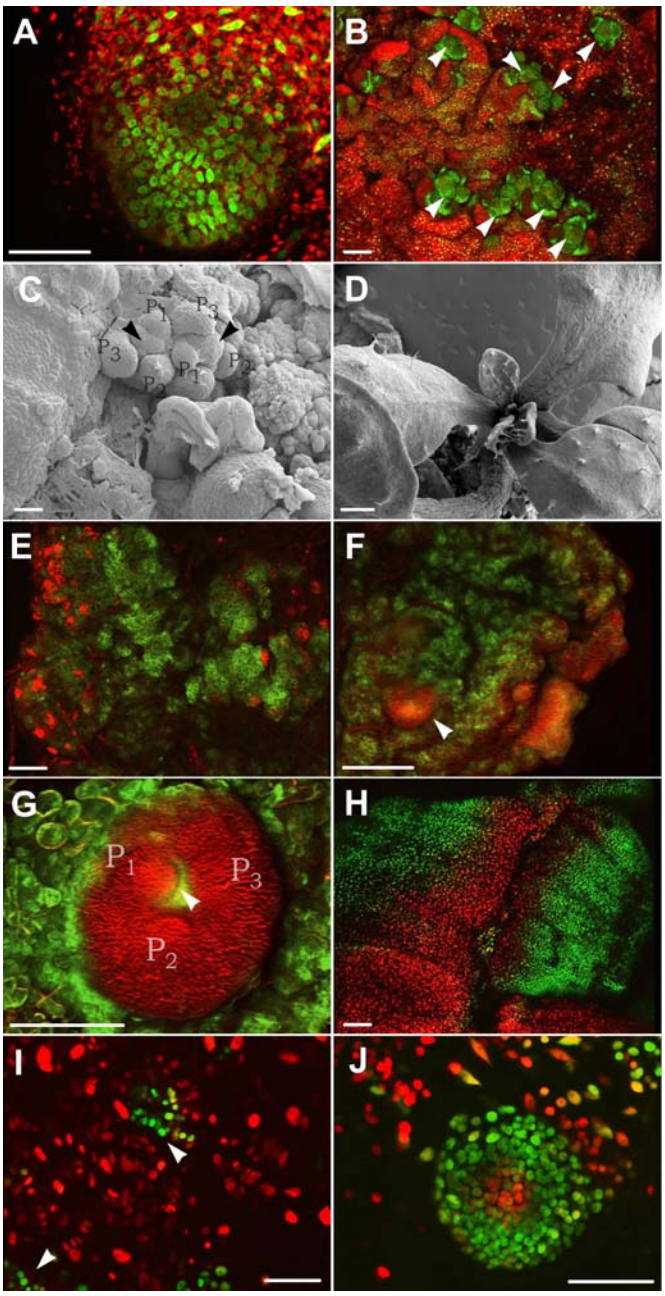


**Figure 2.3 Partition of gene expression and cell identity within callus**
(A) Mounds of small dividing cells marked by the *pCUC2::3XVENUS-N7* reporter (green) formed and (B) gave rise to new shoot meristems (arrowheads), often observed in clusters. Chlorophyll autofluorescence is in red. (C) Scanning electron micrograph of early regenerating meristems (arrowheads), and (D) a late stage regenerated shoot emerging from callus. (E) The *pWUS::mGFP-ER* reporter (green) was expressed in callus cells poorly stained by FM4-64 dye (red) following five days induction on SIM. (F) Shoot progenitors (arrowhead, 12 days on SIM) were labeled with FM4-64 dye, and emerged from regions with peripheral *pWUS::mGFP-ER* expression, and formed (G) mature shoot

meristems, also strongly stained by FM4-64 dye. The *pWUS::mGFP-ER* reporter was upregulated in the center of the developing meristem (arrowhead). (H) *pCUC2::3XVENUS-N7* (green) and *pWUS::DsRed-N7* (red) reporters were active in opposing domains of cells, sometimes in gradients, shown here after 10 days SIM. (I) Higher magnification after 11 days on SIM, showing clusters of cells expressing the *CUC2* reporter (arrowheads) surrounded by *pWUS::DsRed-N7* expressing cells. (J) At later stages, *WUS::DsRed-N7* expression was initiated in the center of the mound of shoot progenitors while *pCUC2::3XVENUS-N7* was restricted to the future peripheral zone, shown here after 12 days on SIM. Scale bars: 50µm (A, C, I, J) or 100µm (B, E-H) or 300µm (D). Primordia ($P_n$) and incipient primordia ($I_n$) are labeled.

### *2.2.3 Partition of hormone response within callus*

Our results show that induction on cytokinin-rich SIM leads to partitioning of cell identity and cell behavior within callus. We next questioned if hormonal response was partitioned within callus in similar fashion. The cytokinin responsive *ARR5* reporter was expressed in areas of shoot meristem initiation and within developing shoot meristems, but was downregulated in organ primordia (Figure 2.4A, green). *ARR5* reporter expression was absent from areas of callus which initiated root tissues or which did not regenerate at all, but strongly labeled regenerating root meristems (Figure 2.12G). In contrast, auxin responsive *DR5* reporter signal (red) was low or undetectable in areas of shoot initiation, but marked surrounding regions of callus which did not initiate shoot tissues (Figure 2.4B). In such areas, shoot meristems and shoot promeristems were marked by expression of a *PIN1* reporter (green), consisting of *PIN1* regulatory sequences driving expression of a PIN1-GFP fusion protein. Higher magnification images show that *PIN1-GFP* expression (green) initiates in cells with low *DR5* activity (blue) (Figure 2.4C). *DR5* signal was observed within the developing shoot meristem after *PIN1* reporter upregulation at future sites of leaf primordium formation (Figure 2.4D). As primordia grew outward *DR5* signal increased at the primordium tip (Figure 2.4E).

Local application of auxin paste to areas of shoot meristem development induced strong *DR5* signal (red) from callus surrounding the meristems marked by the PIN1 reporter

(green) (Figure 2.4F, G), while no response was observed in control experiments. Only cells directly associated with the mature meristem did not show *DR5* reporter upregulation. Thus, lack of strong *DR5* signal in the vicinity of shoot meristem initiation is likely due to lower auxin concentrations in such areas and not simply due to an inability of the cells to respond to auxin.

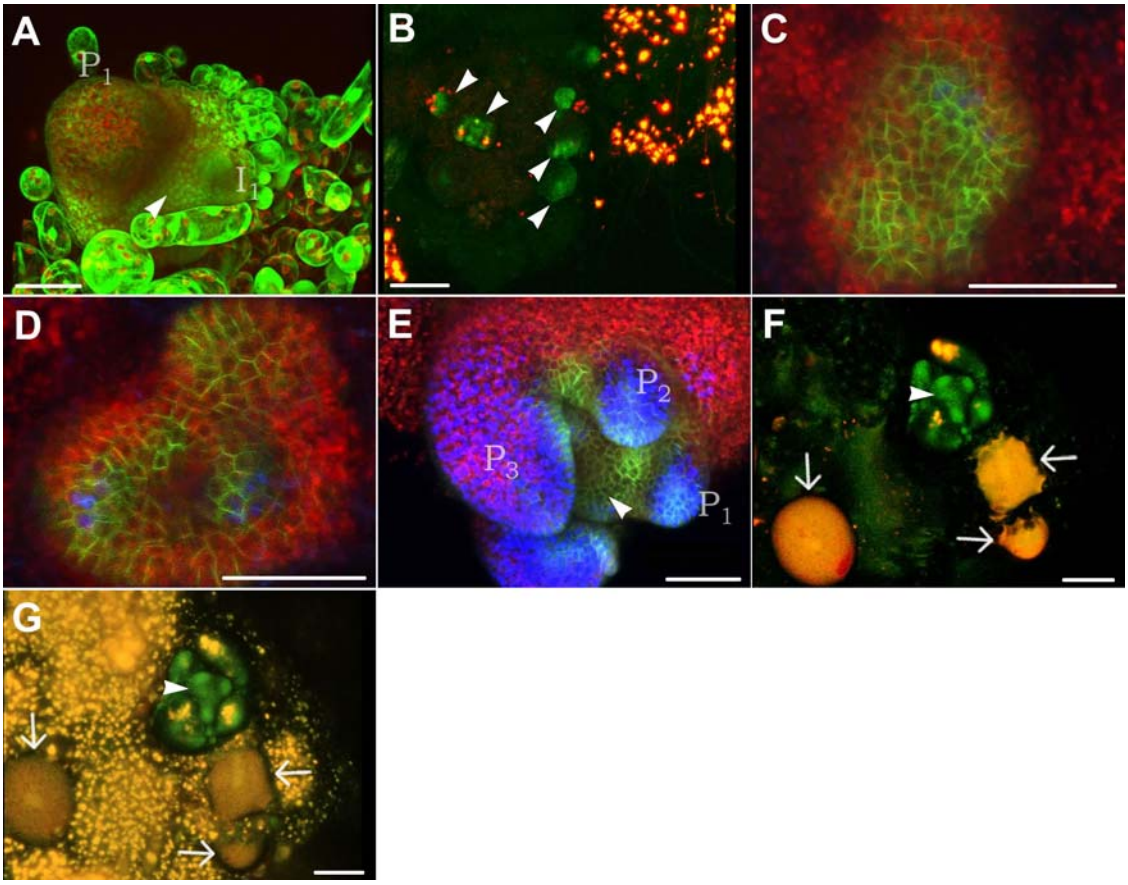


## Figure 2.4 Partition of hormone response within callus

(A) The *pARR5::GFP* reporter (green) was active in callus forming shoot meristems (arrowhead), but downregulated in primordia ($I_1$ and $P_1$). Chlorophyll autofluorescence is in red. (B) Regenerating meristems (arrowheads) marked by *pPIN1::PIN1-GFP* (green) expression, emerged from callus with low *pDR5rev::3XVENUS-N7* (red) expression, while *pDR5rev::3XVENUS-N7* signal was observed in peripheral callus and within initiating primordia flanking meristems. (C) *pPIN1::PIN1-GFP* reporter expression (green) within the shoot progenitors precedes strong *pDR5rev::3XVENUS-N7* expression (blue) which was later detected during (D, E) the initiation and outgrowth of organ primordia ($P_1$-$P_3$). Chlorophyll autofluorescence is in red. (F) *pDR5::3XVENUS*-N7 signal (red) was not observed 1 minute after application of auxin paste (arrows) to callus initiating shoot

meristems (arrowhead), marked by *pPIN1::PIN1-GFP* (green). (G) 4 hours after application of auxin paste (arrows) *pDR5::3XVENUS*-N7 signal (red) was observed throughout callus in contrast to the meristem itself (arrowhead), in which *pDR5::3XVENUS*-N7 signal was only in developing primordia. Scale bars: 50µm (A, C-E) or 100µm (B, F, G). Primordia ($P_n$) and incipient primordia ($I_n$) are labeled.

### *2.2.4 Pattern formation within the shoot promeristem*

*PIN1* reporter upregulation was associated with the morphogenesis and patterning of phyllotatic shoot meristems from mounds of promeristem cells. We therefore investigated *PIN1* expression relative to other developmental genes: *CUC2*, *REV*, *FIL*, *STM*, *CLV3*. We documented simultaneous *PIN1* and *CUC2* reporter activity using *pPIN1::PIN1-GFP; pCUC2::3XVENUS-N7* transgenic plants. *PIN1* (green) was upregulated in the superficial layers of shoot promeristem labeled by the *CUC2* reporter (red) (Figure 2.5A). Higher levels of PIN1-GFP were observed at future sites of primordium initiation. As primordia initiated growth, the *CUC2* reporter was expressed in the primordial/meristem boundary (Figure 2.5B). Using plants transgenic for *pPIN1::PIN1-GFP; pWUS::DsRed-N7* reporters we observed that PIN1-GFP protein (green) was localized within the cell membrane directed towards the apical tip of the shoot promeristem and away from non-progenitor cells (blue) (Figure 2.5C).

At the periphery of the *Arabidopsis* meristem, organ primordia are specified with adaxial/abaxial polarity with respect to the shoot meristem, in part by the HD-ZIP gene *REVOLUTA* (*REV*) and the YABBY transcription factor *FILAMENTOUS FLOWER (FIL)*. Early *PIN1* reporter expression (green) was closely followed by upregulation of a *pREV::REV-VENUS* reporter (red) in a subset of internal cells of the developing shoot meristem (Figure 2.5D). 24 hours laters, as *PIN1* reporter expression was upregulated at sites of primordium initiation, *REV* expression extended toward the adaxial side of initiating primordia (Figure 2.5E) and later was observed in the adaxial side of leaf primordia (Figure 2.5F). Fluorescent signal from a *FIL* reporter (red), *pFIL::DsRed-N7,* was first observed at the periphery of the early *PIN1* domain and clearly demarcated early

primordia (Figure 2.5G), and its expression was later maintained in the abaxial sides of primordia (Figure 2.5H, I).

Upregulation of *PIN1* reporter expression within shoot promeristem was also associated with upregulation of the *SHOOTMERISTEMLESS (STM)* gene. Time-lapse imaging of transgenic plants containing reporters for *PIN1, STM*, and *WUS* showed that the *STM* reporter (blue) is upregulated during the onset of *PIN1* reporter expression (green). *STM* was expressed in a ring of cells surrounding the shoot promeristem and a subset of cells within the promeristem as the *PIN1* reporter was upregulated in primordia initials ($I_1$ and $I_2$) (Figure 2.5J and Figure 2.12H-S). After 24 hours, the *PIN1* reporter marked growing primordia ($P_1$ and $P_2$) while the *STM* reporter became upregulated through the center of the shoot promeristem (Figure 2.5K) and was maintained in this domain through 48 hours of observation (Figure 2.5L).

Stem cells of the shoot reside at the apical tip of the meristem, marked by expression of the *CLAVATA 3 (CLV3)* gene (Fletcher et al., 1999; Reddy and Meyerowitz, 2005). We observed that *CLV3* expression (green), was absent from shoot progenitor cells, which were marked by the *pPIN1::PIN1-CFP* reporter (white) in plants transgenic for *pCLV3::GFP-ER*, *pPIN1::PIN1-CFP*, and *pWUS::DsRed-N7* reporters (Fig. 5M). *CLV3* reporter expression appeared during upregulation of *WUS* reporter expression (red) within the center of the new meristem and the initiation of primordia ($P_1$ and $P_2$) from the meristem periphery (Figure 2.5N). *CLV3* reporter activity was confirmed in plants bearing a *p35S::YFP 29-1* transgene (yellow), which express membrane localized YFP within all cells of the mature meristem (Figure 2.5O).

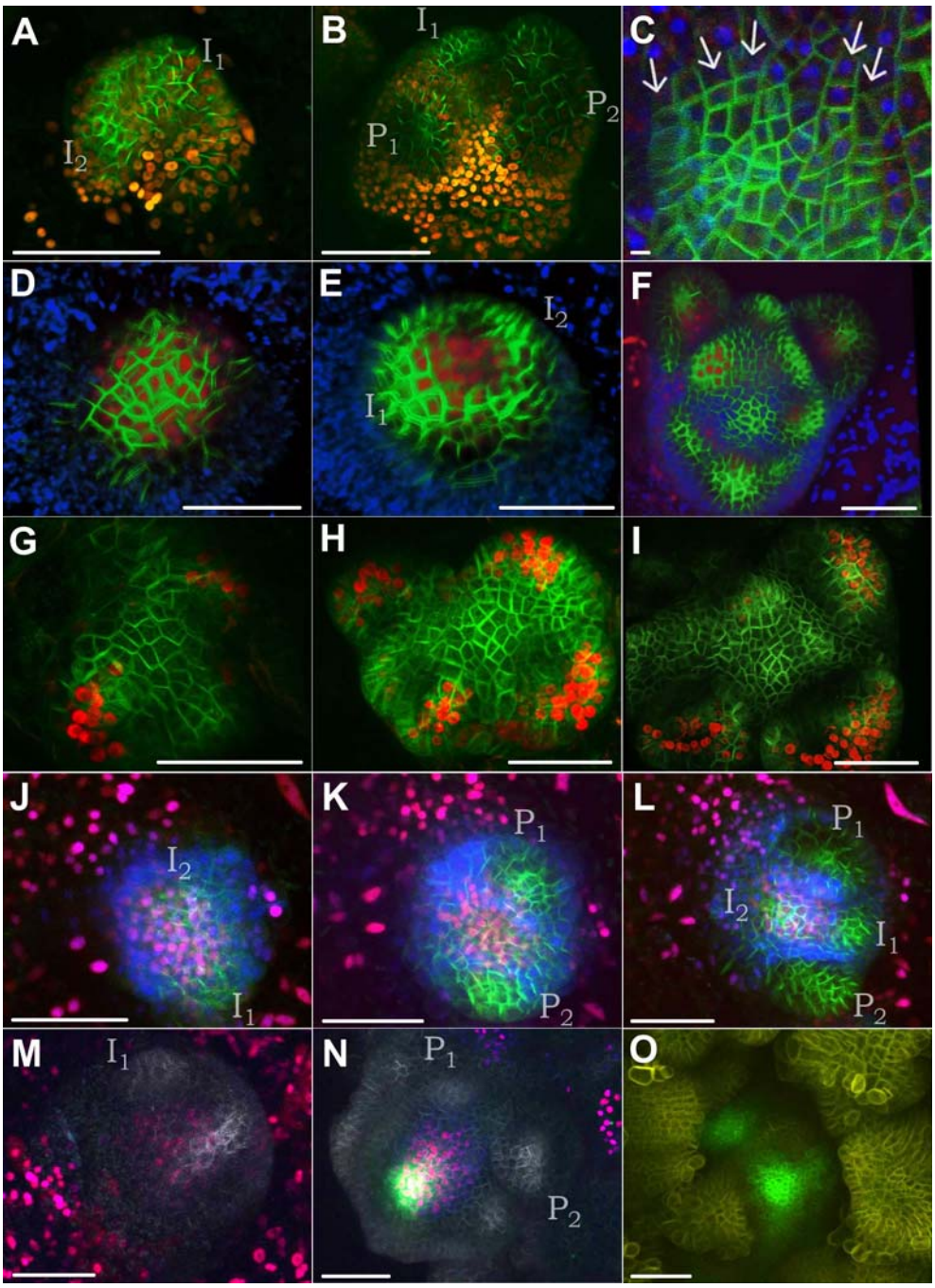


**Figure 2.5 Pattern formation within the shoot promeristem**

(A) *pPIN1::PIN1-GFP* expression (green) was upregulated in the superficial layer of shoot meristem progenitor cells marked by *pCUC2::3XVENUS-N7* reporter expression (red), and labeled primordial initials ($I_1$ and $I_2$). (B) After 24 hours, primordium initials grew into primordia ($P_1$ and $P_2$) and *pCUC2::3XVENUS-N7* (red) was expressed in the meristem boundaries. (C) PIN1-GFP protein was polarized towards the apex of the shoot progenitors (arrows) and away from peripheral cells marked by the *pWUS::DsRed-N7*

reporter (blue). (D) Early *pREV::REV-VENUS* expression (red) was observed in the center of the progenitors underneath the *pPIN1::PIN1-GFP* (green) domain. Chlorophyll autofluorescence is in blue. (E) 24 hours later in the same developing meristem, *pREV::REV-VENUS* expression (red) was expressed in adaxial sides of initiating primordia ($I_1$ and $I_2$), and (F) was similarly expressed in primordia ($P_1$-$P_6$) within later stage shoot meristems. (G) *pFIL::DsRed-N7* expression (red) was upregulated flanking the early *pPIN1::PIN1-GFP* (green) domain and (H) was later upregulated on the abaxial side of early primordia and (I) older primordia. (J) *pSTM::STM-VENUS* (blue) was expressed in a ring surrounding shoot progenitors and a subset of cells within the promeristem (eleven days on SIM) while local *pPIN1::PIN1-GFP* reporter (green) upregulation marked sites of primordium initiation ($I_1$ and $I_2$) and *pWUS::DsRed-N7* reporter (red) was expressed in peripheral cells and upregulated in the center of the developing meristem. (K) 24 hours later in the same shoot progenitors, *pSTM::STM-VENUS* (blue) was upregulated within the meristem between the developing primordia ($P_1$ and $P_2$) and (L) was maintained through 48 hours of imaging during which primordia grew and two new primordia were initiated ($I_1$ and $I_2$). (M) *pCLV3::mGFP5-ER* expression (green) was absent from shoot progenitors marked by *pPIN1::PIN1-CFP* expression (white) and peripheral cells marked by the *pWUS::DsRed-N7* reporter (red). (N) *pCLV3::mGFP5-ER* expression (green) was detected after primordial outgrowth from the periphery of the developing meristem. (O) *pCLV3::mGFP5-ER* expression (green) was also observed in later stage shoot meristems which expressed a *p35S::YFP 29-1* transgene (yellow). Scale bars: 50µm (A,B, D-O) or 5µm (C). Primordia ($P_n$) and incipient primordia ($I_n$) are labeled.

### *2.2.5 L1 layer specification and development of meristem structure*

The homeodomain transcription factor *ARABIDOPSIS THALIANA MERISTEM L1 LAYER (ATML1)* is redundantly required for specification of the epidermal layer in *Arabidopsis* (Abe et al., 2003) and is restricted to the protodermal layer at the 16 cell stage onwards (Lu et al., 1996). We used a transgenic line containing *pATML1::GFP-ER* and *pCUC2::3XVENUS-N7* reporters in order to understand relative timing of L1 cell-type specification with regards to meristem organization. The *ATML1* reporter was restricted to a subset of superficial cells within the shoot promeristem marked by the *CUC2* reporter (Figure 2.6A, B). In contrast, the *ATML1* reporter was often not L1-specific when expressed in callus (Figure 2.6C). Primordium initiation began after approximately 72 hours of development and was associated with homogenous expression of the *ATML1* reporter within the protoderm (Figure 2.6E).

We further followed the shoot regeneration process in a *pPIN1::PIN1-GFP; pSTM::STM-VENUS; pRIBO::2XCFP-N7* marker line. The *pRIBO::2XCFP-N7* marker labeled all cells within callus, enabling us to observe that shoot promeristems were composed of variable numbers of cells (Figure 2.6G). Shoot promeristems composed of smaller numbers of cells developed into shoot meristems with fewer initial leaf primordia compared to larger promeristems (Figure 2.6J).

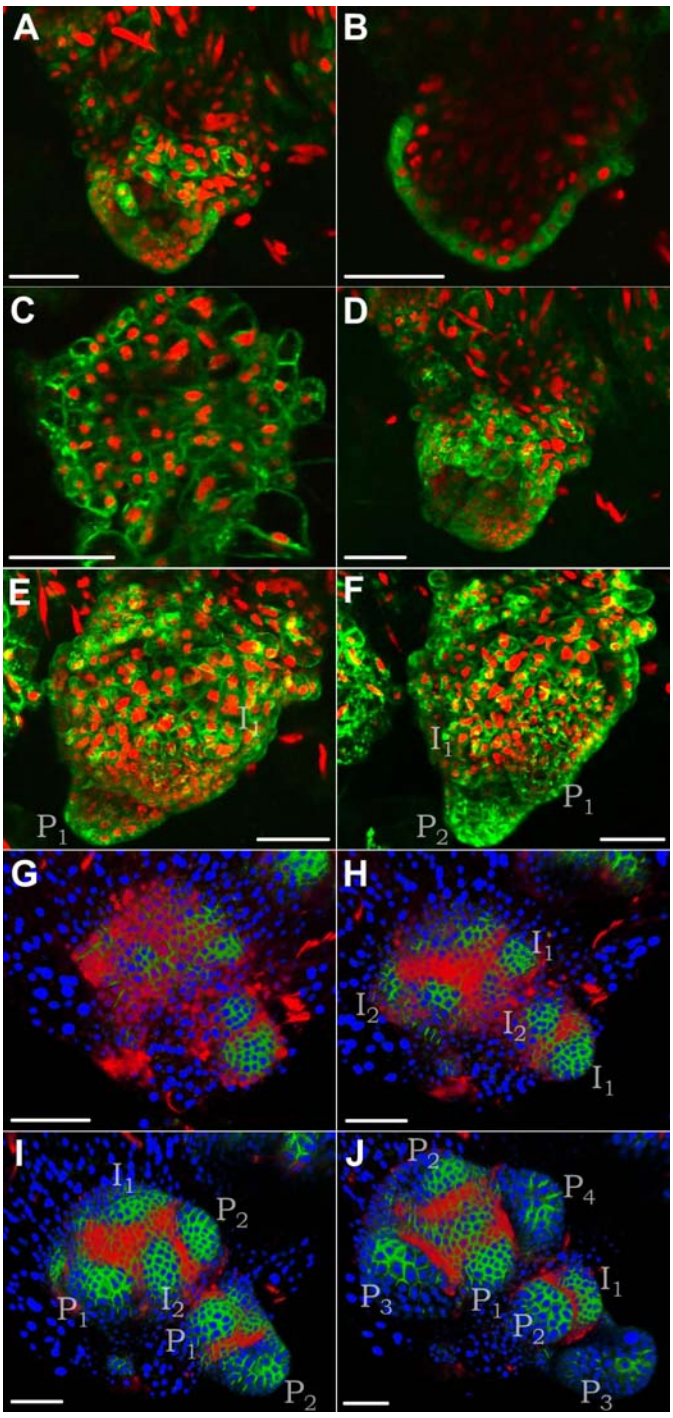


**Figure 2.6 L1 layer specification and development of meristem structure**
(A) *pML1::GFP5-ER* reporter (green) was upregulated in a subset of superficial shoot meristem progenitors, marked by the *pCUC2::3XVENUS-N7* (red) marker. (B) Expression of the *pML1::GFP5-ER* reporter (green) was L1 specific within the shoot progenitors but (C) not L1 specific in cross-sections of callus. (D) 24 hours later, *pML1::GFP5-ER*

expression was upregulated in the shoot progenitors. (E) 72 hours later, *pML1::GFP5-ER* expression was homogeneously expressed within the L1 of the meristem as primordia ($I_1$ and $P_1$) were initiated. (F) 96 hours later, two early primordia ($P_1$ and $P_2$) were evident. (G) *pPIN1::PIN1-GFP* (green) and *pSTM::STM-VENUS* (red) were upregulated with similar timing in small patches of cells marked by the ubiquitous *pRIBO::2XCFP-N7* marker (blue). (H) 24 hours later, *pPIN1::PIN1-GFP* marked initiating primordia ($I_1$, $I_2$). (I) After 48 hours, primordia ($P_1$ and $P_2$) labeled by *pPIN1::PIN1-GFP* have grown outwards and *pSTM::STM-VENUS* expression was expressed in the developing meristem. (J) After 72 hours of observation, meristems derived from variable numbers of initial cells gave rise to greater or lesser numbers of primordia, respectively. Scale bars: 50µm (A-J). Primordia ($P_n$) and incipient primordia ($I_n$) are labeled.

## *2.2.6 Requirement of WUS and PIN1 for shoot meristem induction*

To determine if *WUS* and *PIN1* are necessary for efficient initiation of new shoot meristems, we quantified the number of shoots formed from 2 centimeter callus explants in the strong *wus-1* and *pin1-4* mutants after four weeks of growth on SIM. The average number of shoots formed in the *wus-1* mutant (n = 91) decreased to 5% of wildtype (n = 106) (0.25 ± 0.08 versus 5.06 ± 0.04), while the average number of shoots formed in the *pin1-4* mutant (n = 174) decreased to approximately 20% of wildtype (n = 166) (0.90 ± 0.07 versus 5.16 ± 0.24) (Figure 2.7A).

**Quantitation of an early versus late defect in *wus-1***

The decrease in the number of shoot meristems observed in the *wus-1* mutant could be due to an early defect in which fewer shoot promeristems are initiated or a late defect in which shoot promeristems arrest at later stages of development prior to quantification. We differentiated between these two possibilities by examining the number of early shoot promeristems, marked by *pPIN1::PIN1-GFP* and *pSTM::STM-YFP* co-expression, formed in *wus-1*. The number of early shoot promeristems was decreased in the *wus-1* mutant (n = 45) to only 20% of wildtype (n = 48) (7.63 ± 0.92 versus 1.67 ± 0.43) (Figure 2.7B). However, we observed that in those shoot

promeristems that do form, the *PIN1* and *STM* reporters are initially expressed in similar relative domains as during wildtype shoot meristem assembly (Figure 2.7C-E).

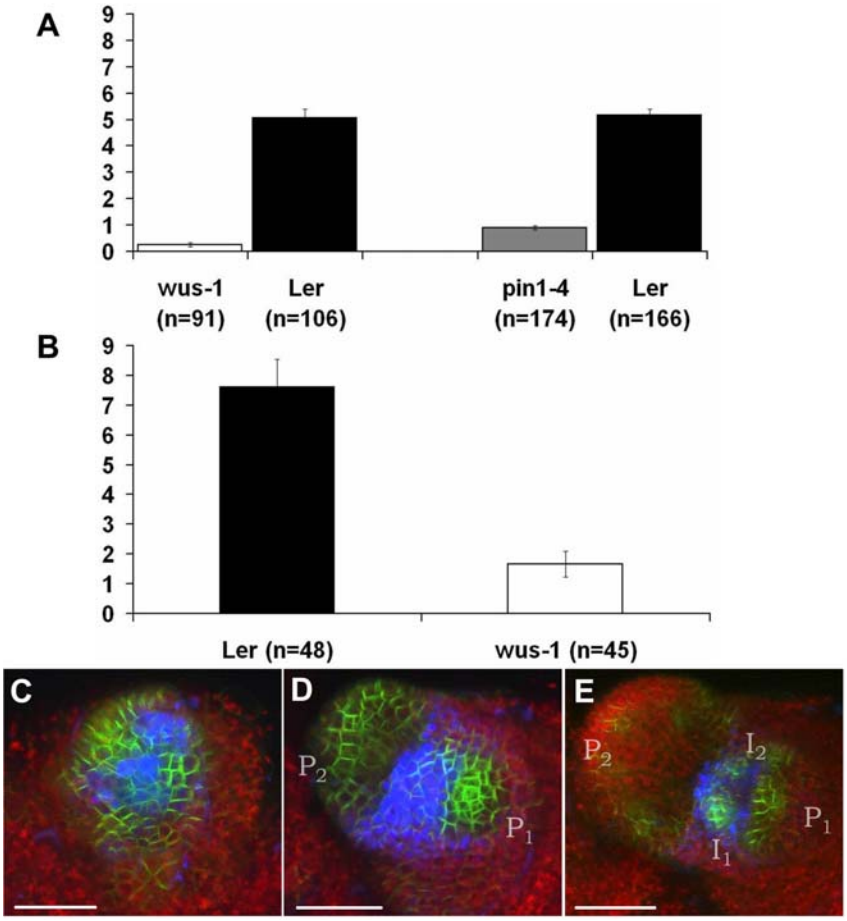


## Figure 2.7 *WUS* and *PIN1* are functionally required for efficient shoot meristem induction.

(A) Histogram showing average numbers of shoots formed after four weeks of induction on SIM from 2 centimeter callus explants in wildtype (L*er*) versus *wus-1,* and in separate experiment L*er* versus *pin1-4*. (B) Histogram showing number of shoot promeristems, marked by *pPIN1::PIN1-GFP* (green) and *pSTM::STM-VENUS* (blue) coexpression, in L*er* versus *wus-1*. (C) *pPIN1::PIN1-GFP* and *pSTM::STM-VENUS* expression in a shoot promeristem initiated in the *wus-1* mutant. Chlorophyll autofluorescence is in red. (D) 24 hours later, the shoot promeristem initiated early primordia ($P_1$ and $P_2$) marked by *pPIN1::PIN1-GFP*, while *pSTM::STM-VENUS* marked the presumptive shoot meristem. (E) 48 hours later, primordia ($P_1$ and $P_2$) have further developed and two early primordia initials ($I_1$ and $I_2$) have formed near the apex of the meristem. Scale bars: 50µm (C-E). Primordia ($P_n$) and incipient primordia ($I_n$) are labeled.

### *2.2.7 Turing-like model of shoot meristem induction*

Our observations demonstrate that culture on medium with high cytokinin/auxin ratio induces a partition of cell identity within callus marked by expression of the early developmental regulators, *CUC2* and *WUS*. *CUC2* and *PIN1* expression mark a small number of progenitor cells that proliferate to form a relatively homogeneous cell mass, which is then later patterned into a new shoot meristem de novo. Patterning of the shoot promeristem involves local upregulation of genes expressed in the mature shoot meristem such as *STM*, *REV*, *FIL, ATML1* and *CLV3* and the progressive refinement of their expression to domains found during later development (Heisler et al., 2005). We therefore break the shoot organization process into distinct events: callus induction, cytokinin-induced partition of cell identity within callus, radial patterning within shoot progenitors, and meristem morphogenesis (Figure 2.8).

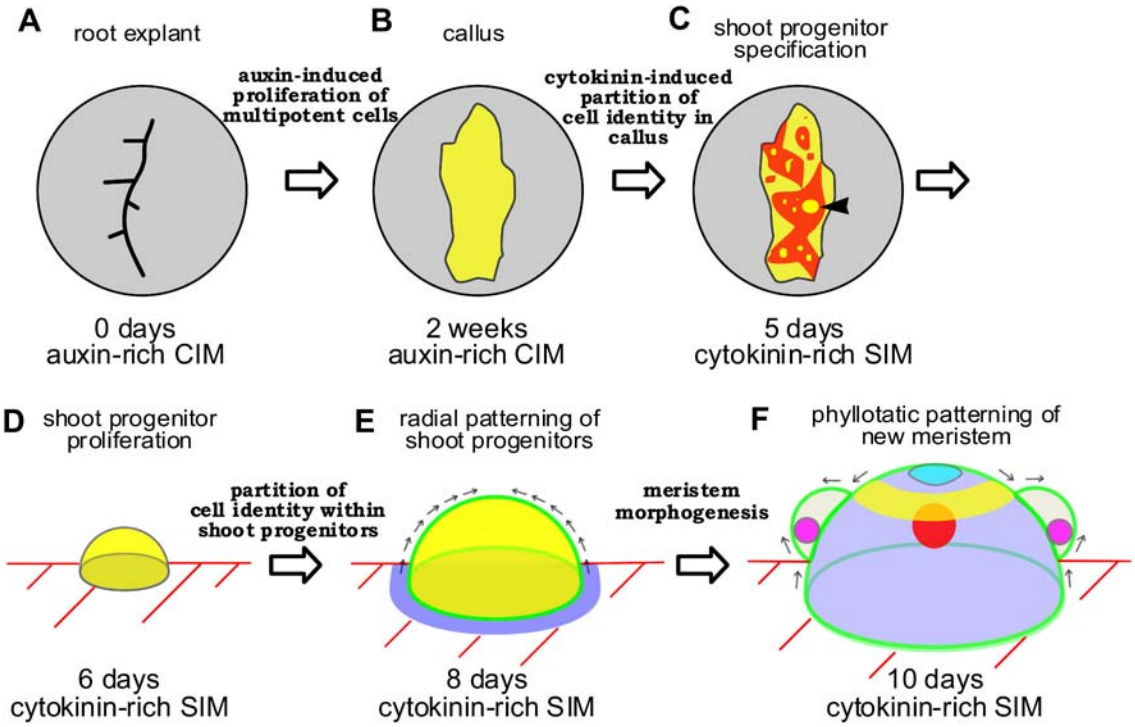

**Figure 2.8 Schematic of *de novo* shoot meristem organization from callus.** (A) Auxin-rich CIM induces proliferation of multipotent cells in the root leading to (B) callus formation. (C) Transfer to cytokinin-rich SIM induces partition of cell identity and behavior within callus marked by the *CUC2* (yellow) and *WUS* (red) reporters. (D) Clusters of *CUC2* labeled shoot progenitors proliferate among neighboring *WUS* expressing (red lines) non-progenitor cells in areas of high cytokinin and low auxin response. (E) 24-48 hours later, *PIN1* and *ML1* reporters (both green) are upregulated within the superficial layer of the shoot promeristem while *STM* (blue) is upregulated in a ring of surrounding cells and within the promeristem. Within the membrane of shoot progenitors, PIN1 protein is directed towards the apex of the promeristem (arrows), and thus is predicted to transport auxin into the promeristem from surrounding cells. (F) 48-96 hours later, *PIN1* becomes locally upregulated within the peripheral zone and marks sites of primordial initiation. PIN1 protein becomes locally polarized towards sites of primordia formation (arrows). *FIL* (magenta) is expressed in the abaxial sides of newly initiated primordia. *CLV3* expression (teal) is initiated within the central zone after *WUS* expression (red) initiates within the center of the meristem. *pSTM::STM-VENUS* is expressed within the meristem.

A primary goal of our documentation of molecular patterning events during de novo meristem induction was to gain insight into the mechanism behind the patterning process. The above data are consistent with a model for *de novo* shoot meristem regeneration in which founder cells are specified in part by gradients of auxin and cytokinin. In our model the antagonistic interaction of auxin and cytokinin is similar to an activator inhibitor system. We propose that auxin acts as an activator of founder cell identity and shoot meristem morphogenesis. Local fluctuations of auxin stimulate PIN1 expression which further increases the local concentration of auxin. Higher auxin levels stimulate the production of cytokinin which acts as an antagonist of auxin function (inhibitor). However, cytokinin freely diffuses from cells away from the site of activation. Such a system is similar to a classical Turing mechanism. In this section we develop a preliminary series of mathematical models based on a Turing-like mechanism as applied to shoot regeneration which may be a more general model for patterning in plants. For example, floral primodia are specified through the PIN-mediated accumulation of auxin (activator) within clusters of initial cells at the meristem

periphery. This is followed by activation of reporters for cytokinin response (inhibitor) within the developing primordia (see Chapter 3).

In our novel Turing-like model, patterning of hormone response and gene expression feedback on one another in order to explain the self-organizing nature of regeneration. For example, restriction of CUC2 expression to founder cells is correlated with the induction of *PIN-FORMED1 (PIN1)* within these cells. PIN1 is a polarized auxin efflux carrier required for the initiation and maintenance of auxin gradients within various tissues of the plant (Friml et al., 2003; Heisler et al., 2005). During selection of founder cell identity, PIN1 is polarized within these and surrounding cells towards the center of the founder cell niche. *PIN1* is itself an auxin regulated gene. Therefore a spike in local auxin concentration might induce *PIN1* expression which positively feeds back on auxin distribution to build a peak of auxin response. Indeed, models based on PIN1 auxin transport accurately reproduce phyllotatic patterning of organ primordia from the shoot meristem (Marcus and Henrik). CUC2 which marks founder cells has been shown induce STM in the embryo. STM has been recently shown to activate transcription of cytokinin synthesis enzymes. In contrast, WUS has been shown to be induced by cytokinin treatment (Lindsay et al., 2006). Furthermore, WUS has been shown to enhance cytokinin signaling. Thus cytokinin may induce *WUS* during regeneration and WUS may then feedback to enhance cytokinin signaling. From this data we built the preliminary Turing-like network displayed in Figure 2.9.

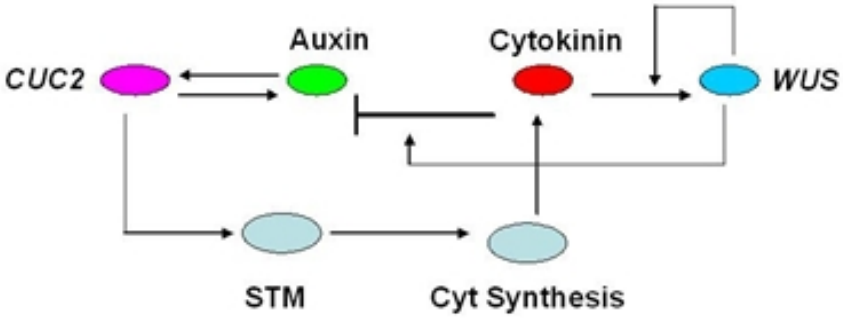


**Figure 2.9 Schematic of Turing-like activator inhibitor model of shoot regeneration.**
In this model auxin acts as an activator of cell differentiation and shoot progenitor fate which feedsback on itself through *CUC2* activity (instead of modeling PIN1, used in subsequent models). Cytokinin antagonizes auxin accumulation and function. Auxin leads to production of the inhibitor, cytokinin, through activation of *STM* thereby inducing cytokinin synthesis enzymes. The strength of inhibitor function is strengthened by its activation of WUSCHEL which suppresses negative regulators of cytokinin signaling.

Intuitively, the network in Figure 2.9 is similar to a Turing-like activator/inhibitor model. Auxin (activator) feeds back on itself through *CUC2*, however, auxin also leads to activation of cytokinin synthesis through *STM*. Cytokinin (inhibitor) inhibits the action of auxin. Auxin is assumed to diffuse slower from the site of activation than cytokinin due to polar transport by PIN transporters. Preliminary computational models representing this network are sufficient to self-assemble patterns of auxin, cytokinin and CUC2 expression observed experimentally.

Recent work has shown that auxin and cytokinin interact antagonistically. Cytokinin reduces auxin response by activating transcription of the *SHY2/IAA3* (*SHY2*) gene which leads to suppression of auxin response and therefore negatively regulates PIN expression (Dello Ioio et al., 2008; Ruzicka et al., 2009). PIN1 as mentioned above acts to locally slow the diffusion of auxin away from founder cells. Thus cytokinin modulates the diffusion of auxin through regulation of *PIN1*. This suggests that auxin will diffuse faster in areas of high cytokinin. Auxin counteracts cytokinin action by directing the degradation of SHY2 protein, enabling auxin response and PIN expression. Auxin has

also has a positive effect on cytokinin. Auxin leads to expression of the cytokinin biosynthetic gene adenosine diphosphate isopentenyltransferase 5 (IPT5) (Dello Ioio et al., 2008). Thus, auxin stimulates the production of its antagonist. From this data we built a revised network displayed in Figure 2.11.

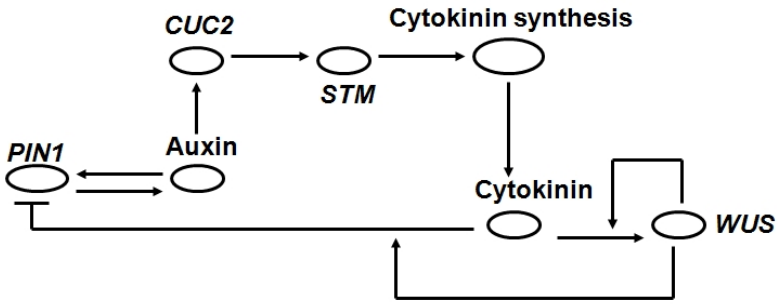


**Figure 2.10 Turing-like model of cytokinin-regulated auxin transport.**
In this revised model the inhibitor (cytokinin) negatively regulates feedback on the activator (auxin) through repression of PIN-mediated directional auxin transport. Auxin promotes PIN1 expression which mediates positive feedback on auxin levels by mediating auxin transport to neighboring cells which have the highest auxin. This effectively retards the diffusion of auxin out of a group of cells with higher auxin levels building a peak of auxin accumulation. Cytokinin response leads to suppression of PIN expression which prevents the sequestering of auxin within particular cells. Thus, the action of cytokinin essentially prevents the positive feedback of auxin on its own accumulation.

From the data gathered above we have developed preliminary computational models of how auxin and cytokinin interact through modulating various gene and protein activities. We found that a Turing-like mechanism fits with available experimental data for partitioning cell fate during regeneration. In this model auxin acts as activator of shoot progenitor cell fate whereas cytokinin act as an inhibitor of shoot progenitor fate. Similar to the classical Turing model, the activator (auxin) positively feeds back on its own accumulation. However, the activator (auxin) stimulates production of the inhibitor (cytokinin) which inhibits the increase in activator accumulation (auxin). Key to the pattern formation process, the inhibitor (cytokinin) diffuses away faster from the site of activation than the activator, allowing a peak of activation to form surrounded by

a zone of inhibition. Novel to our system is the fact that accumulation of the activator occurs not through positive feedback on auxin synthesis but through positive feedback on auxin transport.

## 2.3 Discussion

### *Characterization of hormone response and gene expression during callus induction*

Prior studies have shown that good auxin efflux substrates, such as indole-3-acetic acid (IAA) or [alpha]-naphthalene acetic acid (NAA), induce lateral root growth in wildtype root explants, but callus-like proliferation in mutants for *pin* auxin efflux carriers (Benkova et al., 2003). Furthermore, a reporter for *CUC3* expression was expanded in roots simultaneously treated with IAA and the auxin transport inhibitor NPA. 2,4-D is an auxin analog that is poorly transported by the auxin efflux system (Delbarre et al., 1996). Our data shows that CIM containing 2,4-D as the sole added hormone in the growth medium is sufficient to induce callus formation, which involves proliferation of multipotent cell-types including root pericycle cells, lateral root progenitors, and cells of the root meristems. Combined, these findings suggest that callus induction is due to an inability of root tissue to regulate auxin distribution, leading to unrestrained proliferation of multipotent cells of the root.

Recently, it has been shown that pericycle cells uniquely continue division through the elongation and differentiation zones of the root after exit from the root meristem (Dubrovsky et al., 2000). Later, a subset of these cells gives rise to lateral root primordia. The ability of these cells to continue division may be linked with their enhanced response to environmental stimuli, such as the availability of hormones. Consistent with this model, we observe that most cells initiating and proliferating as callus are marked by the auxin-responsive *DR5* and cytokinin-responsive *ARR5*

reporters. The enhanced capacity to divide in response to hormone induction and ability to give rise to multiple cell types may explain the preferential proliferation of these cells on CIM and their plasticity during induction of shoot tissues when transferred to a high cytokinin environment.

The different quantitative requirements for auxin and cytokinin in order to induce various tissues in culture is likely in part due to different endogenous concentrations of these hormones within explants (Skoog, 1950). Root meristems are sites of endogenous cytokinin production (Aloni et al., 2005; Nordstrom et al., 2004). The upregulation of the cytokinin responsive *ARR5* reporter within callus forming on CIM containing 2,4-D but no exogenous cytokinin suggests that callus induced from root meristems may endogenously produce cytokinin.

## *Partition of cell identity and hormone response within callus during shoot meristem initiation*

Previous studies have shown that mosaic overexpression of either of the redundant transcription factors CUC1 or CUC2 is sufficient to enhance the number of shoots initiated in culture while the respective mutants are deficient in this process (Daimon et al., 2003). Another recent study has shown that broad expression of a *CUC1* enhancer trap on auxin-rich CIM is progressively restricted within callus upon transfer to cytokinin-rich SIM (Cary et al., 2002). We show similar dynamics for the partially redundant gene *CUC2*. In addition, we show that *CUC2* downregulation within cells during induction on cytokinin-rich SIM is synchronized with upregulation of *WUS* expression, leading to a partition of cell identity and behavior within callus (i.e. progenitor/not progenitor). We therefore propose that the dynamic partitioning of *CUC2* and *WUS* expression may underlie the gradual localization and promotion of shoot meristem cell fate within callus tissue.

It was recently reported that *WUS* overexpression downregulates expression of *ARR* genes which negatively regulate cytokinin signaling (Leibfried et al., 2005). On the other hand, *CUC2* has been shown to be downregulated in mutants defective in auxin transport (*PIN1)* and auxin regulated gene activation (*MONOPTEROS)* (Aida et al., 2002; Leibfried et al., 2005). Indeed, we observed that a *CUC2* transcriptional reporter is upregulated on auxin-rich CIM medium and downregulated on cytokinin-rich SIM medium. Furthermore, expression of *CUC2* is maintained in shoot promeristems which express PIN1-GFP, polarized such that it is predicted to transport auxin into the shoot promeristem from surrounding cells. In contrast, *WUS* is induced only after culture on cytokinin-rich SIM medium and the *WUS* reporter forms gradients of expression relative to the *CUC2* reporter in non-overlapping domains. We show that shoot meristems initiate in areas of low auxin and high cytokinin response. Our data is therefore consistent with a model in which gradients of auxin and cytokinin specify cell identities within callus through induction of gene regulators.

## *Wuschel and WOX genes in diverse regeneration processes*

Our observations of *WUS* reporter expression in callus is consistent with previous studies which have described ectopic induction of *WUS* during cell respecification after cell ablations in the shoot meristem (Reinhardt et al., 2003a). Furthermore, the *WUSCHEL related homeobox 5* gene (WOX5), normally active in the quiescent center (QC), is ectopically induced in surrounding cells after QC ablation in the root meristem (Haecker et al., 2004; Xu et al., 2006). In addition, mosaic over-expression of *WUS* has been shown to induce shoot tissues directly from root explants (Gallois et al., 2004). Thus it appears that broad induction of *WUS* and related *WOX* genes may be a general phenomenon associated with regeneration of specific tissues in plants.

## *Necessity of WUS and PIN1 function for proper shoot formation*

The strong *wus-1* mutant regenerated only 5% of the shoots observed in wildtype samples and *WUS* expression was required for initiation of wildtype numbers of shoot promeristems, marked by coexpression of the *PIN1* and *STM* markers. These data support a model in which early *WUS* expression within callus in required to promote shoot meristem progenitor cell identity and late *WUS* expression is required for further shoot development. However, once shoot promeristems are initiated, they are largely autonomous in their development and express *PIN1* and *STM* in a pattern that is initially similar to wildtype. Other factors may compensate for loss of *WUS* function to initiate shoot promeristem development, such as members of the *WOX* gene family or *ESR1*, which confers cytokinin-independent shoot regeneration (Banno et al., 2001). The *pin1-4* mutant was also deficient in shoot regeneration, though not as severe as *wus-1* mutant tissue. The *pin1-4* deficiency was similar to previously reported data for *stm-1* mutant tissue (Barton and Poethig, 1993). *PIN1* activity may be more dispensable for shoot induction than *WUS*, due to greater redundancy including other PIN proteins (Vieten et al., 2005), consistent with higher levels of NPA blocking shoot regeneration (Christianson and Warnick, 1984; Murashige, 1965) and redundancy of *PIN* family members during embryogenesis (Friml et al., 2003).

## *Classical tissue culture methods for studying developmental patterning*

Over a century ago, Haberlandt noted the possible utility of tissue and cell culture for understanding development. He pointed out that cell culture was particularly well suited to determine the potential of individual cells as well as their reciprocal influences on each other (Haberlandt, 1902). Our study represents an early step towards realizing this potential. In vitro culture experiments support the idea that cell identity in plants is largely governed by positional cues mediated by specific hormones (Steward et al., 1964). We propose a model in which partition of cell identity within callus on SIM is mediated through non-homogeneous distributions of auxin and cytokinin, which are initially broadly distributed and therefore induce broad *CUC2* and *WUS* expression, respectively. The expression of these genes may further feed back on hormone

synthesis, transport or perception to enhance gradients of hormone signaling, which then alters *CUC2* and *WUS* expression. This feedback could lead to self-organizing patterns observed during de novo shoot meristem initiation. If this is the case, the primary difference between shoot meristem initiation *in planta* and shoot meristem induction in culture is the initial distribution of auxin and cytokinin. Auxin and cytokinin distribution is tightly controlled at all stages during development *in planta*, whereas this distribution must be gradually reorganized from disrupted initial conditions during shoot induction in culture. In vivo imaging of this dynamic process during gene and hormone perturbations should test the validity of this model.

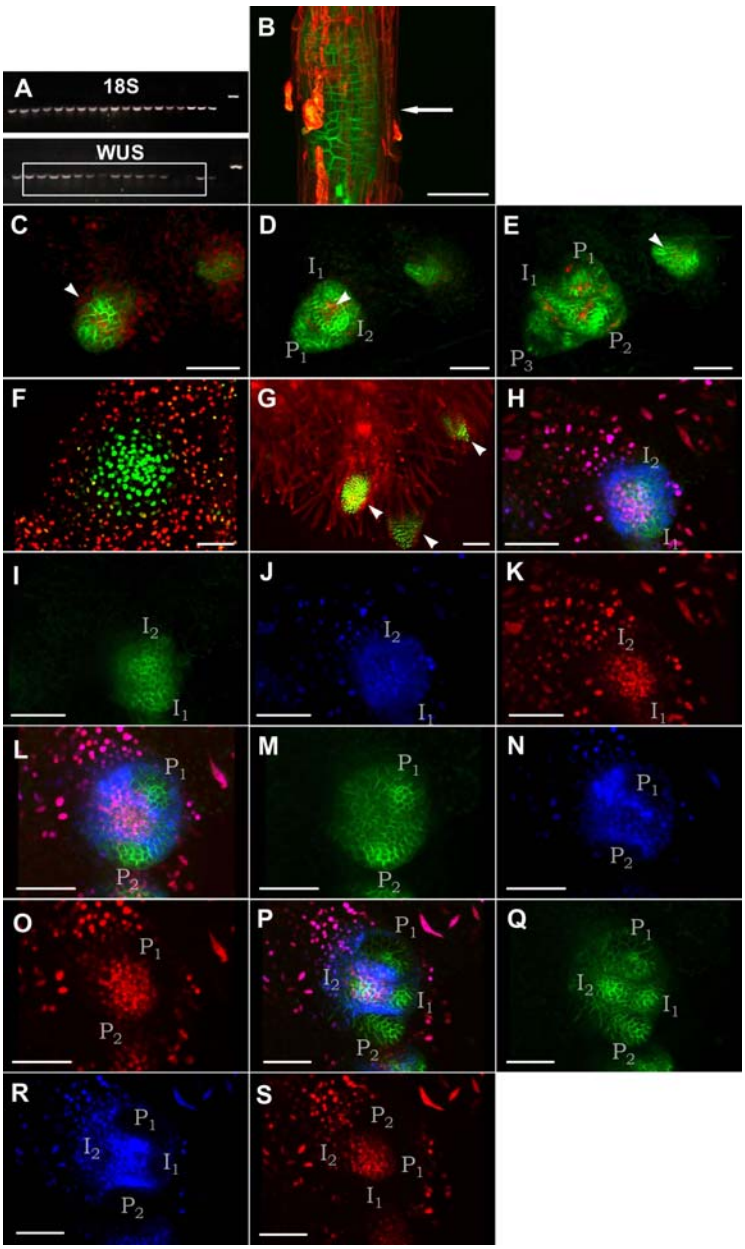


**Figure 2.11 Supplemental data figure.** (A) RT-PCR for 18S rRNA or *WUS* transcript from *pCLV3::GFP-ER*; *pWUS::DsDed-N7* bearing plants. Two week old callus samples induced for 9 days on SIM medium were imaged for *WUS* reporter signal and against *CLV3* reporter signal (selecting against mature meristems). *WUS* transcript was observed in 14 out of 15 samples in which the *WUS* reporter was observed (boxed lanes). (B) PIN1-GFP signal (green) was upregulated after incubation on CIM (four days) in the vicinity of callus formation (arrow). Propidium iodide (red). (C) *pCUC2::CUC2-VENUS* signal (red) was observed in meristem progenitor cells (arrowhead), colabeled by *pPIN1::PIN1-GFP* expression (green). (D) After 24 hours of observation, *pCUC2::CUC2-VENUS* signal (red) was upregulated in the shoot progenitors (arrowhead). *pPIN1::PIN1-*

*GFP* expression was upregulated in early primordia. (E) After 48 hours, *pCUC2::CUC2-VENUS* was expressed in the meristem/primordia boundaries. Another cluster of shoot progenitors was initiated nearby (arrowhead). (F) Cells marked by the *CUC2* reporter (green) proliferated to form mounds of progenitor cells which are encompassed by cells expressing the *WUS* reporter (red) which did not divide rapidly. (G) Root meristems (arrowheads), marked by strong *pARR5::GFP-ER* reporter (green), formed in regions of low *ARR5* reporter signal and were stained by propidium iodide (red). (H-S) Same as in Fig. 5 J-L but with separated channels for *pPIN1::PIN1-GFP* (green), *pSTM::STM-VENUS* (blue), and *pWUS::DsRed-N7* (red). Scale bars: 50µm (B-F, H-S) or 100µm (G). Primordia ($P_n$) and incipient primordia ($I_n$) are labeled.

**Author Contributions** S.P.G. designed experiments, collected data, and performed analysis; V.G.R. provided the *pWUS::DsRed-N7*, *p35S::29.1-mYFP, pWUS::mGFP5-ER* and pCLV3::mGFP-ER constructs; C.K.O., M.G.H., and P.D. provided the *pPIN1::PIN1-GFP, pSTM::STM-YFP, pREV::REV-YFP, pCUC2::3xVenus-N7*, *pDR5rev::3XVENUS-N7*, *pFIL::DsRED-N7, pPIN1::PIN1-CFP* and *pRIBO::2xCFP* plant lines. E.M.M. was involved in study design and management. S.P.G. and E.M.M. contributed to writing of the article.

## 2.4 Material and Methods

### *2.4.1 Plant materials*

All plants used in this study are in the Landsberg *erecta* (L*er*) ecotype except when stated otherwise. Plants and tissue cultures were grown at 22 °C under continuous light. Transgenic plants were produced using the *Agrobacterium*-mediated floral dip method (Clough and Bent, 1998). The strong *wus-1* mutant allele and the strong *pin1-4* allele have been described previously (Bennett et al., 1995; Mayer et al., 1998).

### *2.4.2 Construction of GFP reporters*

The translational protein fusion constructs including the *pPIN1::PIN1-GFP*, *pSTM::STM-VENUS*, *pREV::REV-VENUS*, and *pCUC2::CUC2-VENUS* constructs have been described previously (Heisler et al., 2005). The upstream regulatory sequence reporters including the *pDR5rev::3XVENUS-N7*, *pCUC2::3XVENUS-N7*, and the *pFIL::DsRED-N7* markers were

described previously (Heisler et al., 2005; Sieber et al., 2007). The transcriptional *pCLV3::GFP-ER* reporter was described previously in plants bearing a construct consisting of a 35S promoter driving 29.1 plasma membrane-localized yellow fluorescent protein (YFP) (Reddy and Meyerowitz, 2005). The *pARR5::GFP* reporter in WS ecotype has been described previously (Yanai et al., 2005) and was generously provided by Joseph Kieber (Department of Biology, University of North Carolina).

The previously published *pWUS::mGFP5-ER* construct (Jonsson et al., 2005) contains 3Kb upstream and 1.5Kb of downstream WUS genomic regulatory sequences separated by the *mGFP-ER* coding sequence in the T-DNA vector *pPZP222* conferring gentamycin resistance in plants (Hajdukiewicz et al., 1994). The *pWUS::DsDed-N7* construct, also in *pPZP222,* is composed of 4.4Kb upstream and 1.5Kb of downstream WUS genomic regulatory sequences separated by the DsRed coding region fused to the N7 nuclear localization sequence. The *pWUS::DsDed-N7* construct was transformed into L*er* harboring the *pCLV3::GFP-ER* reporter. The *pWUS::DsDed-N7* reporter line gave a pattern of expression confined to the rib zone of shoot meristems and floral meristems. A putative additive signal or strong autofluorescence was detected in the older leaves of the *pWUS::DsDed-N7* transformants, which was not found in *pWUS::mGFP5-ER* transformants. Spatial expression of the *pWUS::DsRed-N7* marker was verified by semi-quantitative RT-PCR to strictly correspond to areas of callus samples with *WUS* transcript (supplemental, S1A), in contrast to random samples of callus.

The *pRIBO::2XCFP-N7* construct in the T-DNA vector *pPZP222* is composed of 2.6 kb of upstream regulatory sequence from the 60S ribosomal protein L2 gene (At2g18020) fused to 2 tandem copies of eCFP (Clontech) followed by the N7 nuclear localization sequence (Cutler et al., 2000).

The *pML1::GFP-ER* construct in the T-DNA vector *pPZP222* is composed of 3.4 kb of upstream regulatory sequence from the *ML1* gene containing a fragment demonstrated to drive L1-specific expression, fused to *mGFP-ER* (Sessions et al., 1999).

The *pPIN1::PIN1-CFP* construct was created by substituting the *CFP* coding sequence for the *GFP* coding sequence in the published *pPIN1::PIN1-GFP* construct. Plants bearing multiple transgenes and the mutant alleles were combined by genetic crossing.

### *2.4.3 Regeneration conditions*

Root explants were harvested from 2 week old seedlings grown in sterile culture on Murashige and Skoog basal salt mixture (MS) plates. Explants were cultured on callus-inducing medium (CIM) consisting of modified Gamborg's B-5 medium (Sigma) containing 20g/L glucose, 0.5 g/L MES (Sigma) and supplemented with 1X Gamborg's vitamin solution (Sigma), 50 µg/mL of 2,4-D (Sigma) and 5 µg/mL of Kinetin (Sigma). Samples were incubated on CIM tissue culture plates for 2 weeks. Callus samples were cut into 2 centimeter length sections which were cultured on shoot-inducing medium (SIM) plates, consisting of MS medium containing 10g/L sucrose, 0.5 g/L MES and supplemented with 1X Gamborg's vitamin solution, 2µg/mL Zeatin (BioWorld, Dublin, OH), 1 µg/mL d-biotin (Sigma), and 0.4 µg/mL indole-3-butyric acid (IBA) (Sigma).

For quantifying shoot meristem induction, samples were cultured in tall tissue culture plates (USA Scientific) for a further two weeks, at which point the number of shoots per 2 centimeter callus explant was recorded. Shoots were defined as described previously (Daimon et al., 2003). Each experiment contained independent wild type controls using the same media batch and growth conditions.

### *2.4.4 Exogenous application of IAA*

Indole-3-acetic acid (IAA) lanolin paste from Carolina Biological Supply Company at a concentration of 500 ppm labeled with 1 µg/mL of propidium iodide was applied directly to callus in the vicinity of developing shoot meristems.

### *2.4.5 Imaging conditions*

Callus and regenerating shoots were imaged directly on respective media. For each marker line, at least 25 samples were imaged to confirm that observed patterns were representative of respective markers. Propidium iodide for staining cell outlines of root tissues was applied to samples at a concentration of 10 µg/ml 10 minutes prior to imaging. The lipophilic dye FM4-64 (Molecular Probes) was used at a concentration of 10 µg/ml to demarcate cell membranes and specifically labeled regenerating shoot tissues initiating from root-derived callus.

All imaging was done using a Zeiss 510 Meta laser scanning confocal microscope with either a 10x air objective, 20x air objective, or a 40x 0.8 NA water dipping lens using the multi-tracking mode. Specific sets of filters used for the respective markers were similar to those already described (Heisler et al., 2005; Reddy and Meyerowitz, 2005). Projections of confocal data were exported using Zeiss LSM software. Alternatively, volume renderings were made using Amira (Mercury Computer Systems).

## *2.5 Acknowledgements*

We thank Joe Keiber for the *ARR5::GFP* seeds. We thank Kaoru Sugimoto for assistance with the supplemental RT-PCR data, Annick Dubois and Arnavaz Garda for technical advice, and Elizabeth Haswell for critical comments on the manuscript. This work was funded by National Science Foundation grant IOS-0211670 to E.M.M.

Chapter 3

# Multiple feedback loops control stem cell number within the *Arabidopsis* SAM

Sean P. Gordon, Vijay S. Chickarmane, Carolyn Ohno, and Elliot M. Meyerowitz

A chapter submitted to *Science* (2009)

Pluripotent stem cells, residing in a specialized niche termed the shoot apical meristem (SAM), are the source of the above-ground tissues of flowering plants (Sablowski, 2007)[,](Fletcher and Meyerowitz, 2000). Stem cell identity in the SAM is genetically regulated by the *CLAVATA/WUSCHEL* circuit (Clark, 2001; Tucker and Laux, 2007). The plant hormone cytokinin also regulates stem cell number through regulating gene expression (Lindsay et al., 2006; Muller and Sheen, 2007). However, the mechanism by which cytokinin-regulated gene expression controls stem cell number and activity is unclear. Previous studies suggested that *WUSCHEL* regulates SAM function through controlling cytokinin signaling (Leibfried et al., 2005). Here we show that cytokinin signaling controls *WUSCHEL* expression through both *CLAVATA*-dependent and independent pathways. We provide evidence that a gradient of cytokinin signaling decreasing from the center of the SAM acts as spatial reference to inform cells of their position within the stem cell niche. Based on these data we develop a computational model in which interactions between components within the network predict their relative patterning, which we confirm experimentally. This study reveals that cytokinin signaling acts as a spatial cue which triggers domain-specific gene expression as cells pass through different zones of the SAM. This result also explains a critical aspect of *de*

*novo* plant regeneration in tissue culture, that is, how increasing cytokinin concentration leads to the first steps in reestablishing the shoot stem cell niche in vitro.

## 3.1 Introduction

Plants ranging from the small weed *Arabidopsis* to the Giant Sequoia tree (arguably ranking as the world's largest individual organism) maintain growth of stems, leaves, flowers, and branches through the action of stem cells. A central unanswered question in stem cell biology, both in plants and in animals, is how the spatial organization of stem cell niches are maintained as cells move through them, differentiating along the way.

Stem cell identity in the Arabidopsis SAM is genetically regulated by feedback between the *CLAVATA (CLV)* and *WUSCHEL (WUS)* genes (Clark, 2001; Tucker and Laux, 2007). *WUS* is expressed in RM cells and promotes stem cell identity in overlying CZ cells. Previous studies suggested that *WUSCHEL* regulates SAM function through controlling activation of a signal transduction pathway regulated by the plant hormone cytokinin (Leibfried et al., 2005). However, here we show that cytokinin signaling itself regulates *WUSCHEL* expression. This leads to multiple positive feedback loops which ensure that the *WUSCHEL* expression pattern follows from the distribution of cytokinin signaling in the SAM. We demonstrate the existence of a gradient of cytokinin perception and signaling decreasing from the center of the SAM which acts as spatial reference to trigger RM cells to express WUSCHEL. Application of exogenous cytokinin extends the cytokinin signaling gradient within the SAM and leads to respecification of surrounding cells to express *WUSCHEL*. Based on these data we develop a computational model in which interactions between components within the network predict their relative patterning, which we confirm experimentally. This study reveals that cytokinin signaling

acts as a spatial cue to triggers domain-specific gene expression as cells pass through different zones of the SAM and thus maintaining meristem function.

The Arabidopsis SAM is composed of three functionally distinct zones. The central zone (CZ) at the tip of the SAM harbors pluripotent stem cells which are necessary for the indeterminate growth and development of the plant. As the plant grows, CZ cells become either multipotent peripheral zone (PZ) cells on the sides of the meristem, capable of differentiating to leaf and flower primordia, or multipotent rib meristem (RM) cells beneath, which can differentiate to the cell types of the stem (Clark, 2001). Positions of zones within the meristem are maintained even as individual cells are displaced from the CZ through the PZ and RM into differentiating tissues. Molecular mechanisms by which meristematic zones are maintained as cells comprising these domains change remains a fundamental question in plant biology (Haecker and Laux, 2001; Sablowski, 2007). One mechanism involves the transmembrane receptor kinase CLAVATA1 (CLV1), expressed in cells of the rib meristem (Clark et al., 1997). Its ligand, the extracellular peptide product of the *CLAVATA3* (*CLV3*) gene, is produced in the CZ (Fletcher et al., 1999), and when it signals the RM cells, they reduce the activity of the *WUSCHEL* (*WUS*) gene, which codes for a homeodomain transcription factor also expressed in the RM (Brand et al., 2000; Mayer et al., 1998). WUS activity is nonautonomously necessary for the maintenance of the CZ cells as pluripotent stem cells, and therefore for persistence of the SAM (Schoof et al., 2000). Loss of CLV3 activity causes enlargement of the CZ by conversion of PZ cells on the PZ-CZ border to CZ cells within hours, followed by enlargement of the SAM through increased cell division over days (Reddy and Meyerowitz, 2005).

Multiple lines of evidence show that the plant hormone cytokinin is involved in the *CLV*/*WUS* circuit, as well as SAM formation, maintenance and growth (Sablowski, 2007). Cytokinins stimulate the formation of new shoot apical meristems in culture(Skoog and Miller, 1957). Cytokinin application rescues the SHOOTMERISTEMLESS (STM) mutant, which lacks the ability to maintain the SAM (Long et al., 1996), and *STM* induces

cytokinin biosynthetic genes (Yanai et al., 2005). Cytokinins act via receptors of the histidine kinase class (AHK2, 3 and 4), which when activated transfer phosphoryl groups to histidine phosphotransfer proteins (HPTs) and thence to two classes of *Arabidopsis* response regulators (ARRs). The Type-B ARRs activate transcription of cytokinin-induced target genes; Type-A ARRs negatively regulate cytokinin signaling (Muller and Sheen, 2007; To et al., 2004; To and Kieber, 2008). WUS has recently been shown to repress the genes for Type-A ARRs, thus likely increasing cytokinin signaling(Leibfried et al., 2005). Furthermore, overexpression of a Type-A ARR reduces *WUS* RNA levels, and can mimic the *wus* mutant phenotype which results in SAM termination (Laux et al., 1996; Leibfried et al., 2005). Cytokinin treatment induces *CLV* loss of function phenotypes and causes increased *WUS* and decreased *CLV1* expression (Clark et al., 1993; Lindsay et al., 2006).

## 3.2 Results

### *3.2.1 CLV-independent regulation of WUS by cytokinin*

These data led us to build the network shown in Figure 3.1a, in which *WUS* is regulated by cytokinin through suppression of the *CLV* pathway (Lindsay et al., 2006). We show through experiment that cytokinin is in addition a *CLV*-independent activator of *WUS*, regulating both levels and the spatial profile of *WUS* transcription. Computational modeling and experimentation suggests that cytokinin signaling acts as a spatial cue which triggers domain-specific gene expression as cells pass through different zones of the SAM.

To test our starting model (Figure 3.1a), we quantified the effect of cytokinin treatment (N6-benzylaminopurine; BAP) on *CLV1* and *ARR5* transcription, as measured by quantitative reverse transcriptase polymerase chain reaction (qRT-PCR). As previously reported (Lindsay et al., 2006; To and Kieber, 2008), 24hrs of cytokinin treatment (1mM) reduced *CLV1* RNA levels and increased RNA for the Type-A ARR, *ARR5* (Figure 3.1b,c).

To test whether repression of the *CLV* pathway is the only mechanism of *WUS* induction by cytokinin (Lindsay et al., 2006), we performed cytokinin treatments in a *clv1-11* loss-of-function mutant. At 4 and 24 hours after cytokinin treatment, *WUS* RNA increased in both wild-type and mutant lines compared to mock-treated samples (Figure 3.1d,e); by 24 hours *WUS* transcript was increased ~ 40-fold in both genotypes. Pretreatment of the plants with the protein synthesis inhibitor cycloheximide did not prevent this induction (Figure 3.1f), suggesting a direct effect. Cytokinin treatment also induced *WUS* transcript accumulation in a *clv3-2* loss-of-function mutant background, suggesting that induction in the *clv1-11* mutant is not due to redundant function of related CLV3-dependent kinases active in the SAM, such as BAM1, 2 and 3 (DeYoung et al., 2006), CLV2 (Kayes and Clark, 1998) or CORYNE (Muller et al., 2008). We observed greater phenotypic enhancement of floral organ number (an indicator of increased floral meristem size) by cytokinin in *clv1* and *clv3* mutants compared with wild type, suggesting a synergistic effect between cytokinin and *clv* loss of function (Figure 3.1g, two-way ANOVA, $P < 0.0001$). In contrast to wild type, BAP treatment of *clv* mutants resulted in massive enlargement of the SAM and floral meristems (Figure 3.3). Similar fold induction of *WUS* transcript in wild type and *clv* mutants after continuous cytokinin treatment reveals the existence of CLV-independent mechanisms of cytokinin-induced *WUS* expression (Figure 3.1d-f). However, greater phenotypic enhancement in CLV loss of function background indicates that the CLV pathway limits the effect of transient perturbations in cytokinin signaling and therefore indicates that there are also CLV-dependent effects.

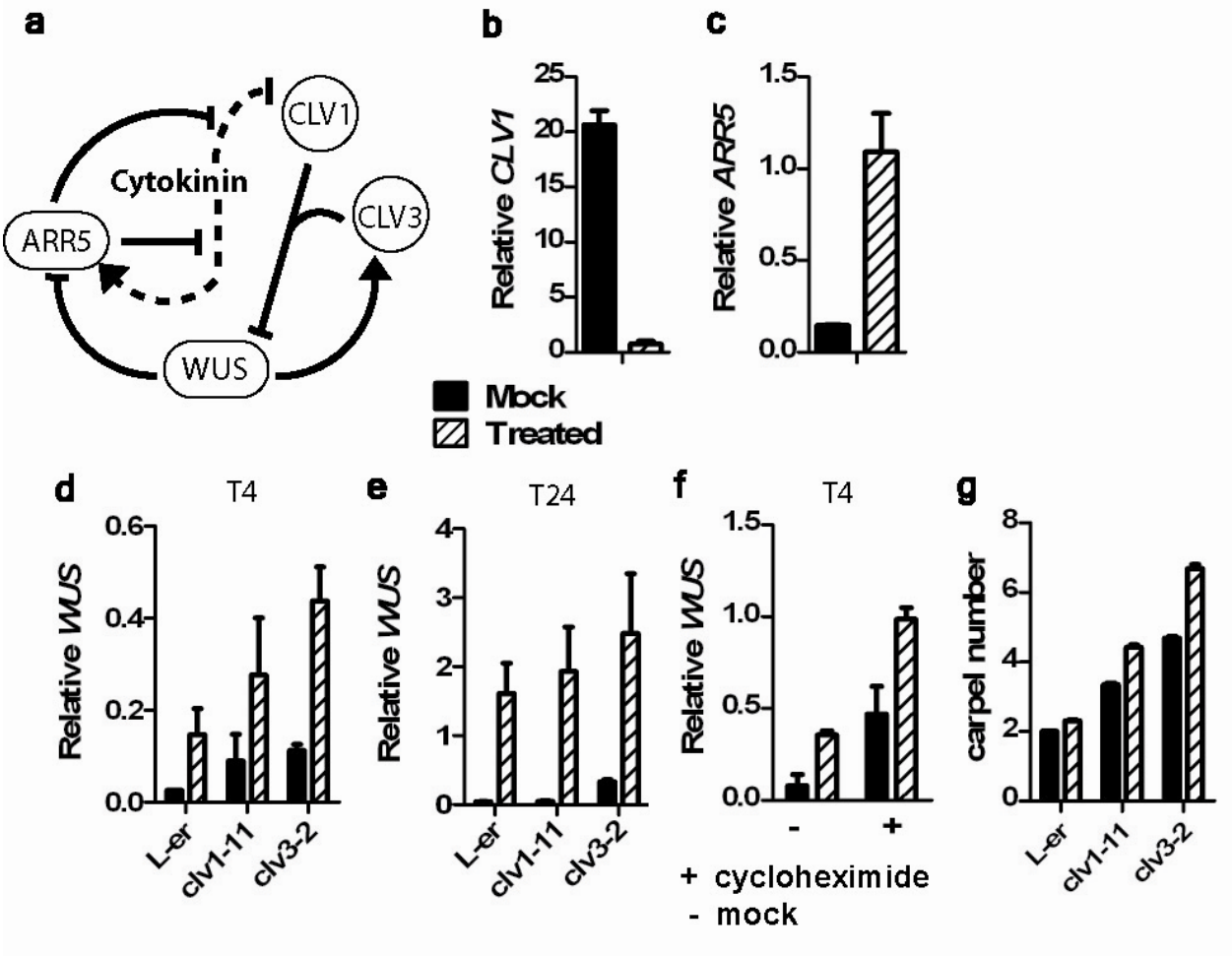


**Figure 3.1 CLV-independent regulation of *WUS* by cytokinin.**
**a**, known cytokinin signaling and CLV/WUS interactions. **b**,**c**, *CLV1* (**b**) or *ARR5* (**c**) transcript after 24hrs of mock treatment or cytokinin treatment (1mMBAP). **d**,**e**, relative *WUS* transcript in wild type, *clv1-11* and *clv3-2* seedlings after mock treatment or cytokinin treatment (1mMBAP) for (**d**) 4hrs, or (**e**) 24hrs. **f**, Cytokinin induction of *WUS* for 4hrs in absence (-) or presence (+) of 30min cycloheximide (10µM) pretreatment. **g**, Synergistic enhancement of carpel number in cytokinin treated (1mMBAP) *clv1* and *clv3-2* mutants compared to wild type (Two-way ANOVA, $P < 0.0001$). qRT-PCR error bars indicate S.E.M. from three biological replicates**.**

### *3.2.2 feedback influences patterning of gene expression*

After 24hrs, *CLV1* and *ARR5* transcript levels were altered at low cytokinin concentrations. However, increase in *WUS* transcript occurred only at high

concentration (Figure 3.2a). Finer dilutions showed a steep rise in *WUS* transcript and corresponding decrease in *ARR5* beginning at 400µM and peaking near 600µM (Figure 3.3). The *WUS* response curve implies that high cytokinin signaling and high *WUS* expression should overlap spatially within the SAM. Consistent with this hypothesis, a reporter for cytokinin signaling output, *pTCS::GFP* (Muller and Sheen, 2008) was expressed in a similar domain to *WUS* (Figure 3.2b-d). *pTCS::GFP* expression mirrored temporal dynamics of *WUS* reporter expression during floral meristem development and SAM regeneration in culture (Figure 3.5), consistent with a model where *WUS* is spatially regulated by cytokinin signaling during development (Gordon et al., 2007).

The similar spatial profiles of cytokinin signaling and *WUS* expression led us to investigate how patterning of components within our model network might be influenced by different mechanisms of interaction. Our results indicate that multiple feedbacks between cytokinin signaling, *WUS* and *CLV1* expression could explain the shape of the response curves shown in (Figure 3.2a). For example, *CLV*-independent regulation of *WUS* by cytokinin could be either Type-A ARR dependent Fig. 2e(1) or independent Fig. 2e(2). We used computational modeling (see *Discussion of Computational Modeling*) to plot predicted steady state values of *WUS* for these networks as a function of cytokinin signaling (Figure 3.2f). The difference in dynamics between networks 1 and 2, is that in 1, a higher threshold of cytokinin signaling is required for *WUS* expression due to suppression by Type-A ARR negative feedback. This suppression is relieved when high levels of signaling produce sufficient *WUS* to repress Type-A ARRs, leading to positive feedback of *WUS* on itself (Figure 3.2f). In contrast, there is a lower threshold for *WUS* induction in network 2 because WUS is activated independently of Type-A ARR negative regulation on signaling. Addition of the CLV pathway Fig. 2e(3) to networks 1 and 2 results in negative feedback of *WUS* on itself, which is relieved by the *CLV1* downregulation that results from cytokinin signaling. This increases the threshold of cytokinin signaling for *WUS* induction (Figure 3.2f). Of the plots in Figure 3.2f, networks 1 and 3 together most accurately resemble the

experimental response of *WUS* to cytokinin. In Figure 3.2g-l we display predicted spatial distributions of *WUS* and Type-A ARR for Type-A dependent *WUS* activation (network 1+3; Figure 2g-i) or Type-A independent activation (network 2+3; Figure 3.2j-l), assuming a central peak of cytokinin signaling input as seen experimentally in Figure 2b-d (see *Discussion of Computational Modeling*). Plots for these alternative models show that Type-A ARR-dependent *WUS* activation consistently predicts a narrow peak of *WUS* expression from which Type-A ARR is repressed (Figure 3.2h,i ) whereas Type-A independent activation leads to broader *WUS* expression which does not consistently correlate with Type-A ARR suppression (Figure 3.2k,l).

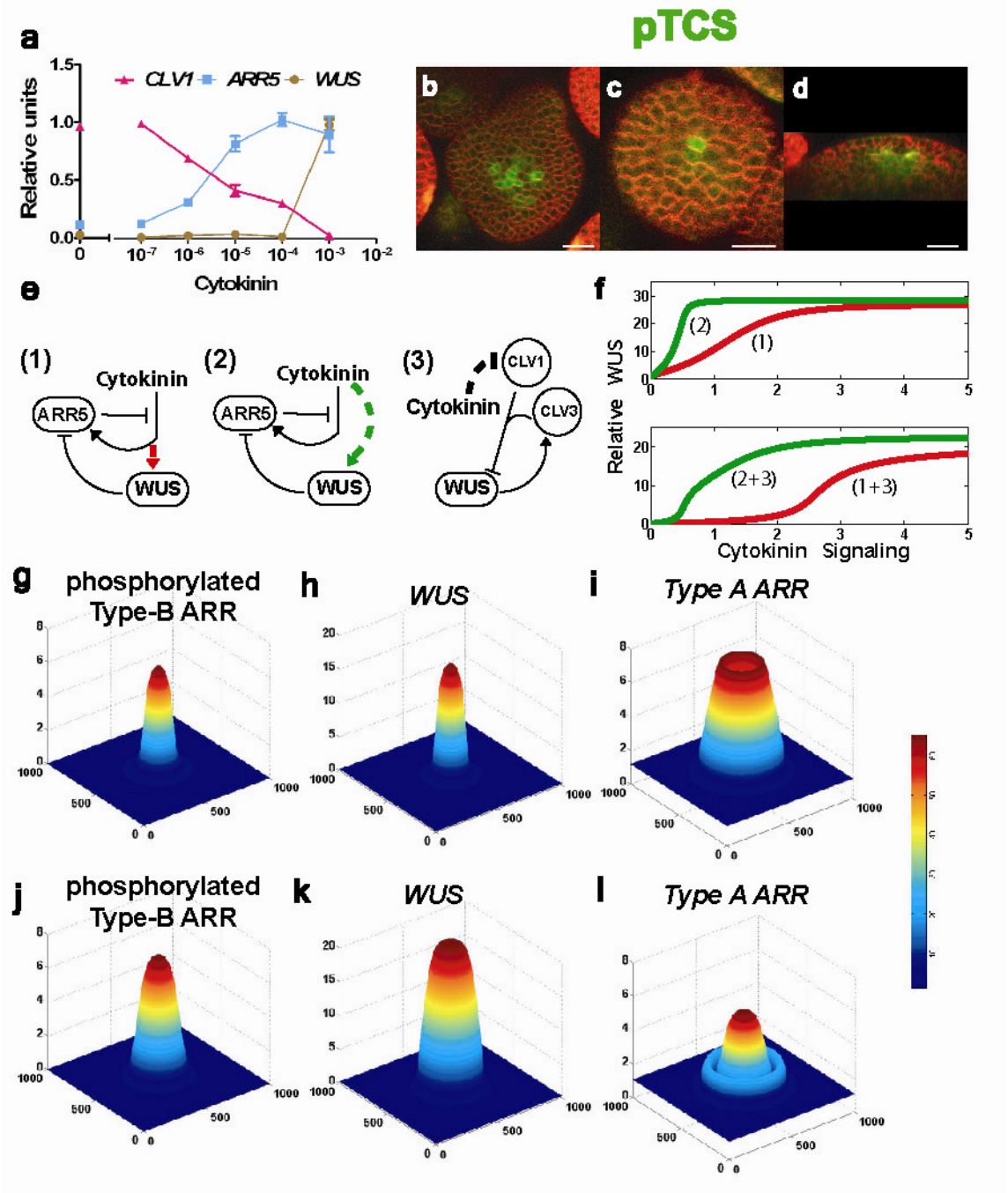


**Figure 3.2 feedback between cytokinin signaling and the *WUS/CLV* circuit influences patterning of gene expression.** **a**, Transcriptional regulation of *CLV1*, *ARR5,* and *WUS* at varying cytokinin concentrations. **b**-**d**, *pTCS::GFP* expression in the SAM (**b**), early flower bud (**c**) or cross section of SAM (**d**). **e**, (**1**) Cytokinin activates *WUS* through a Type-A ARR-regulated (red line) or (**2**) independent pathway (green line). (**3**) Negative regulation of *WUS* through the CLV pathway is relieved by cytokinin induced

suppression of *CLV1*. **f**, Predicted steady state *WUS* levels at varying levels of cytokinin signaling for (**1, red line**), (**2, green line**), (**1+3, red line**), or (**2+3, green line**). **g-i**, spatial distribution of phosphorylated B-type ARR (**g**), *WUS* (**h**), or *Type-A ARR* (**i**) for network (1+3). **j-l**, spatial distribution of phosphorylated B-type ARR (**j**), *WUS* (**k**), or *Type-A ARR* (**l**) for network (2+3). Error bars indicate S.E.M from two biological replicates**.**

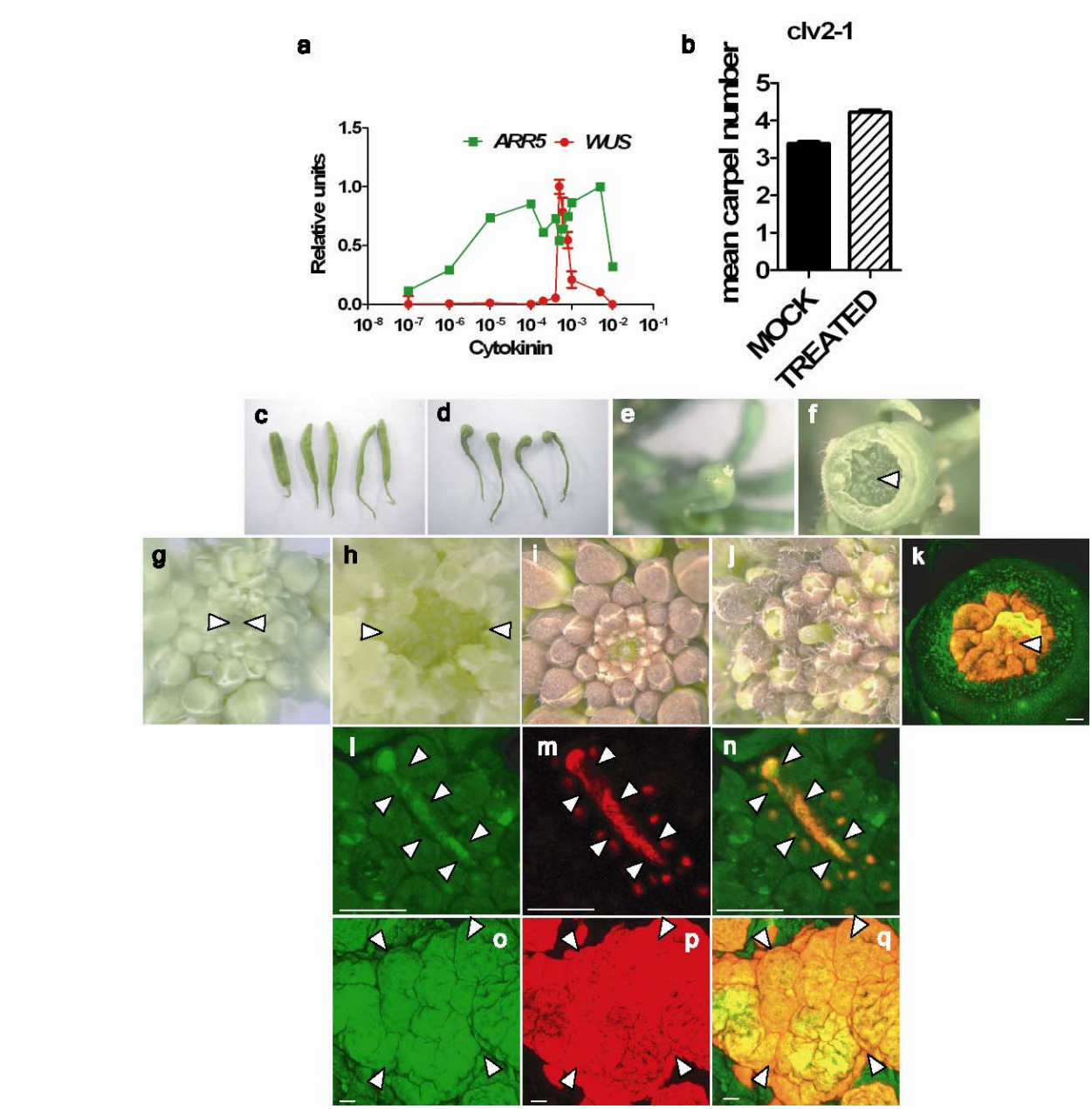


**Figure 3.3 Cytokinin-induced changes to meristem structure and gene expression.** **a**, Finer serial dilutions reveal a steep rise in *WUS* transcript starting

around 400µM and peaking near 600µM, overlapping with a dip of *ARR5* transcript. **b**, mean carpel numbers from either mock or cytokinin treated *clv2-1* flowers. Error bars are shown for all data as S.E.M. **c**,**d**, Phenotypes of mock (**c**) or treated (**d**) *clv1-11* carpels showing their phenotypic enhancement. **e**,**f**, *clv3-2* mock (**e**) or cytokinin treated (**f**) flowers. Treated flowers were observed with 14 carpels with a central mass of undifferentiated tissue (arrowhead) which was never observed in mock treated flowers. **g**,**h**, Mock (**g**) or cytokinin treated (**h**) *clv3-2* meristems showing massive enlargement of the *clv3-2* SAM (bounded by arrows) after cytokinin treatment. **i**,**j**, Mock (**i**) or treated (**j**) *clv1-11* meristems. Treated meristems were slightly wider (50 vs ~100 microns) and qualitatively taller than mock treated meristems. **i**, undifferentiated tissue within the center of the gynoecium (arrowheads, Fig. S1f) formed after repeated treatment of *clv3-2* flowers was marked by *WUS* (red) and *AHK4* (green) reporter expression. **j**-**l**, *AHK4* (green) and *WUS* (red) reporter expression in the untreated linear fasciated *clv3-2* SAM (arrows) and floral meristems or **m**-**o**, in the grossly enlarged cytokinin treated *clv3-2* SAM (arrows) and floral meristems. Scale bars represent 100µm.

### *3.2.3 Patterning of ARR5, WUS, and AHK4 expression*

In order to resolve which of the predictions is correct, we experimentally determined the relative spatial expression of *WUS* and Type-A ARR. We observed that a transcriptional reporter for the Type-A ARR, *ARR5,* was suppressed in the *WUS* domain but expressed strongly in adjacent cells (Figure 3.4a-c), consistent with Type-A dependent *WUS* activation.

Activation of *WUS* expression by cytokinin suggests that a distribution of cytokinin perception within the SAM might act as a positional cue for patterning WUS transcription. Higher cytokinin perception within the meristem center could be achieved through localized receptor expression. Indeed, fluorescent reporters for the cytokinin receptor *AHK4* (Mahonen et al., 2006), and *WUS* transcription were expressed in overlapping domains within the SAM and were correlated in individual cells (Figure 3.4d-h). *AHK4* and *WUS* reporters were similarly regulated during floral meristem development, expanded similarly in the *clv3-2* mutant and were both altered in super-enlarged cytokinin-treated *clv3-2* SAMs (Figure 3.4i-l, Figure 3.3). *AHK4* and *WUS* reporters also overlapped during SAM regeneration in culture. *AHK4* reporter was

induced in cultured cells during pretreatment on auxin-rich medium known to promote regeneration (Figure 3.5). Transfer to cytokinin-rich medium results in *WUS* induction (Gordon et al., 2007) in cells marked by the *AHK4* reporter in developing SAMs (Figure 3.4).

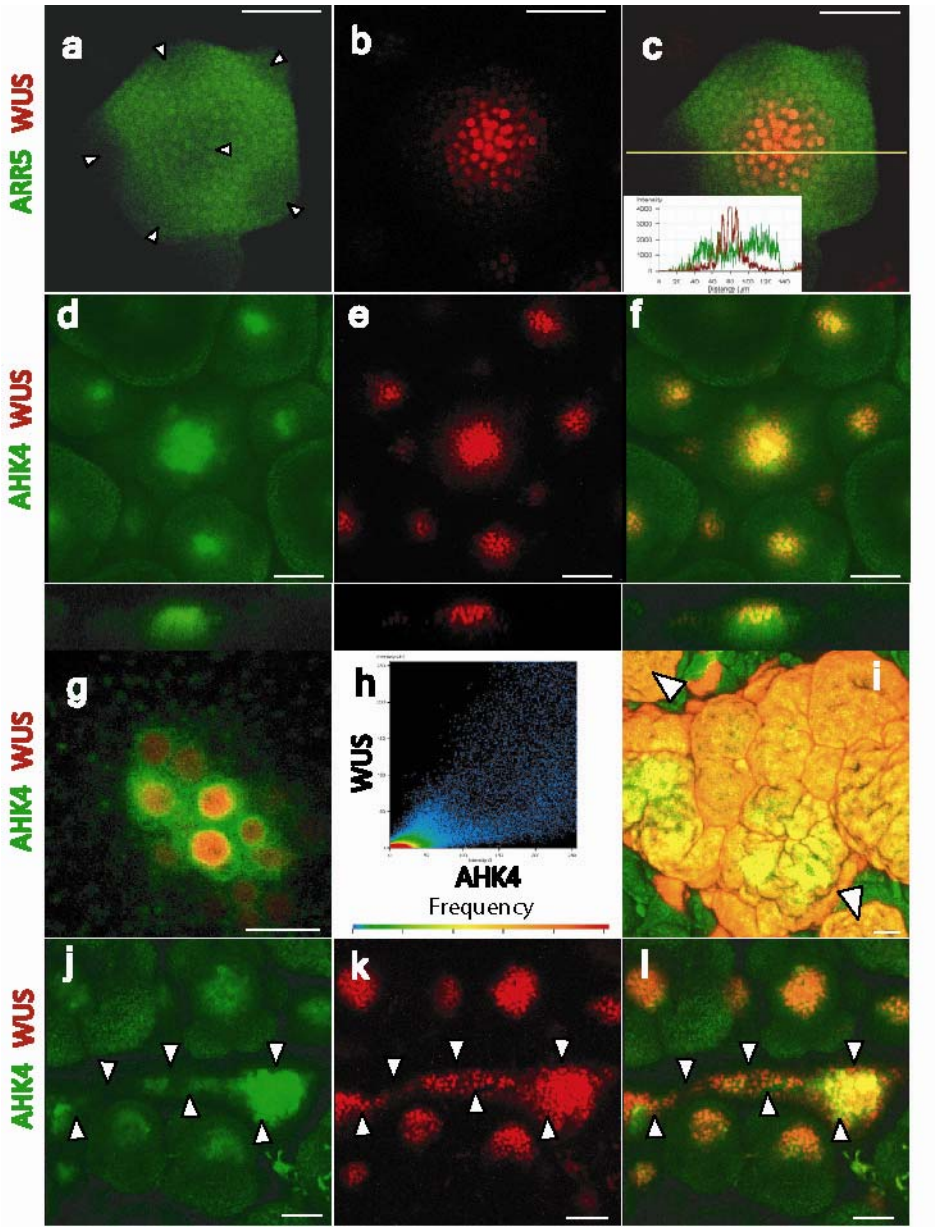


**Figure 3.4 *AHK4* and *WUS* expression correlate in individual cells where *ARR5* is suppressed.** **a**-**c**, *ARR5* (green) reporter down regulation within the *WUS* domain (red) and organ primordia (*AHP6* domain, Supplementary Fig. 3). **d**-**f**, Cytokinin

receptor (*AHK4*, green) and *WUS* reporter (red) overlap within the SAM (center) or floral meristems (peripheral). Cross sections displayed below. **g**, *AHK4* and *WUS* overlap in single cells (correlation coefficient R = 0.79). **h**, pixel intensity of *AHK4* (x-axis) and *WUS* (y-axis) reporters in wild type flowers. **i**, *WUS* (red) and *AHK4* (green) in cytokinin treated *clv3-2* SAM and floral meristems (arrows) compared to untreated *clv3-2* mutants (**j**-**l**). Error bars represent 20µm except for 10µm in (**g**) and 100µm in (**i**).

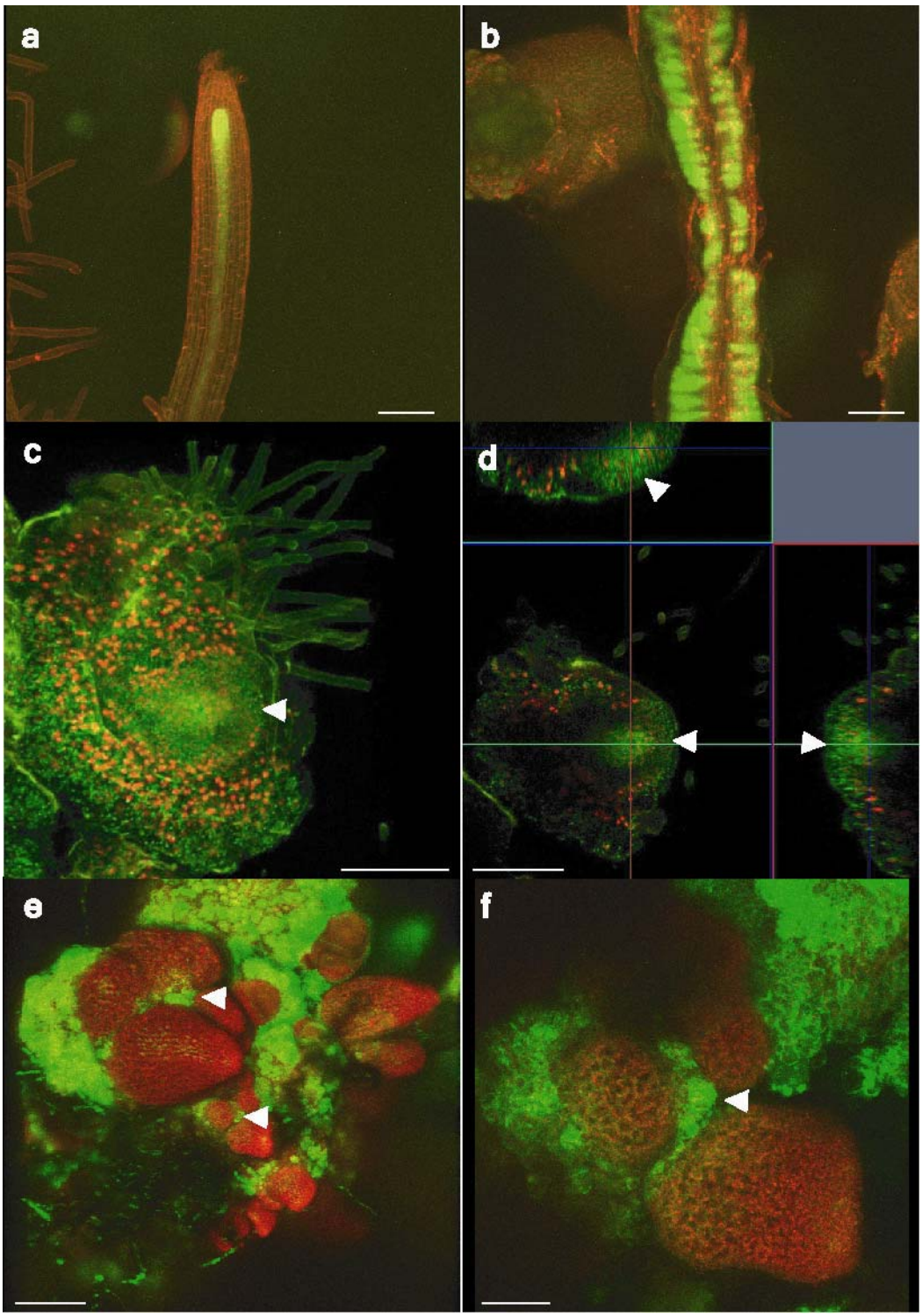


**Figure 3.5 *AHK4*, *WUS* and cytokinin signaling output during *de novo* regeneration.** **a**,**b**, *AHK4* reporter expression in the untreated root (**a**) and proliferating cells after culture on auxin-rich medium (**b**). Receptor expression is both stronger and broader in auxin treated samples. **c**,**d**, *AHK4* and *WUS* reporter overlap in

the developing rib zone of new shoot meristems forming from callus. **e**,**f**, *pTCS::GFP* report is also active in the developing RM of regenerating SAMs in culture and peripheral callus cells. Error bars represent 100µm in (**a**,**b**) 200 µm in (**e**) and 50µm in (**c**,**d,f**). Arrowheads mark regenerating SAMs.

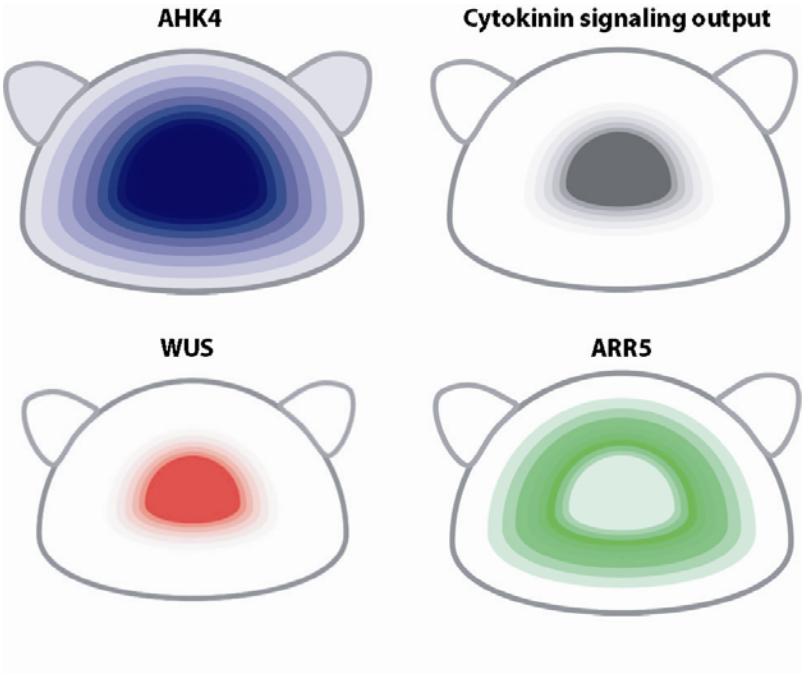


**Figure 3.6 Summary of experimentally determined gene expression patterns.** The patterns for *AHK4* expression (blue), cytokinin signaling output reporter (grey), *WUS* expression (red), and *ARR5* expression (green) are drawn.

### *3.2.4 Cytokinin signaling regulates cell fate within the SAM*

It thus appears that cytokinin receptor distribution initiates a gradient of cytokinin signaling which patterns *WUS* expression in multiple contexts. This suggests that treatment of plants with exogenous cytokinin could extend sufficient signaling to cells farther down the receptor gradient, causing *WUS* activation in an expanded domain. Indeed, live imaging before and after 24hrs of cytokinin treatment showed expansion of *WUS* reporter expression (Figure 3.7a-d, Supplementary Fig. 3) and led to increased *pTCS::GFP* and *pCLV3::GFP-ER* reporter expression within inflorescence and floral

meristems which was not observed in mock treated samples (Figure 3.7e-h). Within 12hrs of cytokinin treatment we observed respecification of cells that previously did not express *WUS,* indicating that *WUS* expansion was not solely due to increased cell division in the RM (Figure 3.7), and also showing that the RM, like the CZ (Reddy and Meyerowitz, 2005), can recruit surrounding cells. Cytokinin treatment was also sufficient to induce ectopic *WUS* expression (Figure 3.8), but only in tissues which express the cytokinin receptor *AHK4* (Mahonen et al., 2006).

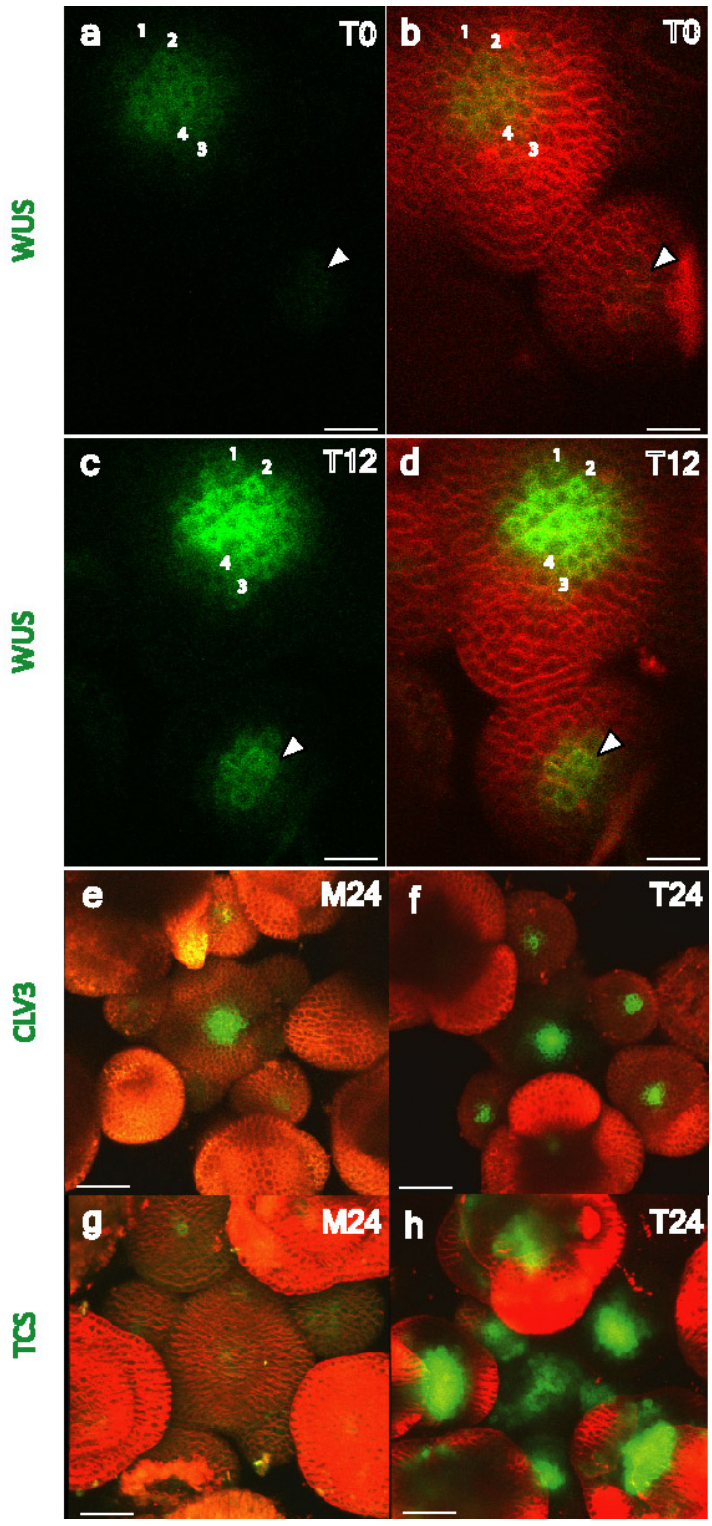


**Figure 3.7 Cytokinin signaling regulates *WUS* and *CLV3* expression.** **a-d,** live imaging of *WUS* reporter (green) before (**a**,**b,**) and after 24hrs of cytokinin treatment (1mMBAP) (**c**,**d**,). **e**, *CLV3* reporter (green) in plants after 24hrs of mock

treatment (n=5) or (**f**) cytokinin treatment (n=5). **g**, *pTCS::GFP* reporter (green) after 24hrs of mock treatment (n=5) as compared to **h,** 24hrs of cytokinin treatment (n=5). Membranes are marked with FM4-64 dye (**a**-**d** and **g,h**) or 29-1 membrane YFP marker (Reddy and Meyerowitz, 2005) (**e**,**f**). Scale bars represent 50µm. Numbering in **a**-**d** registers floral meristems in (**a**,**b**) to the same floral meristems in (**c**,**d**) after 24hrs.

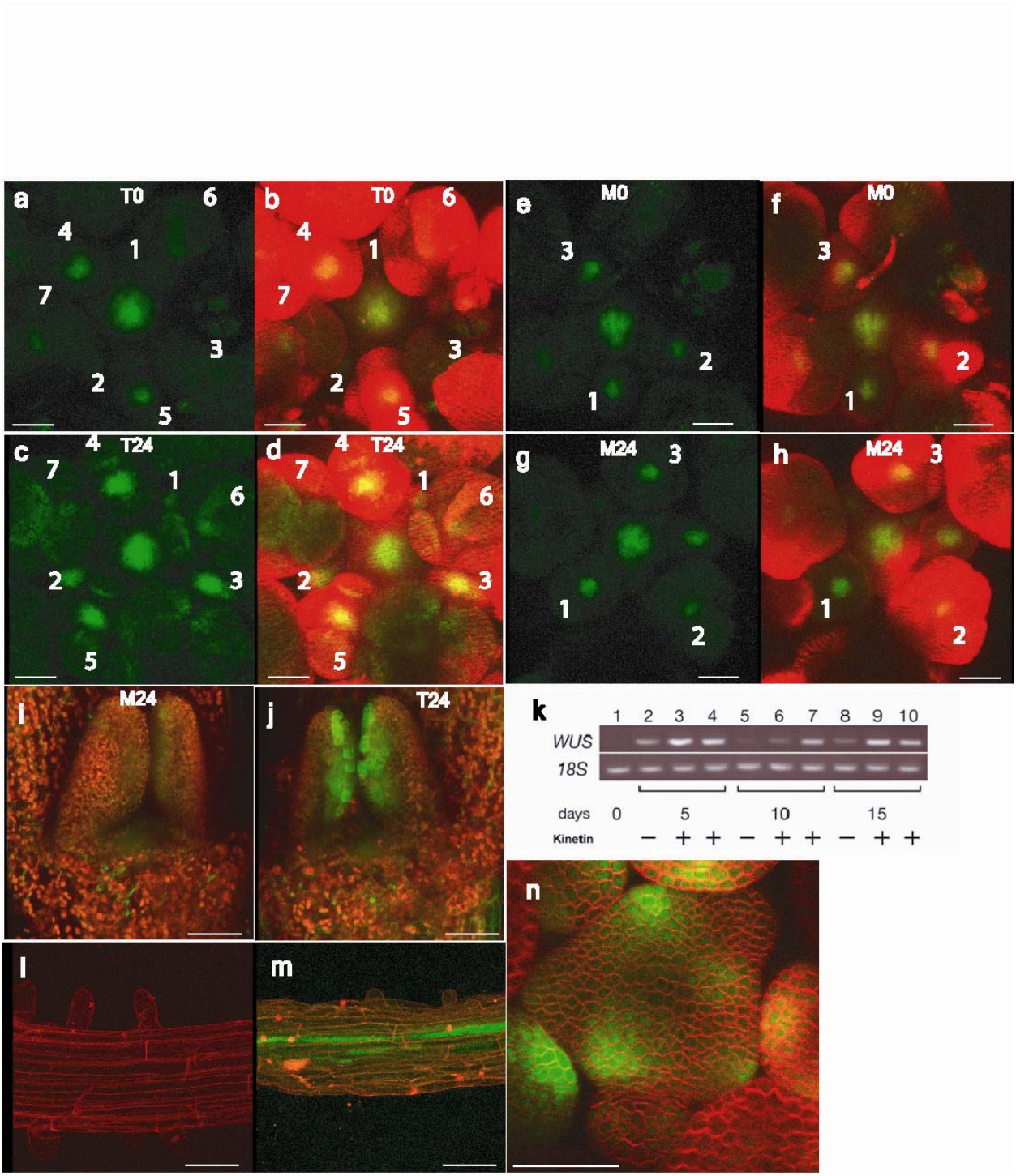


**Figure 3.8 Cytokinin is sufficient to respecify differentiated cells as multipotent rib meristem cells.** **a-d,** are representative results of live imaging experiments of *WUS* reporter (green) before (**a**,**b,**) (n=10) and after 24hrs of cytokinin treatment (**c**,**d**,) (n=10). **e-h,** are representative results of live imaging experiments of *WUS* reporter (green) before (**e**,**f,**) (n=10) and after 24hrs of mock

treatment (**g**,**h**,) (n=10). *WUS* expression is induced in the adaxial sides of cytokinin treated leaves (**j**) but not mock treated samples (**i**). **k**, Cytokinin treatment induces *WUS* expression in root explants. Semi-quantitative RT-PCR on root explants after 0, 5, 10, and 15 days of culture in the absence (**-**) or presence (**+**) of the cytokinin (50µg/L kinetin). *WUS* is not expressed in root plants at 0 days of culture (lane 1) but becomes expressed after prolonged culture on MS media (lane 2-10) and this expression is enhanced by the presence of cytokinin (lanes 3, 4, 6, 7, 9, 10). **l**,**m**, *WUS* reporter expression (green) in the vasculature of cytokinin treated root explants (**m**) but not untreated roots (**l**). **n**, AHP6 reporter, *pAHP6::AHP6-GFP* (green), a component known to repress cytokinin signaling(Mähönen et al., 2006a) is expressed in organ primordia where Type-A ARRs are down-regulated. Scale bars represent 50µm.

## 3.3 Discussion

Previous studies suggested that *WUSCHEL* regulates SAM function through controlling activation of a signal transduction pathway regulated by the plant hormone cytokinin (Leibfried et al., 2005). However, here we show that cytokinin signaling itself regulates *WUSCHEL* expression. This leads to multiple positive feedback loops which ensure that the *WUSCHEL* expression pattern follows from the distribution of cytokinin signaling in the SAM.

The mechanism by which spatial organization of stem cell niches are maintained as cells move through them, is a poorly understood but important field of study (Sablowski, 2007). We partly answer this question for the shoot stem cell niche of plants, by showing that response to the plant hormone cytokinin establishes a spatial domain in which cells take a rib meristem fate. Within the stem cell niche, the rib meristem is necessary for promoting adjacent cells to assume stem cell fate. Therefore, this result also explains a critical aspect of de novo plant regeneration in tissue culture. Increasing cytokinin concentration leads to the induction of *WUS* which reestablishes the shoot stem cell niche *in vitro*. The reestablished stem cell niche then promotes adjacent cells to assume stem cell fate leading to self-organization of a new plant. Thus *de novo* regeneration of plants in culture can be thought of as proceeding through first re-

establishing the shoot stem cell niche. Once established this niche promotes surrounding cells to assume stem cell fate and produce a new plant.

We propose that within the shoot meristem a standing gradient of cytokinin signaling decreasing from the rib meristem acts as spatial reference to inform cells of their position. This spatial reference allows cells to recognize their entry and departure from the RM domain, to regulate the level and spatial expression of *WUS*, an RM marker, and to control shoot stem cell number (Figure 3.8). During *in vitro* shoot induction, high cytokinin signaling triggers ectopic *WUS* expression which is sufficient for regeneration of shoot tissues (Gallois et al., 2002). The ability of cytokinin signaling to promote *WUS* expression is a common thread that links regeneration of shoot tissues and normal shoot development.

## *Discussion of Computational Modeling*

In order to guide our interpretation of experimental results we developed the first computational model describing cytokinin signaling dynamics. In addition, we interrogate the experimentally identified interactions between the cytokinin signaling pathway and the WUS/CLV circuit. Computational modeling was done based on thermodynamic models for transcription and translation for the network shown in Figure 3.9. Simulations were carried out using MATLAB software (The Mathworks) and the Systems Biology Workbench (SBW/BioSPICE) tools [10]: JDesigner, and Jarnac. The bifurcation diagrams which were used to generate steady state curves for various species were generated using Oscill8 [11].

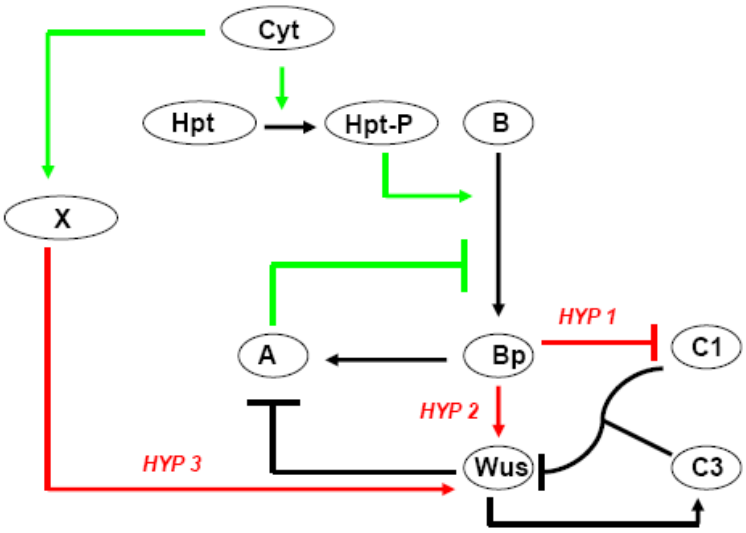


**Figure 3.9 Hypothetical regulatory networks by which cytokinin regulates WUS expression.** Cytokinin could activate WUS expression through Type-A ARR regulated suppression of CLV1 transcription through B-Type ARRs (HYP1). Alternatively, B-Type ARRs could directly lead to induction of *WUS* transcript, again in a Type-A ARR regulated manner (HYP2). Lastly, WUS induction could occur by an unknown pathway which is Type-A ARR independent (HYP3). All other links except those labeled (HYP) are shared between the three hypothetical models. Simulations comparing the three alternative models were run using the same parameters which are shown in section 3.4.6.

The above network was translated into a set of differential equations for the concentration of the various species (Figure 3.10).

$$
\begin{aligned}
\frac{d[AHPT_P]}{dt} &= \left(\frac{[Cyt][AHPT]}{K_{h1}+[AHPT]}\right) - \frac{v_{h1}[AHPT_P]}{K_{h2}+[AHPT_P]}, \\
\frac{d[B_P]}{dt} &= \left(\frac{[AHPT_P][B]}{K_1+[B]}\right)\left(\frac{1}{1+\alpha[A]}\right) - \frac{v_1[B_P]}{K_2+[B_P]}, \\
\frac{d[A]}{dt} &= \frac{a_0+a_1[B_P]}{1+a_0+a_1[B_P]+a_2[Wus]^n} - \gamma_1[A], \\
\frac{d[Wus]}{dt} &= \frac{b_0+b_1[B_P]+b_2[X_P]}{1+b_0+b_1[B_P]+b_2[X_P]+b_3[CLV]} - \gamma_4[Wus] \\
\frac{d[CLV1]}{dt} &= \frac{c_0}{1+c_0+c_1[B_P]} - k_1[CLV1][CLV3] + k_2[CLV] - \gamma_2[CLV1] \\
\frac{d[CLV3]}{dt} &= \frac{d_1[Wus]}{1+d_1[Wus]} - k_1[CLV1][CLV3] + k_2[CLV] - \gamma_3[CLV3] \\
\frac{d[CLV]}{dt} &= k_1[CLV1][CLV3] - k_2[CLV] \\
\frac{d[X_P]}{dt} &= \frac{[AHPT_P][X]}{K_{c1}+[X]} - \frac{v_{c2}[X_P]}{K_{c2}+[X_P]},
\end{aligned}
$$

**Figure 3.10 Differential equations used for modeling cytokinin signaling.**
Differential equations used for modeling the concentrations of the various species shown in the network diagram in Figure 3.9.

We started our modeling using a sub-system consisting of AHPT, Type-A ARR, and Type-B ARR using the differential equations shown in Figure 3.10. Cytokinin treatment first leads to a rise in activated (phosphorylated) Type-B ARR, which immediately increases transcription of Type-A ARR. The Type-A ARR, negatively feeds back on signaling, which in turn, restricts Type-B ARR activation. Hence as the feedback strength is increased (increasing $\alpha$), we see from the plots that both Type-A ARR as well as Type-B ARR levels rise and fall over shorter time scales. Type-A negative feedback therefore leads to a quick response of the system to perturbations.

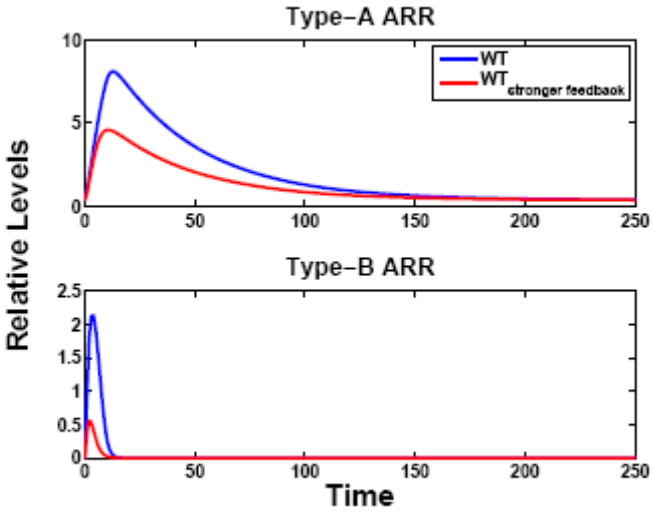


**Figure 3.11 Simulation of Type-B ARR phosphorylation and Type-A ARR transcription dynamics as a function of time (mins).** We began by analyzing the sub-system which consists of AHPT, Type-A ARR, and Type-B ARR using the above differential equations. We excluded all other interactions, since we were first interested in the dynamics of core negative feedback of Type-A ARR on signaling. In Figure 3.11 we plot Type-A ARR and Type-B ARR levels, for a perturbation in cytokinin concentration (cytokinin concentration which starts at a high value (10), and degrades in time). This is plotted for the wild type, and for higher negative feedback, *i.e* $\alpha$ = 1*,* 5, respectively.

Figure 3.12 shows simulated dose response curves for (HYP1) and (HYP2) alone compared to the combined case (HYP1+HYP2). The curves show that HYP1 alone or HYP2 alone lead to low levels of *WUS* induction. Suppression of *CLV1* leads to higher levels of WUS but this increase is bounded. The maximum increase through this mechanism is equivalent to the clv1 mutant which we show experimentally has a 3 fold higher level of WUS than wildtype not the 38 fold increase observed after treatment. HYP2 and HYP3 alone also does not lead to massive induction of *WUS*, since the CLV-mediated negative feedback restricts WUS levels. In comparision, the combined case (HYP1+HYP2), in which both mechanisms operate, leads to robust *WUS* induction. In summary, CLV negative feedback must be reduced, in addition to CLV independent activation to obtain the large fold inductions of *WUS* observed.

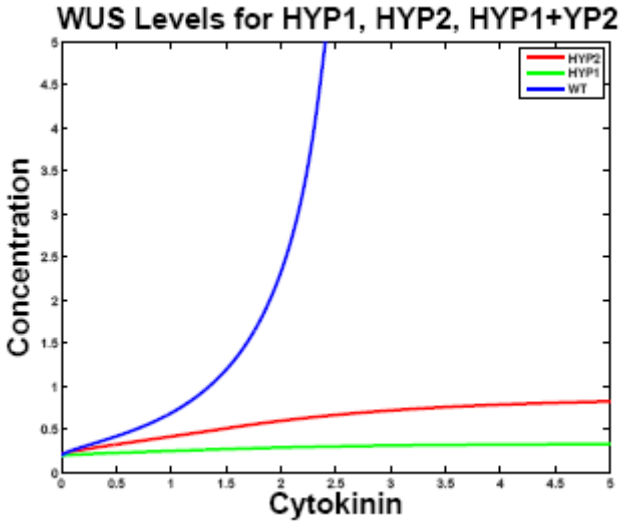


**Figure 3.12 Direct activation of WUS or CLV1 suppression alone do not reproduce WUS induction by cytokinin.** Simulation of either hypothetical model (HYP) 1 and 2 as well as a model including both regulatory links. Simulations of the models reveal that HYP1 or HYP2 alone do not lead to large increases in *WUS* concentration. In HYP1, *CLV1* suppression leads to a small increase in *WUS*, comparable to the 3 fold increase in the clv1 mutant. HYP2 does not lead to large increases in WUS as CLV-mediated negative feedback prevents unrestrained *WUS* induction. The combined model (HYP1 + HYP2) does lead to massive induction of *WUS* as CLV negative feedback is not able to suppress the direct activation of *WUS* by cytokinin.

Our experiments revealed that transient cytokinin treatments alter floral development leading to a quantitative excess stem cell phenotype. The quantitative nature of this phenoptype allowed us to show that cytokinin treatment leads to greater increase in stem cell activity in CLV loss of function background (two-way ANOVA, $P < 0.0001$). To understand why loss of CLV function leads to greater perturbation in stem cell activity after cytokinin treatment we simulated transient cytokinin treatments (Figure 3.13). This can be explained by CLV negative feedback in the system leading to a quicker response in damping out fluctuations.

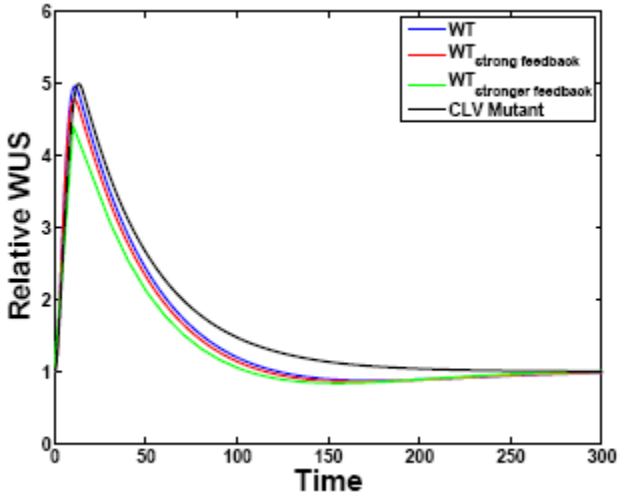


**Figure 3.13 Simulation of WUS transcript levels during transient cytokinin perturbation.** We compared models including CLV negative feedback (WT), the same model with stronger negative feedback parameters ($WT_{stronger\ feedback}$), or a model omitting CLV negative feedback (CLV mutant). The plot shows that higher levels of CLV negative feedback results in quicker damping out of WUS induction and quicker return to WUS levels before treatment.

Figure 3.13 shows that negative feedback provided by the CLV pathway damps out perturbations in *WUS* levels.

## *Discussion of Spatial Interpretation of Computational Modeling Results*

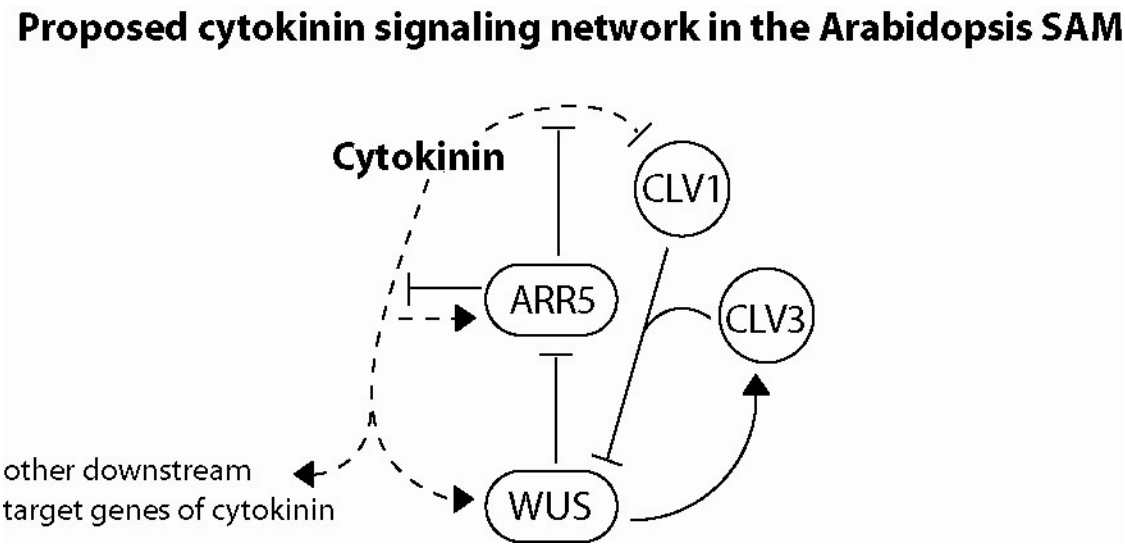


**Figure 3.14 Schematic of cytokinin signaling circuit.** Our experimental analysis leads to the above network in which cytokinin signaling interacts with *WUS*, and *ARR5* to determine the level of cytokinin signaling output within a given cell and the relative abundance of *WUS* and *ARR5*.

Simulation of our model indicates that feedback between cytokinin signaling and gene expression determines their relative spatial pattern. For example, the network predicts *WUS* expression and the cytokinin signaling maximum to overlap. Furthermore, Type-A ARR should be repressed within areas of highest signaling and *WUS* expression.

**Author Contributions** S.P.G. designed experiments, collected data, and performed analysis; V.C. developed the mathematical models, performed simulations and was involved in data analysis; C.K.O. cloned the *pWUS::DsRed-N7* construct; and E.M.M. was involved in study design and management. S.P.G., V.C., and E.M.M. contributed to writing of the article.

## 3.4 Materials and Methods

### *3.4.1 Plant materials*

*clv1-11* and *clv3-2* and *clv2-1* alleles in L-*er* background have been previously described (Clark et al., 1995; Dievart et al., 2003). The *pWOL::GFP* line in Columbia (Col-0) background has been previously described (Birnbaum et al., 2003) which recapitulates expression patterns observed in the shoot and root via in situ hybridization (Mähönen et al., 2006b). The *pARR5::GFP* line in WS ecotype has been previously described (Yanai et al., 2005).

### *3.4.2 Growth conditions and cytokinin treatments*

Plants were grown as previously described (Gordon et al., 2007). N6-benzylaminopurine (BAP; Sigma–Aldrich Co., St. Louis, MO) was dissolved in 1M KOH to make a 0.5M stock which was then diluted in water to make a final treatment concentration containing 0.05% Tween20 (Sigma–Aldrich Co., St. Louis, MO). Mock treatments were performed with the same solution, only lacking cytokinin. Cytokinin treatments with N6-benzylaminopurine (BAP) were performed as described(Lindsay et al., 2006) except that shoots were sprayed with the respective solutions. Shoots were sprayed with respective solutions beginning at the 5 five rosette leaf stage. For phenotypic analysis of carpel number, plants were treated either 3 times at 1 week intervals or alternatively once weekly for continuous treatments. *clv3-2* mutants and wild type plants in Fig. 3f and Supplementary Fig. 1f,i,k were treated once every second day. Phenotypic analysis was performed on soil. Flowers at positions 3-20 of at least 10 plants were counted for carpel numbers of cytokinin and mock treated samples. At least two independent biological experiments were performed for each genotype. Imaging was performed as previously described (Gordon et al., 2007). Membranes were stained with FM4-64 dye unless otherwise noted (Gordon et al., 2007).

### *3.4.3 Construction of GFP reporters*

The *pWUS::dsRED-N7* construct in the T-DNA vector pMLBART (Gleave, 2002) conferring Basta resistance in plants is composed of 3.33 kb of upstream regulatory sequence from the *WUS* gene fused to dsRED followed by the N7 nuclear localization sequence (Cutler et al., 2000) with 1.31 kb of *WUS* 3'-untranslated sequence. For double transgenic plants, *pWUS::DsRed-N7* was transformed into respective backgrounds.

### *3.4.4 Real-time quantitative reverse transcriptase-mediated PCR (qRT-PCR)*

Quantitative real-time PCR (qRT-PCR) was performed with Roche Universal Probe Library hydrolysis probes. Sequences of primers and probes used in this study and additional information is provided in Additional Methods. Each sample represents tissue harvested from 50 two week old seedlings just transitioned to flowering. Relative expression by qRT-PCR was normalized to *NM_128399.2* and similar trends were observed using *UBIQUITIN 10* (Czechowski et al., 2005). All samples were run in at least triplicate. Error bars of real-time qRT-PCR experiments in Fig. 1 are derived from 3 independent biological experiments except for the cytokinin serial dilution curve in Fig. 2a which is derived from two independent biological experiments. We show the mean and s.e.m. between respective biological replicates

Seeds were germinated on MS agar medium and grown for 13 days to the 5 leaf stage (day 1 being 24 hours after removal from cold shock) under continuous light. Meristem tissue from 50 plants was harvested and pooled from seedlings after dissecting off leaves, cotyledons and root tissue followed by liquid nitrogen flash freezing and homogenization. Total RNA was isolated using the RNeasy mini kit (Qiagen). RNA concentration and quality was assayed using nanodrop spectrometer (Agilent). First-strand cDNA synthesis was performed with 2µg of total RNA using Superscript II RNase H- reverse transcriptase (Invitrogen) and 20mer oligo dT primers according to the

manufacturer's instructions. Real-time PCR amplifications were performed in triplicate in 96-well plates in a 20 ul reaction volume on a Roche LightCycler 480 system. Unlabeled gene-specific primers in combination with a gene-specific hydrolysis probe from the Roche Universal Probe Library Set were used to detect gene-specific amplification products. For WUS quantification, primers spanned two intron sequences which eliminated products from potential genomic DNA contamination under our PCR settings. Relative WUS concentration ratios were calculated by normalizing to the transcript for SAND family protein (NM_128399.2) which has been shown to be a superior reference gene for qRT-PCR analysis, constant against various treatments, including cytokinin treatments (Czechowski et al., 2005). Transcript abundance of this gene is 1/10 of *UBQ10* transcript levels and similar to *WUS* transcript levels. Additional experiments using *UBQ10* as a reference gene gave similar trends between mock and treated samples. Gene specific primers 5'-ggattttcagctactcttcaagcta-3' and 5'-ctgccttgactaagttgacacg-3'with UPL probe 157 were used to amplify and detect *NM_128399.2*, the primers 5'-tcagagaacatcttgcctcgt-3' and 5'-atttcacaggcttcaataagaaatc-3' with UPL probe 17 were used to amplify *ARR5*, 5'-ggatacatcgccccagagt-3' and 5'-tccaaattcaccaacaggttt-3' with UPL probe 33 were used for *CLV1*, the primers 5'-aaccaagaccatcatctctatcatc-3' and 5'- ccatcctccacctacgttgt-3' with probe 33 were used to amplify *WUS*, the primers 5'-ggagcctcaagcaagagttc-3' and 5'-ggcgagcttttgttgctc-3' with UPL probe 35 were used to amplify and detect *STM*, and the primers 5'-gaagttcaatgtttcgtttcatgt-3' and 5'-ggattatacaaggccccaaaa-3' with UPL probe 119 were used to amplify and detect *UBQ10*. Error bars of real-time qRT-PCR experiments in figure 1 are derived from 3 independent biological experiments showing the mean and s.e.m. between respective samples. Error bars in all other experiments are derived from at least two independent biological experiments. In all cases, error calculated between qRT-PCR triplicate reactions or between independent runs on the same biological sample was negligible.

Cycloheximide treatments: Plants were pretreated with 10 µM cycloheximide (Sigma–Aldrich Co., St. Louis, MO) for 30 min. then treated with respective BAP or mock solutions also containing 10 µM cycloheximide and harvested 4hrs after treatment.

### *3.4.5 Imaging conditions*

Callus and regenerating shoots were imaged directly on respective media. For live imaging of the SAM plants were grown for 2 weeks on respective MS agarose plates, after which they were transferred to MS agarose boxes for further growth and imaging. For each marker line, at least 10 samples were imaged to confirm that observed patterns were representative of respective markers. Propidium iodide for staining cell outlines of root tissues was applied to samples at a concentration of 10 µg**/**ml 10 minutes prior to imaging. The lipophilic dye FM4-64 (Molecular Probes) was used at a concentration of 10 µg**/**ml to demarcate cell membranes and specifically labeled regenerating shoot tissues initiating from root-derived callus.

All imaging was done using a Zeiss 510 Meta laser scanning confocal microscope with either a 10x air objective, 20x air objective, or a 40x 0.8 NA water dipping lens using the multi-tracking mode. Specific sets of filters used for the respective markers were similar to those already described (Heisler et al., 2005; Reddy and Meyerowitz, 2005). Projections of confocal data were exported using Zeiss LSM software. Alternatively, volume renderings were made using Amira (Mercury Computer Systems).

### *3.4.6 computational modeling*

Computional modeling is described in "*Discussion of Computational Modeling"* above. Parameter values used in the modeling section are described in the table below.

| $K_{h1}$ | $v_{h1}$ | $K_{h2}$ | $K_1$ | $\alpha$ | $v_1$ | $K_2$ | $a_0$ | $a_1$ | $a_2$ | $b_0$ | $b_1$ | $b_2$ |
|---|---|---|---|---|---|---|---|---|---|---|---|---|
| 5 | 2 | 5 | 1 | 1 | 1 | 1 | 0.01 | 5 | 10 | 0.025 | 0.25 | 0.25 |

| $b_3$ | $c_0$ | $c_1$ | $k_1$ | $k_2$ | $d_1$ | $K_{c1}$ | $K_{c2}$ | $v_{c2}$ |
|---|---|---|---|---|---|---|---|---|
| 1 | 0.5 | 5 | 0.025 | 0.5 | 1 | 1 | 1 | 1 |

**Table 1: Parameter values.** The concentration of the network components are in dimensionless units, the rate constants (transcription and degradation) are in units of *min*−1, and the Michaelis-Menton constants are dimensionless. We assume no form of cooperativity unless specifically mentioned, hence *n* = 1 (in the section on bistable response of the circuit, we use *n* = 2, since multiple binding sites for WUS were found on the Type A ARR promoter (Leibfried et al., 2005). Although the results obtained from the model are robust to a wide range of parameters, one guideline we have adhered to is to set the parameters for the AHPT, Type-A ARR, and Type-B ARR, such that certain relevant time scales are obtained. Namely, the phosphorylation/dephosphorylation time scales of the AHPT's are 10*min*, and the time scales of the Type-A & Type-B ARRs, are 1hr. To obtain these results we assume a degradation rate for the Type A ARR to be 0.025*min*−1. We also assume that all degradation rates *γi* = 0.025*min*−1 (i=1:5), the transcription/translation rates are chosen to be scaled to a maximum of unity. For parameter values used in typical models of bacterial signaling regulatory networks see: (Mitrophanov and Groisman, 2008). The total amount of AHPT, Type B ARR and X in their two different forms obey, *AHPT* + *AHPTP* = 10*, B* + *BP* = 10*, X* + *XP* = 10.

## 3.5 Acknowledgements

I would like to acknowledge Vijay Chickermane for his development of the mathematical models and simulations used here. I would also like to acknowledge Carolyn Ohno who cloned the *pWUS::DsRed-N7* construct. We thank P. Benfey for the *pWOODENLEG::GFP* line which we refer to here as the *AHK4* reporter, *pAHK4::GFP*. The *pARR5::GFP* line was kindly provided by J. Kieber and Y. Helariutta provided the *pAHP6::AHP6-GFP* line. T. Kakimoto provided additional reagents. We thank members of the Computable Plant group (http://computableplant.org/) including H. Jönsson, M. Heisler, A. Roeder and P. Tarr for comments on the manuscript; K. Sugimoto for advice with RT-PCR analysis of cytokinin treated root explants; A. Martin for sample collection of cytokinin serial dilutions; and A. Garda for technical support. This study was supported by National Science Foundation grants IOS-0846192 and IOS-0544915 to E.M.M.

CHAPTER 4

# Feedback model of cytokinin signaling

## 4.1 Introduction

The limited modeling data in Chapter 3 address how cytokinin signaling and the function of proteins such as WUS, Type-A ARRs interact to regulate their own spatial expression as well as the spatial distribution of cytokinin signaling. A computational model of such dynamics accurately generated patterns of activity which we subsequently confirmed experimentally.

However, we considered only the case involving a single cytokinin receptor which activates a single class of Type-A ARR and omitted other components which negatively feedback on cytokinin signaling. In reality, at least 3 cytokinin receptors, 11 Type-B ARRs and 12 type-A ARRs are known to exist (Muller and Sheen, 2008; To et al., 2007). Only 4 Type-A ARRs (ARR5,6,7,15) are known to be repressed by WUS (Leibfried et al., 2005). Furthermore, other feedback networks are known to regulate cytokinin signaling. For example, the ARABIDOPSIS HISTIDINE PHOSPHOTRANSFER PROTEIN 6 (AHP6) is known to suppress cytokinin signaling (Mähönen et al., 2006a). Cytokinin signaling also represses *AHP6* transcription leading to positive feedback on signaling. The significance of the apparent redundancy in components both involved in the positive and negative regulation of cytokinin signaling is unknown. In fact, although the transcription of most Type-A ARRs is promoted by cytokinin, different Type-A ARRs are activated with different kinetics after treatment (D'Agostino et al., 2000; Kagan et al., 1997). Furthermore, the basal transcription patterns of Type-A ARRs vary (To et al., 2004). *ARR3* and *ARR4* are expressed mainly in the shoot vasculature, *ARR5* and *ARR6* are expressed in the shoot meristem, while *ARR8* and *ARR9* are most strongly expressed in the root. Lastly, mutant analysis of both Type-B and Type-A ARRs suggests that

individual members are required for different physiological functions (Mason et al., 2005).

In this chapter, we investigate putative specificity in two component cytokinin signaling. We consider the effect of multiple cytokinin receptors and the action of AHP6. We show that the three different cytokinin receptors considered are required for activation of different antagonistic downstream targets of cytokinin signaling. Secondly, the expression pattern of *AHP6* appears to in part follow from its interaction with cytokinin signaling and the ahp6 mutant has enhanced clv-like phenotypes after treatment with cytokinin revealing its connection to the WUS/CLV pathway.

## 4.2 Results

### *4.2.1 Specificity cytokinin receptor signal transduction pathways*

Our previous work in Chapter 3 showed that cytokinin signaling promotes the expression of *WUS*, a positive regulator of stem cell fate in the shoot stem cell niche. In order to understand the specificity of signaling leading to the activation of *WUS* in response to cytokinin treatment we quantified *WUS* activation in loss of function mutants for the three individual cytokinin receptors, the *Arabidopsis* histidine kinases 2,3,4 (AHK2,3,4) (Figure 4.1). Quantitative real-time PCR showed that basal levels of *WUS* were higher in the ahk3-3 mutant and lower in the ahk2-2 mutant as compared to the wildtype or the ahk4 mutant (cre1-12). Treatment with cytokinin strongly increased *WUS* transcript in wildtype. This induction was slightly reduced in the cre1-12 mutant and completely abolished in the ahk2-2 mutant. In contrast, *WUS* induction was stronger in the ahk3-3 mutant background.

The Type-A ARRs *ARR5,6,7,15* are direct targets of WUS-mediated repression. Over expression of these Type-A ARRs leads to lower *WUS* transcript levels. This evidence

suggests that WUS and this subset of Type-A ARRs antagonistically suppress each other's transcription. Although the basal expression of the Type-A ARR, *ARR5* was only slightly lower in the ahk3-3 mutant its induction by cytokinin was severely reduced in this mutant background. In contrast, induction of *ARR5* was only slightly reduced in the cre1-12 mutant and was higher in the ahk2-2 mutant than wildtype. As compared to the results for *WUS* and *ARR5*, cytokinin-dependent repression of *CLV1* transcript was similar between wildtype and each of the cytokinin receptor mutants (non-specific).

The above results demonstrate unappreciated specificity within cytokinin-activated signal transduction pathways (Figure 4.1). Our data shows that different downstream targets are activated through partially insulated signal transduction originating from the activation of different cytokinin receptors. Lower basal levels of *WUS* and the absence of induction in response to cytokinin in the ahk2-2 mutant as compared to wildtype or the other receptor mutants suggests that signaling through the AHK2 receptor is the primary pathway for cytokinin-induced activation of *WUS* transcription. In contrast, severely reduced *ARR5* expression in the ahk3-3 mutant suggests that the AHK3 receptor is the primary pathway for cytokinin-induced activation of ARR5 transcription. Higher induction of *WUS* transcript in the ahk3-3 mutant and higher *ARR5* induction in the ahk2-2 mutant suggest that these alternative pathways are antagonistic in the regulation of *WUS* and *ARR5* expression.

Cytokinin treatment results in a quantifiable phenotype associated with excess stem cells (Lindsay et al., 2006). In order to see whether opposite consequences of cytokinin treatment on *WUS* and *ARR5* expression in the ahk2-2 and ahk3-3 mutants is physiologically important for this phenotype we quantified excess carpel number in these backgrounds. We observed that cytokinin treatment increased carpel number in wildtype and ahk3-3 mutants. However, we never observed any instance of increased carpel number in cytokinin treated ahk2-2 mutants. In contrast, cytokinin treatment reduced carpel number in ahk2-2 mutants or more frequently resulted in partial loss of

carpel tissue. These results indicate that functional AHK2 receptor is necessary for excess stem cell phenotypes in response to cytokinin treatment.

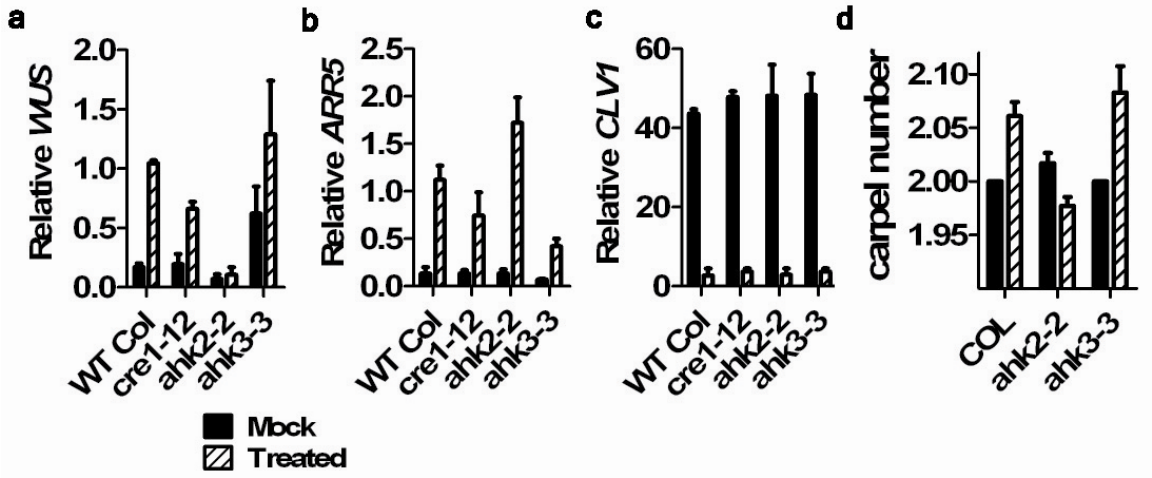


**Figure 4.1 Specificity in two component signaling in Arabidopsis.** a-c, qRT-PCR analysis of *WUS*, *ARR5* and *CLV1* transcript levels in wildtype (WT), the ahk4 mutant (cre1-12), the ahk2 mutant (ahk2-2), or the ahk3 mutant (ahk3-3) after 24hrs of mock treatment or cytokinin treatment (1mMBAP). **a**, *WUS* transcript is increased in the ahk3 mutant and decreased in the ahk2 mutant. This trend is accentuated by cytokinin treatment. **b**, *ARR5* transcript is increased in the ahk2 mutant but decreased in the ahk3 mutant. This trend is also accentuated by cytokinin treatment **c**, *CLV1* transcript is decreased after cytokinin treatment in all single mutants similar to WT. Carpel number is increased in WT and ahk3 mutant plants after treatment with cytokinin. In contrast, cytokinin treatment induces a decrease in carpel number in ahk2 mutant plants. qRT-PCR error bars indicate S.E.M. from two biological replicates**.**

The above data suggests that individual receptors signal through distinct subsets of cytokinin signaling components to activate transcription of downstream targets. In Figure 4.2 we present a schematic summarizing the interactions suggested from our data.

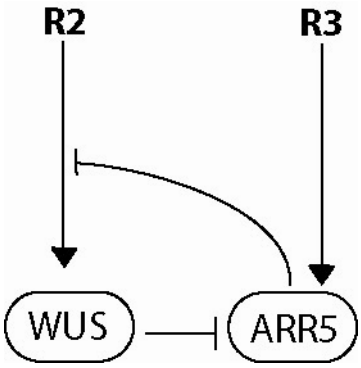


**Figure 4.2 Network diagram of signaling specificity in the cytokinin signaling pathway.** Diagram of interactions suggested from our qRT-PCR data in different cytokinin receptor mutant backgrounds. AHK2 signaling (R2) activates WUS transcription which suppresses ARR5 transcription. AHK3 signaling (R3) induces ARR5 transcription which negatively regulates signaling through the R2 pathway. Not diagrammed here, AHK4 signaling (R1) activates transcription of both WUS and ARR5.

### *4.2.2 Functional importance of antagonistic pathways*

Cytokinin perception by different receptors which have different downstream targets could be physiologically important for plant growth and development. The three cytokinin receptors (*AHK2,3,4*) have partially overlapping but also distinct expression patterns (Higuchi et al., 2004). For example, *AHK2* appears to be expressed at highest levels in the shoot while *AHK3* is highest in leaves and *AHK4* is highest in roots. In the context of the shoot stem cell niche, the three receptors appear to partially overlap (Mähönen et al., 2006b). However better data will likely show that the patterns of the three receptors are at least partially unique.

As demonstrated in Figure 4.1, AHK3 is required for cytokinin-induced upregulation of *ARR5*. AHK2 is in contrast required for cytokinin-induced increase of *WUS* transcript. These pathways are also antagonistic. WUS directly suppresses *ARR5* expression while ARR5 suppresses *WUS* induction by reducing cytokinin signaling through the AHK2 pathway. Thus the ratio of AHK2 to AHK3 signaling within a cell could play a significant

role in influencing the spatial expression of *ARR5* and *WUS*. For example, we propose the hypothetical case in which AHK3 is expressed more broadly than AHK2 (Fig. A3). In contrast, we showed in Chapter 3 that *AHK4* is specifically expressed in the *WUS* domain within the SAM. Cells expressing only *AHK3* would express only *ARR5*, while cells with a high ratio of AHK2 to AHK3 would express *WUS* and thus lower levels of *ARR5*.

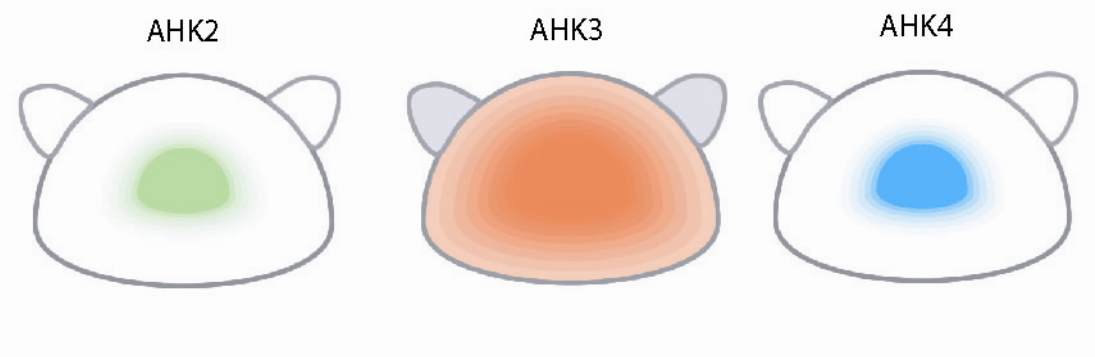


**Figure 4.3 Hypothetical combinatorial expression of AHK2,3,4 within cells.** Hypothetical expression patterns of the three cytokinin receptors AHK2,3,4. Different combinations or ratios of the three receptors could influence which downstream targets are activated by cytokinin signaling within particular cells of the shoot stem cell niche.

### *4.2.3 Differential regulation of Type-A ARR family members.*

In the preceding analysis we demonstrated that *WUS* is activated by cytokinin through an AHK2 receptor-dependent pathway while the Type-A ARR, *ARR5*, is activated through an AHK3 receptor-dependent pathway. WUS and ARR5 function leads to antagonism between the AHK2 and AHK3 pathways. However, of the 12 type-A ARRs in *Arabidopsis* only 4 Type-A ARRs (ARR5,6,7,15) are known to be directly repressed by WUS (Leibfried et al., 2005). In this section we characterize specificity of the entire Type-A ARR family at the receptor level as well as their response curves to cytokinin. We show that Type-A ARRs can be grouped into classes sharing similar receptor specificities and responses to

exogenous cytokinin. Using this data we further support a model in which the AHK3 receptor pathway activates the majority of Type-A ARRs, thus mediating negative feedback on cytokinin signaling through the AHK2 pathway.

Quantitative real-time PCR showed that transcript levels of different Type-A ARRs are regulated differently in the background of the three individual cytokinin receptor loss of function mutants (Figure A.4). Similar to observed for ARR5, the direct targets of WUS repression (ARR5,6,7,15) all required AHK3 for their induction and their transcript levels were increased in AHK2 loss of function background. This subgroup of Type-A ARRs appears to be activated through the AHK3 pathway and is suppressed by the AHK2 pathway. Although not known to be directly suppressed by WUS, *ARR4* and *ARR17* transcript levels were regulated in a similar manner as compared to *ARR5,6,7* and *15*. This may be due to direct repression by WUS or due to indirect changes in cytokinin signaling dynamics resulting from WUS function. In contrast, induction of ARR3 and ARR16 was largely receptor non-specific. ARR8 and ARR9 transcript levels were suppressed by cytokinin treatment. This data confirms that the AHK3 pathway is the major pathway for induction of Type-A ARRs. As Type-A ARRs negatively feedback on the cytokinin signaling pathway, these results suggests that the AHK3 pathway is largely responsible for mediating negative feedback on cytokinin signaling.

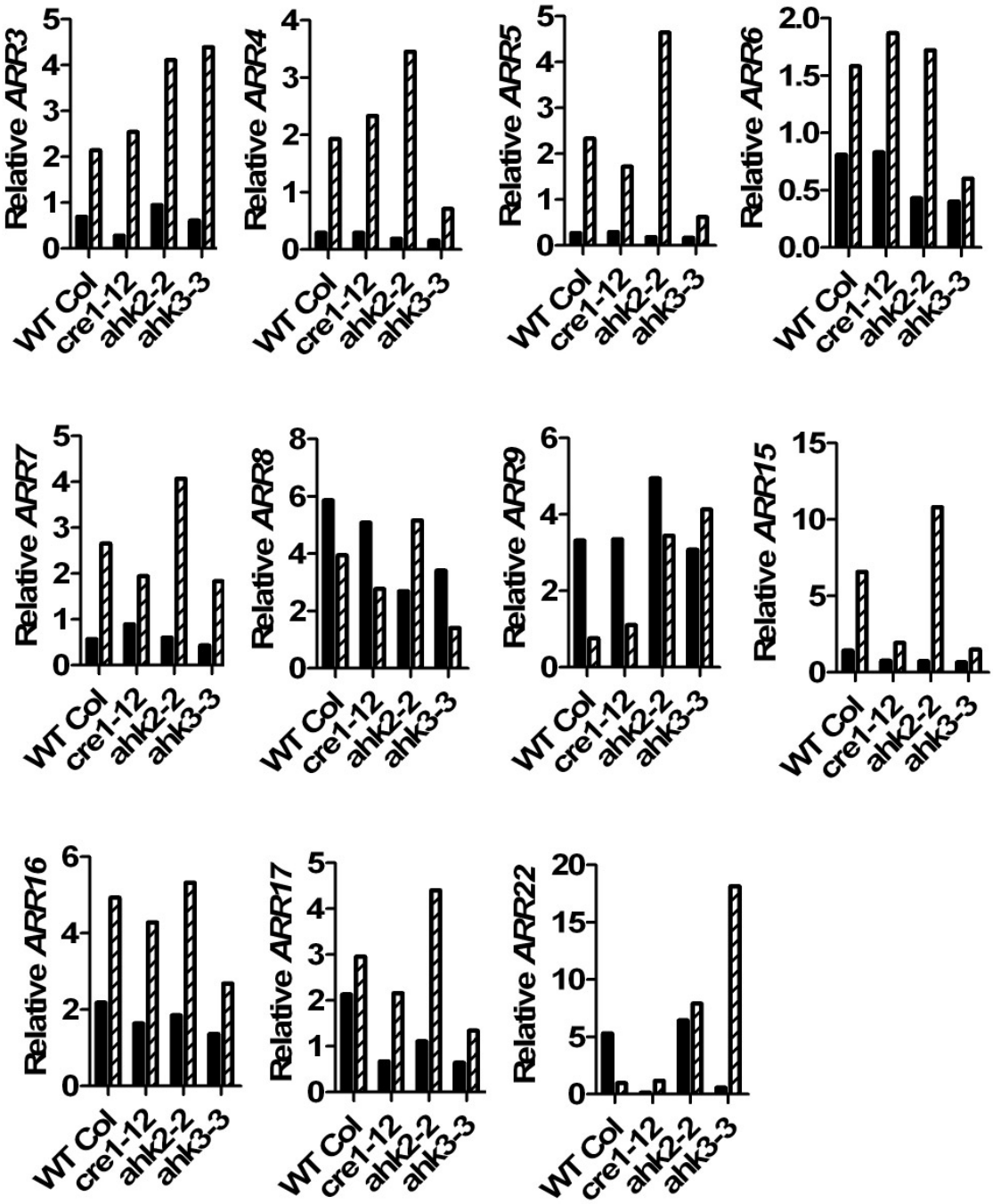


**Figure 4.4 Receptor specificity of Type-A ARR cytokinin-mediated induction.** qRT-PCR analysis of Type-A ARR transcript levels in mock treated (solid black bar) or cytokinin treated (1mMBAP) (stripped bar) in wildtype Columbia (Col), the ahk4 mutant (cre1-12), the ahk2 mutant (ahk2-2), or the ahk3 mutant (ahk3-3). ARR4, 5, 6, 7, 15 and 17 require a functional AHK3 receptor for induction and are suppressed by the AHK2 receptor pathway, shown by their upregulation in the ahk2-2 loss of

function mutant. Induction of ARR3 and ARR16 transcript was largely receptor non-specific. ARR8 and ARR9 were suppressed by the level of cytokinin treatment used in this experiment.

The results in Figure 4.4 show that different Type-A ARRs have different receptors requirements for activation or suppression of their transcription in response to cytokinin. In order to further contrast the mechanisms by which the different members of the Type-A ARR class are transcriptionally regulated, we characterized the response of each Type-A ARR to treatment with a range of cytokinin concentrations (Figure 4.5). We observed that different Type-A ARRs could be grouped according to the shape of their respective response over varying cytokinin concentrations. For example ARR3 and ARR4 transcript continuously increased over increasing concentrations of cytokinin. ARR5 and ARR6 transcript levels increased over higher cytokinin levels but this response was saturated at the highest levels of cytokinin treatment. In contrast, transcript levels of ARR7,8,9,15 and 16 increased over higher cytokinin concentrations but peaked at 10μM, and decreased in samples treated with higher concentrations of cytokinin.

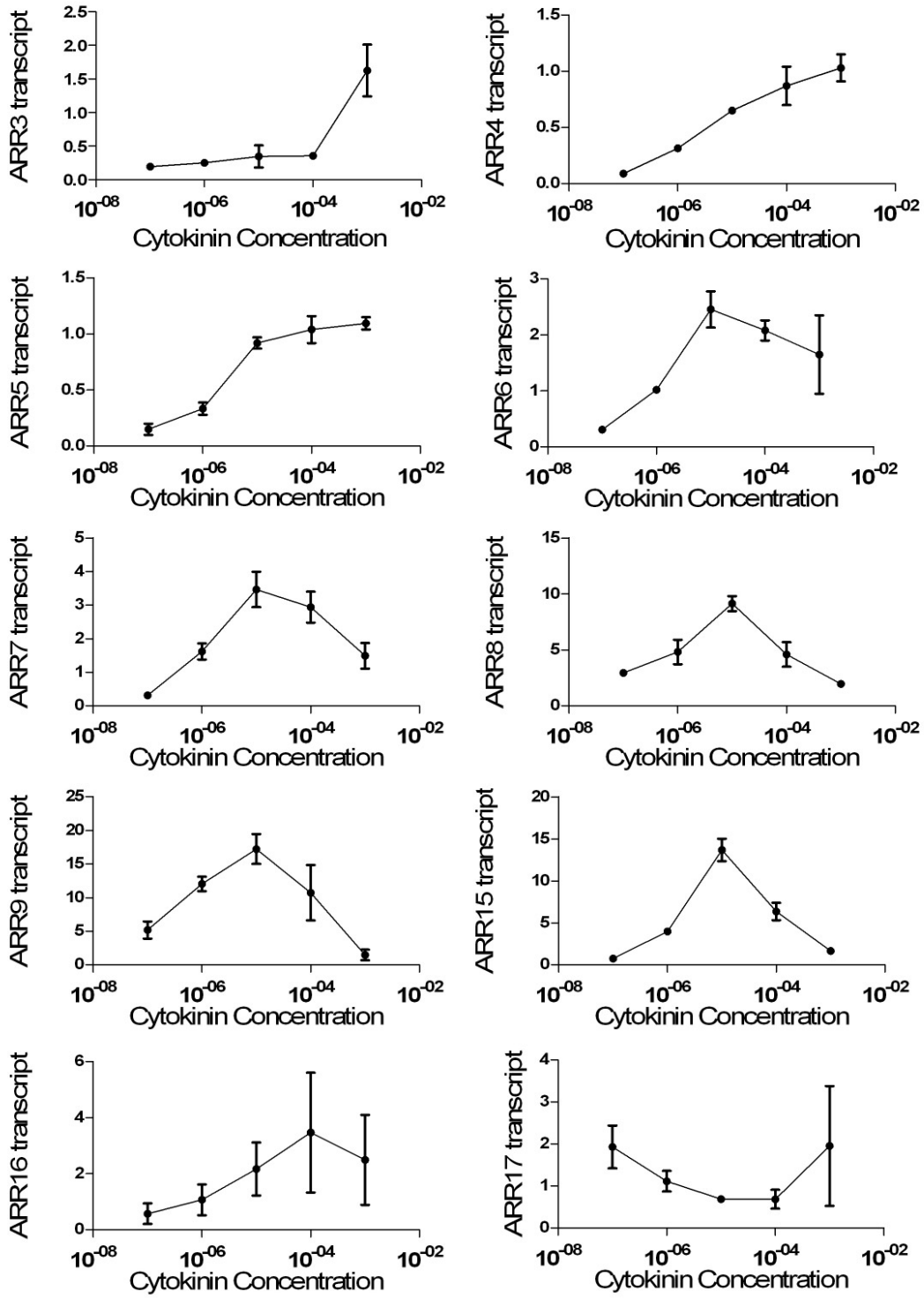


**Figure 4.5 Transcriptional regulation of Type-A ARRs at varying levels of cytokinin.** qRT-PCR analysis of Type-A ARR transcript levels in response to treatment

with serial dilutions of cytokinin. ARR3 and ARR4 transcript is continuously increased over increasing concentrations of cytokinin. ARR5 and ARR6 transcript increased over higher concentrations of cytokinin but response became saturated at the highest cytokinin concentrations. In contrast, transcript levels of ARR7,8,9,15 and 16 increased over higher cytokinin concentrations but peaked at 10µM, and decreased at higher levels of cytokinin. qRT-PCR error bars indicate S.E.M. from two biological replicates each from pooled tissue from 50 SAMs**.**

### *4.2.4 External feedback loop mediated by AHP6*

Cytokinin receptors mediate downstream signaling through phosphorylation of histidine phosphotransfer proteins which then transfer phosphoryl groups to downstream response regulators (RRs). The pseudo histidine phosphotransfer protein AHP6 was discovered as a suppressor of dominant negative alleles of the AHK4 receptor (Mähönen et al., 2006a). It was shown that AHP6 suppresses downstream cytokinin signaling and that *AHP6* transcription is in turn negatively regulated by cytokinin signaling. These two negative interactions lead to a positive feedback loop. Theoretically, AHP6 could, in addition to Type-A negative feedback, regulate the responsiveness of *WUS* to cytokinin signaling. To test if AHP6 has a role in regulating *WUS* transcription in response to cytokinin signaling we documented the cytokinin-induced excess stem cell phenotype on carpel number in the ahp6-3 mutant. Indeed, ahp6-3 loss of function mutants had larger increases in carpel number after cytokinin treatment than wildtype suggesting an interaction between AHP6 loss of function and cytokinin treatment (Figure 4.6; Two-way ANOVA, $F=9.7$, $P < 0.0018$). This suggests that AHP6 function regulates the ability of cytokinin signaling to enhance *WUS* transcription. This data also shows that genetic perturbation of cytokinin signaling can enhance phenotypes associated with *WUS* misregulation.

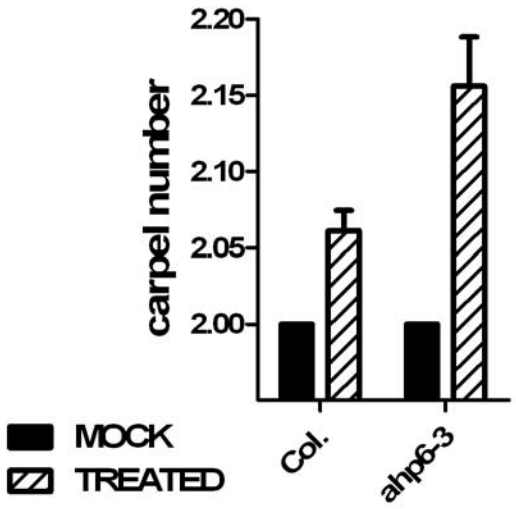


**Figure 4.6 Interaction between AHP6 loss of function and cytokinin-induced carpel number phenotypes.** Two-way ANOVA suggests that AHP6 loss of function interacts with cytokinin treatment to lead to a stronger carpel number phenotype in the ahp6-3 mutant ($F=9.7$, $P < 0.0018$).

### *4.2.5 Modeling consequences of AHP6 function*

Inclusion of the AHP6 feedback loop into our previous model consisting of cytokinin signaling and the CLV/WUS circuit leads to an increase in the cytokinin threshold required to induce *WUS*. Depending on the feedback strength, inclusion of AHP6 feedback into the network leads to switch-like behavior solely due to the 3 positive feedbacks within the network.

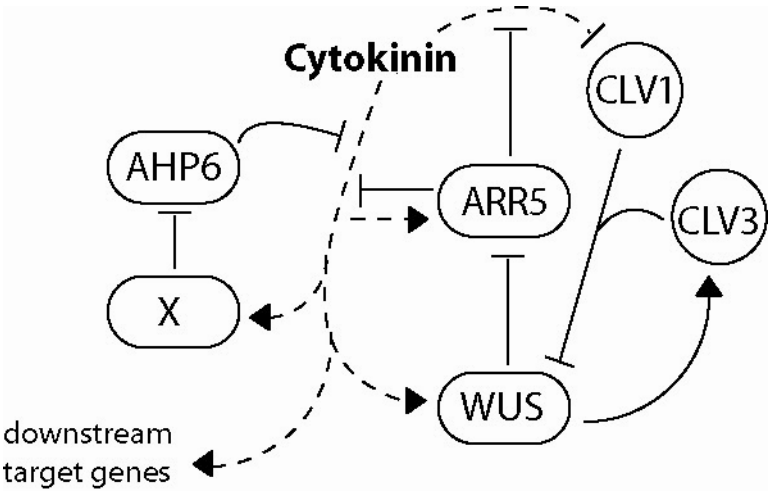


**Figure 4.7 Network diagram of the AHP6 feedback loop within the cytokinin signaling network.** Diagram of our extended network including the AHP6 feedback loop. AHP6 inhibits downstream cytokinin signaling. Higher cytokinin signaling leads to induction of an unknown factor X which suppresses AHP6 transcription leading to positive feedback on cytokinin signaling. Similar to our previous models, gene expression and cytokinin signaling feedback on one another to regulate each other's activity as well as the activity of other downstream genes. Intuitively, AHP6 functions to further increase the threshold of cytokinin required to activate WUS expression and downstream genes.

Intuitively, the network in Figure 4.7 in which AHP6 is suppressed by cytokinin, predicts the experimentally observed pattern shown in Chapter 3 in which AHP6 is expressed at the SAM periphery distal to the cytokinin signaling maximum.

**Author Contributions** S.P.G. designed experiments, collected data, and performed analysis; V.C. developed the mathematical models, performed simulations and was involved in data analysis; and E.M.M. was involved in study design and management. S.P.G., V.C., and E.M.M. contributed to writing of the article.

## 4.3 Discussion

In this thesis we have presented data and modeling which is consistent with multiple feedbacks between gene expression and hormone signaling. Our demonstration that individual cytokinin receptors activate specific downstream targets through antagonistic parallel pathways adds an additional degree of complexity to understanding how cytokinin perception by cytokinin receptors leads to downstream signaling output. The ratio of AHK2 to AHK3 expression could determine the gene expression profile of a given cell and therefore its identity and behavior. In our future work we plan to further reveal additional detail about these antagonistic pathways and the interactions between them that control signaling and patterning within the shoot stem cell niche.

CHAPTER 5

# Concluding Remarks

Unlike animals, plants continuously modify their form through continuous post embryonic development. Auxin and cytokinin are key hormonal regulators of post-embryonic development and pattern formation (Muller and Sheen, 2007; Teale et al., 2006). At the level of the individual cell, the ratio of auxin and cytokinin response influences its profile of gene activity and thereby controls its behavior and fate. Auxin and cytokinin have antagonistic roles in regulating cell differentiation. Auxin is associated with specification of cells into organs and mediating cell differentiation (Teale et al., 2006). In contrast, cytokinin is associated with maintaining undifferentiated cells within the stem cell niche. The goal of this study was to probe the mechanism by which auxin and cytokinin enable self-organizing patterns seen during regeneration and normal development. Furthermore we have focused on how cytokinin influences patterning of the stem cell niche and its role in reestablishing this niche *in vitro* during regeneration.

## *5.1 Plant regeneration*

Recent work in animals indicates that differentiated cells can be reprogrammed into pluripotent stem cells through direct manipulation of gene and protein activity in culture (Park et al., 2008; Yu et al., 2007). Another approach is the determination and use of external factors such as hormones that elicit similar effects by regulation of gene expression without the need for transgenic manipulation of cells.

In plant biology, external factors for regulating cell differentiation in culture have long been known. Auxin and cytokinin have long been used as key factors to manipulate cell differentiation in vitro. For example, single somatic cells can be induced to form entire new plants through stimulation with auxin and cytokinin (Steward et al., 1964). Plants

are routinely cloned in culture through regeneration with the use of these hormones. Nonetheless, the developmental process as well as the molecular mechanism by which auxin and cytokinin stimulate regeneration of new plants from somatic tissue is unknown.

### *5.1.1 Summary of results*

We show transfer of cells from low cytokinin/auxin ratio to a high cytokinin/auxin environment triggers self-organization among a population of cultured cells. This process occurs via spatial partition of cell identity and hormone response into two populations. Small clusters of progenitor cells marked by auxin response, surrounded by cytokinin responsive cells, initiate development of a new shoot stem cell niche (the shoot meristem). Our real-time observations of gene and protein activity lead us the novel hypothesis that a Turing-like mechanism may underlie patterning during de novo plant regeneration. In this model the diffusion rate of the activator (auxin) is increased by the presence of the inhibitor (cytokinin) by suppression of directional auxin transport. This leads to slower diffusion of auxin out of clusters of cells which are already responding to a fluctuation in auxin, building a peak of auxin response. Peaks of auxin response trigger differentiation of cells. High cytokinin response in surrounding cells triggers the first steps in reestablishing the shoot stem cell niche in vitro which involves activation of *WUSCHEL*, a marker for rib meristem fate. *WUSCHEL* non-cell autonomously prevents some cells responding to auxin from fully differentiating, specifying them as new shoot stem cells.

### *5.1.2 Significance of results*

We have characterized the widely used but poorly understood *in vitro* shoot meristem induction system. We show that this system is useful for study of how auxin and cytokinin regulate reestablishment of the shoot stem cell niche. We show how induction of broad cytokinin receptor expression during auxin pre-treatment during

callus growth may underlie the enhanced regeneration from callus as compared to untreated tissue explants. Our results lead to a testable model for how the shoot stem cell niche is reestablished *de novo* during regeneration. This work may allow design and manipulation of patterning during plant regeneration in predictable ways. If our model is correct both the size of regenerating structures as well as the frequency of regeneration could be manipulated. Furthermore, the particular type of Turing-like mechanism discussed here may be the first example of its kind and therefore be an important model for researchers investigating patterning in plant development and other fields.

## *5.2 Cytokinin-regulated patterning of gene expression and SAM zonation*

Plants ranging from the small weed *Arabidopsis* to the Giant Sequoia tree (arguably ranking as the world's largest individual organism) maintain growth of stems, leaves, flowers, and branches through the action of stem cells. A central unanswered question in stem cell biology, both in plants and in animals, is how the spatial organization of stem cell niches are maintained as cells move through them, differentiating along the way. Previous studies suggested that *WUSCHEL* regulates SAM function through controlling activation of a signal transduction pathway regulated by the plant hormone cytokinin (Leibfried et al., 2005). However, it was unclear whether cytokinin signaling itself had any patterning role within the shoot stem cell niche.

### *5.2.1 Summary of results*

In this study, we show that cytokinin plays an important role in patterning the shoot stem cell niche. We provide evidence that a gradient of cytokinin signaling decreasing from the center of the SAM acts as spatial reference to inform cells of their position within the stem cell niche. Furthermore, we show that different genes can be activated through the cytokinin signaling pathway in a threshold-dependent manner. Based on these data we develop a computational model in which interactions between

components within the network predict their relative patterning, which we confirm experimentally. This study reveals that cytokinin signaling acts as a spatial cue which triggers domain-specific gene expression as cells pass through different zones of the SAM. This result also explains a critical aspect of de novo plant regeneration in tissue culture, that is, how increasing cytokinin concentration leads to broad expression of *WUSCHEL* which leads to reestablishment of the shoot stem cell niche in vitro.

### *5.2.2 Significance of results*

Our results indicate that high levels of cytokinin signaling within the rib meristem of the shoot stem cell niche promotes *WUS* expression in these cells. WUS is known to non-cell autonomously promote shoot stem cell fate in overlying CZ cells which in turn produce secreted CLV3 peptide. CLV3 peptide is thought to diffuse through the meristem and bind to CLV1 receptor initiating a signal transduction cascade that leads to *WUS* downregulation. This negative feedback loop restricts *WUS* expression within the shoot meristem (Clark, 2001).

However, some evidence suggested that a positive *WUS* promoting signal might emanate from the stem cells in the shoot apex to preserve the position of the rib meristem relative to the stem cells as cells individual cells comprising the rib meristem are displaced into the growing stem (Tucker and Laux, 2007). In rice, the *LONELY GUY (LOG)* gene encodes an enzyme that converts inactive cytokinin into the active free base form. *LOG* gene expression is localized to the shoot meristem apex overlapping with the shoot stem cell domain (Kurakawa et al., 2007). Thus, LOG activity in the shoot stem cells may release active cytokinins which are perceived by cells in the rib meristem and initiate cytokinin signaling leading to *WUS* production. Consistent with this hypothesis, rice log mutants have smaller shoot meristems which prematurely terminate (similar to *WUS* loss of function mutants) (Tucker and Laux, 2007). In *Arabidopsis*, the expression of a gene homologous to the rice *LOG* gene is also specifically expressed in the apical

shoot stem cells providing support for a similar picture as in rice (Yadav et al., 2009). In this model, active cytokinins are produced in apical stem cells and diffuse down to underlying rib meristem cells where they bind to cytokinin receptor in rib meristem cells to activate *WUS* expression. If this is correct, then cytokinin acts as a diffusible messenger within the meristem to mediate communication between the apical shoot stem cells and the underlying rib meristem. As the stem cells in the shoot apex grow upwards, the release of active cytokinins from these cells would shift the domain of *WUS* expression upwards as well, leading to a standing wave of *WUS* expression relative to the apical stem cells. Additional signals must be required for positioning cytokinin receptor expression within the rib zone as shown in our study. Our preliminary data suggests that this signal is not cytokinin itself but could be auxin (data not shown).

## *5.3 Feedback model of cytokinin signaling*

There is putative redundancy at every step of the hybrid two component signaling pathway activated by the plant hormone cytokinin in *Arabidopsis*. At least three transmembrane receptors are activated by cytokinins which phosphorylate at least five histidine phosphotransfer proteins. This phosphorylation is then transferred to one of 11 Type-B ARRs, many of which regulate gene transcription while others mediate their function through unknown mechanisms (To and Kieber, 2008). Alternatively phosphorylation can be potentially transferred to one of 12 type-A ARRs negatively feedback on signaling through either competition for phosphorylation with Type-B ARRs or through an unknown mechanism (Muller and Sheen, 2008; To et al., 2007).

### *5.3.1 Summary of results*

In this investigation we showed that individual cytokinin receptors signal through partially insulated antagonistic pathways to regulate expression of *WUS* and Type-A ARR transcription. Furthermore we discover an additional level of negative feedback

regulation on cytokinin-induced *WUS* expression by showing that AHP6 limits the cytokinin-induced excess stem cell phenotype during floral development.

### *5.3.2 Significance of results*

We show that AHK2 pathway activation leads to induction of *WUS* which directly suppresses Type-A ARR (ARR5,6,7,15 ) expression. In contrast, Type-A ARRs such as ARR5 are activated through the AHK3 pathway and suppress *WUS* induction by antagonizing the AHK2 pathway. Therefore, our results demonstrate previously unappreciated specificity in two component cytokinin signaling in *Arabidopsis*. Our results also indicate that the ratio of AHK2 to AHK3 signaling within a cell could play a significant role in influencing the spatial expression of *ARR5* and *WUS*. Cells expressing only *AHK3* would express only *ARR5*, while cells with a high ratio of AHK2 to AHK3 would express *WUS* and thus lower levels of *ARR5*. Controlling the ratio of the two receptors within cells could allow fine tuning of cytokinin-induced gene expression. Further studies will show that differences in spatial expression of the three cytokinin receptors plays a role in patterning of the shoot stem cell niche.

## Bibliography

**Abe, M., Katsumata, H., Komeda, Y. and Takahashi, T.** (2003). Regulation of shoot epidermal cell differentiation by a pair of homeodomain proteins in Arabidopsis. *Development* **130**, 635-43.
**Aida, M., Ishida, T., Fukaki, H., Fujisawa, H. and Tasaka, M.** (1997). Genes involved in organ separation in Arabidopsis: an analysis of the cup-shaped cotyledon mutant. *Plant Cell* **9**, 841-57.
**Aida, M., Ishida, T. and Tasaka, M.** (1999). Shoot apical meristem and cotyledon formation during Arabidopsis embryogenesis: interaction among the CUP-SHAPED COTYLEDON and SHOOT MERISTEMLESS genes. *Development* **126**, 1563-70.
**Aida, M., Vernoux, T., Furutani, M., Traas, J. and Tasaka, M.** (2002). Roles of PIN-FORMED1 and MONOPTEROS in pattern formation of the apical region of the Arabidopsis embryo. *Development* **129**, 3965-74.
**Aloni, R., Langhans, M., Aloni, E., Dreieicher, E. and Ullrich, C. I.** (2005). Root-synthesized cytokinin in Arabidopsis is distributed in the shoot by the transpiration stream. *J Exp Bot* **56**, 1535-44.
**Aloni, R., Langhans, M., Aloni, E. and Ullrich, C. I.** (2004). Role of cytokinin in the regulation of root gravitropism. *Planta* **220**, 177-82.
**Baker, C. C., Sieber, P., Wellmer, F. and Meyerowitz, E. M.** (2005). The early extra petals1 mutant uncovers a role for microRNA miR164c in regulating petal number in Arabidopsis. *Curr Biol* **15**, 303-15.
**Banno, H., Ikeda, Y., Niu, Q. W. and Chua, N. H.** (2001). Overexpression of Arabidopsis ESR1 induces initiation of shoot regeneration. *Plant Cell* **13**, 2609-18.
**Barton, M. K. and Poethig, R. S.** (1993). Formation of the shoot apical meristem in Arabidopsis thaliana: an analysis of development in the wild type and in the shoot meristemless mutant. *Development* **119**, 823-831.
**Benkova, E., Michniewicz, M., Sauer, M., Teichmann, T., Seifertova, D., Jurgens, G. and Friml, J.** (2003). Local, efflux-dependent auxin gradients as a common module for plant organ formation. *Cell* **115**, 591-602.
**Bennett, S. R. M., Alvarez, J., Bossinger, G. and Smyth, D. R.** (1995). Morphogenesis in pinoid mutants of Arabidopsis thaliana. *The Plant Journal* **8**, 505-520.
**Birnbaum, K., Shasha, D. E., Wang, J. Y., Jung, J. W., Lambert, G. M., Galbraith, D. W. and Benfey, P. N.** (2003). A Gene Expression Map of the Arabidopsis Root. *Science* **302**.
**Brand, U., Fletcher, J. C., Hobe, M., Meyerowitz, E. M. and Simon, R.** (2000). Dependence of stem cell fate in Arabidopsis on a feedback loop regulated by CLV3 activity. *Science* **289**, 617-9.
**Cary, A. J., Che, P. and Howell, S. H.** (2002). Developmental events and shoot apical meristem gene expression patterns during shoot development in Arabidopsis thaliana. *Plant J* **32**, 867-77.
**Casimiro, I., Marchant, A., Bhalerao, R. P., Beeckman, T., Dhooge, S., Swarup, R., Graham, N., Inze, D., Sandberg, G., Casero, P. J. et al.** (2001). Auxin transport promotes Arabidopsis lateral root initiation. *Plant Cell* **13**, 843-52.
**Christianson, M. L. and Warnick, D. A.** (1984). Phenocritical times in the process of in vitro shoot organogenesis. *Dev Biol* **101**, 382-90.
**Clark, S. E.** (2001). Cell signalling at the shoot meristem. *Nat Rev Mol Cell Biol* **2**, 276-84.
**Clark, S. E., Running, M. P. and Meyerowitz, E. M.** (1993). CLAVATA1, a regulator of meristem and flower development in Arabidopsis. *Development* **119**, 397-418.

**Clark, S. E., Running, M. P. and Meyerowitz, E. M.** (1995). CLAVATA3 is a specific regulator of shoot and floral meristem development affecting the same processes as CLAVATA1. *Development* **121**, 2057-2067.
**Clark, S. E., Williams, R. W. and Meyerowitz, E. M.** (1997). The CLAVATA1 gene encodes a putative receptor kinase that controls shoot and floral meristem size in Arabidopsis. *Cell* **89**, 575-85.
**Clough, S. J. and Bent, A. F.** (1998). Floral dip: a simplified method for Agrobacterium-mediated transformation of Arabidopsis thaliana. *Plant J* **16**, 735-43.
**Cutler, S. R., Ehrhardt, D. W., Griffitts, J. S. and Somerville, C. R.** (2000). Random GFP::cDNA fusions enable visualization of subcellular structures in cells of Arabidopsis at a high frequency. *Proc Natl Acad Sci U S A* **97**, 3718-23.
**Czechowski, T., Stitt, M., Altmann, T., Udvardi, M. K. and Scheible, W.** (2005). Genome-Wide Identification and Testing of Superior Reference Genes for Transcript Normalization in Arabidopsis. *Plant Physiology* **Vol. 139**, 5–17.
**D'Agostino, I. B., Deruére, J. and Kieber, J. J.** (2000). Characterization of the Response of the Arabidopsis Response Regulator Gene Family to Cytokinin. *Plant Physiology* **124**, 1706–1717.
**Daimon, Y., Takabe, K. and Tasaka, M.** (2003). The CUP-SHAPED COTYLEDON genes promote adventitious shoot formation on calli. *Plant Cell Physiol* **44**, 113-21.
**Delbarre, A., Muller, P., Imhoff, V. and Guern, J.** (1996). Comparison of mechanisms controlling uptake and accumulation of 2,4-dichlorophenoxy acetic acid, naphthalene-1-acetic acid, and indole-3-acetic acid in suspension-cultured tobacco cells. *Planta* **Volume 198, Number 4**, 532–541.
**Dello Ioio, R., Nakamura, K., Moubayidin, L., Perilli, S., Taniguchi, M., Morita, M. T., Aoyama, T., Costantino, P. and Sabatini, S.** (2008). A genetic framework for the control of cell division and differentiation in the root meristem. *Science* **322**, 1380-4.
**DeYoung, B. J., Bickle, K. L., Schrage, K. J., Muskett, P., Patel, K. and Clark, S. E.** (2006). The CLAVATA1-related BAM1, BAM2 and BAM3 receptor kinase-like proteins are required for meristem function in Arabidopsis. *Plant J* **45**, 1-16.
**Dievart, A., Dalal, M., Tax, F. E., Lacey, A. D., Huttly, A., Li, J. and Clark, S. E.** (2003). CLAVATA1 dominant-negative alleles reveal functional overlap between multiple receptor kinases that regulate meristem and organ development. *Plant Cell* **15**, 1198-211.
**Dubrovsky, J. G., Doerner, P. W., Colon-Carmona, A. and Rost, T. L.** (2000). Pericycle cell proliferation and lateral root initiation in Arabidopsis. *Plant Physiol* **124**, 1648-57.
**Estelle, M.** (1998). Polar auxin transport. New support for an old model. *Plant Cell* **10**, 1775-8.
**Fletcher, J. C., Brand, U., Running, M. P., Simon, R. and Meyerowitz, E. M.** (1999). Signaling of cell fate decisions by CLAVATA3 in Arabidopsis shoot meristems. *Science* **283**, 1911-4.
**Fletcher, J. C. and Meyerowitz, E. M.** (2000). Cell signaling within the shoot meristem. *Curr Opin Plant Biol* **3**, 23-30.
**Friml, J., Vieten, A., Sauer, M., Weijers, D., Schwarz, H., Hamann, T., Offringa, R. and Jurgens, G.** (2003). Efflux-dependent auxin gradients establish the apical-basal axis of Arabidopsis. *Nature* **426**, 147-53.
**Gallois, J. L., Nora, F. R., Mizukami, Y. and Sablowski, R.** (2004). WUSCHEL induces shoot stem cell activity and developmental plasticity in the root meristem. *Genes Dev* **18**, 375-80.
**Gallois, J. L., Woodward, C., Reddy, G. V. and Sablowski, R.** (2002). Combined SHOOT MERISTEMLESS and WUSCHEL trigger ectopic organogenesis in Arabidopsis. *Development* **129**, 3207-17.

**Gierer, A., Berking, S., Bode, H. R., David, C. N., Flick, K. M., Hansmann, G., Schaller, H. and Trenkner, E.** (1972). Nat. New Biol. **239**, 98-101.
**Gleave, A. P.** (2002). A versatile binary vector system with a T-DNA organizational structure conducive to efficient integration of cloned DNA into the plant genome. . *Plant Mol. Biol.* **20**, 1203 - 7.
**Gordon, S. P., Heisler, M. G., Reddy, G. V., Ohno, C., Das, P. and Meyerowitz, E. M.** (2007). Pattern formation during de novo assembly of the Arabidopsis shoot meristem. *Development* **134**, 3539-48.
**Haberlandt, G.** (1902). Kulturversuche mit isolierten Pflanzenzellen. *Sitzungsb. Akad. Wiss. Wien, Math. Natur.* **Kl., Abt. J.**, 69-92.
**Haecker, A., Gross-Hardt, R., Geiges, B., Sarkar, A., Breuninger, H., Herrmann, M. and Laux, T.** (2004). Expression dynamics of WOX genes mark cell fate decisions during early embryonic patterning in Arabidopsis thaliana. *Development* **131**, 657-68.
**Haecker, A. and Laux, T.** (2001). Cell-cell signaling in the shoot meristem. *Curr Opin Plant Biol* **4**, 441-6.
**Hajdukiewicz, P., Svab, Z. and Maliga, P.** (1994). The small, versatile pPZP family of Agrobacterium binary vectors for plant transformation. *Plant Mol Biol* **25**, 989-94.
**Heisler, M. G., Ohno, C., Das, P., Sieber, P., Reddy, G. V., Long, J. A. and Meyerowitz, E. M.** (2005). Patterns of auxin transport and gene expression during primordium development revealed by live imaging of the Arabidopsis inflorescence meristem. *Curr Biol* **15**, 1899-911.
**Higuchi, M., Pischke, M. S., Mähönen, A. P., Miyawaki, K., Hashimoto, Y., Seki, M., Kobayashi, M., Shinozaki, K., Kato, T., Tabata, S. et al.** (2004). In planta functions of the Arabidopsis cytokinin receptor family. *PNAS* **101**, 8821-26.
**Hobmayer, B., Rentzsch, F., Kuhn, K., Happel, C. M., von Laue, C. C., Snyder, P., Rothbacher, U. and Holstein, T. W.** (2000). WNT signalling molecules act in axis formation in the diploblastic metazoan Hydra. *Nature* **407**, 186-9.
**Hwang, I. and Sheen, J.** (2001). Two-component circuitry in Arabidopsis cytokinin signal transduction. *NATURE* **413**, 383-9.
**Jonsson, H., Heisler, M., Reddy, G. V., Agrawal, V., Gor, V., Shapiro, B. E., Mjolsness, E. and Meyerowitz, E. M.** (2005). Modeling the organization of the WUSCHEL expression domain in the shoot apical meristem. *Bioinformatics* **21 Suppl 1**, i232-40.
**Jonsson, H., Heisler, M. G., Shapiro, B. E., Meyerowitz, E. M. and Mjolsness, E.** (2006). An auxin-driven polarized transport model for phyllotaxis. *Proc Natl Acad Sci U S A* **103**, 1633-8.
**Kagan, R. M., McFadden, H. J., McFadden, P. N., O'Connor, C. and Clarke, S.** (1997). Molecular phylogenetics of a protein repair methyltransferase. *Comp Biochem Physiol B Biochem Mol Biol* **117**, 379-85.
**Kayes, J. M. and Clark, S. E.** (1998). CLAVATA2, a regulator of meristem and organ development in Arabidopsis. *Development* **125**, 3843-51.
**Kurakawa, T., Ueda, N., Maekawa, M., Kobayashi, K., Kojima, M., Nagato, Y., Sakakibara, H. and Kyozuka, J.** (2007). Direct control of shoot meristem activity by a cytokinin-activating enzyme. *NATURE* **445**, 652-5.
**Laux, T., Mayer, K. F., Berger, J. and Jurgens, G.** (1996). The WUSCHEL gene is required for shoot and floral meristem integrity in Arabidopsis. *Development* **122**, 87-96.
**Leibfried, A., To, J. P., Busch, W., Stehling, S., Kehle, A., Demar, M., Kieber, J. J. and Lohmann, J. U.** (2005). WUSCHEL controls meristem function by direct regulation of cytokinin-inducible response regulators. *Nature* **438**, 1172-5.

**Lindsay, D. L., K.Vipen, V. and Bonham-Smith, P. C.** (2006). Cytokinin-induced changes in CLAVATA1 and WUSCHEL expression temporally coincide with altered floral development in Arabidopsis. *Plant Science* **170**, 1111–1117.
**Long, J. A. and Barton, M. K.** (1998). The development of apical embryonic pattern in Arabidopsis. *Development* **125**, 3027-35.
**Long, J. A., Moan, E. I., Medford, J. I. and Barton, M. K.** (1996). A member of the KNOTTED class of homeodomain proteins encoded by the STM gene of Arabidopsis. *Nature* **379**, 66-9.
**Lowenheim, H.** (2003). Regenerative medicine for diseases of the head and neck: principles of in vivo regeneration. *DNA Cell Biol* **22**, 571-92.
**Lu, P., Porat, R., Nadeau, J. A. and O'Neill, S. D.** (1996). Identification of a meristem L1 layer-specific gene in Arabidopsis that is expressed during embryonic pattern formation and defines a new class of homeobox genes. *Plant Cell* **8**, 2155-68.
**Mähönen, A. P., Bishopp, A., Higuchi, M., Nieminen, K. M., Kinoshita, K., Törmäkangas, K., Ikeda, Y., Oka, A., Kakimoto, T. and Helariutta, Y.** (2006a). Cytokinin Signaling and Its Inhibitor AHP6 Regulate Cell Fate During Vascular Development. *Science* **311**, 94-98.
**Mähönen, A. P., Higuchi, M., K.Törmäkangas, Miyawaki, K., Pischke, M. S., Sussman, M. R., Helariutta, Y. and Kakimoto, T.** (2006b). Cytokinins Regulate a Bidirectional Phosphorelay Network in Arabidopsis. *Current Biology* **16**, 1116–1122.
**Mahonen, A. P., Higuchi, M., Tormakangas, K., Miyawaki, K., Pischke, M. S., Sussman, M. R., Helariutta, Y. and Kakimoto, T.** (2006). Cytokinins regulate a bidirectional phosphorelay network in Arabidopsis. *Curr Biol* **16**, 1116-22.
**Mason, M. G., Mathews, D. E., Argyros, D. A., Maxwell, B. B., Kieber, J. J., Alonso, J. M., Ecker, J. R. and Schaller, G. E.** (2005). Multiple type-B response regulators mediate cytokinin signal transduction in Arabidopsis. *Plant Cell* **17**, 3007-18.
**Mayer, K. F., Schoof, H., Haecker, A., Lenhard, M., Jurgens, G. and Laux, T.** (1998). Role of WUSCHEL in regulating stem cell fate in the Arabidopsis shoot meristem. *Cell* **95**, 805-15.
**Mitrophanov, A. Y. and Groisman, E. A.** (2008). Positive feedback in cellular control systems. *Bioessays* **30**, 542-55.
**Morgan, T.** (1901). Regeneration. 1-292.
**Muller, B. and Sheen, J.** (2007). Advances in cytokinin signaling. *Science* **318**, 68-9.
**Muller, B. and Sheen, J.** (2008). Cytokinin and auxin interaction in root stem-cell specification during early embryogenesis. *NATURE* **453**, 1094-7.
**Muller, R., Bleckmann, A. and Simon, R.** (2008). The receptor kinase CORYNE of Arabidopsis transmits the stem cell-limiting signal CLAVATA3 independently of CLAVATA1. *Plant Cell* **20**, 934-46.
**Murashige, T.** (1965). Effects of stem-elongation retardants and gibberellin on callus growth and organ formation in tobacco tissue culture. . *Physiol Plant* **18**, 665-73.
**Nordstrom, A., Tarkowski, P., Tarkowska, D., Norbaek, R., Astot, C., Dolezal, K. and Sandberg, G.** (2004). Auxin regulation of cytokinin biosynthesis in Arabidopsis thaliana: a factor of potential importance for auxin-cytokinin-regulated development. *Proc Natl Acad Sci U S A* **101**, 8039-44.
**Okada, K., Ueda, J., Komaki, M. K., Bell, C. J. and Shimura, Y.** (1991). Requirement of the Auxin Polar Transport System in Early Stages of Arabidopsis Floral Bud Formation. *Plant Cell* **3**, 677-84.
**Park, I. H., Zhao, R., West, J. A., Yabuuchi, A., Huo, H., Ince, T. A., Lerou, P. H., Lensch, M. W. and Daley, G. Q.** (2008). Reprogramming of human somatic cells to pluripotency with defined factors. *Nature* **451**, 141-6.

**Reddy, G. V., Heisler, M. G., Ehrhardt, D. W. and Meyerowitz, E. M.** (2004). Real-time lineage analysis reveals oriented cell divisions associated with morphogenesis at the shoot apex of Arabidopsis thaliana. *Development* **131**, 4225-37.
**Reddy, G. V. and Meyerowitz, E. M.** (2005). Stem-cell homeostasis and growth dynamics can be uncoupled in the Arabidopsis shoot apex. *Science* **310**, 663-7.
**Reinhardt, D., Frenz, M., Mandel, T. and Kuhlemeier, C.** (2003a). Microsurgical and laser ablation analysis of interactions between the zones
and layers of the tomato shoot apical meristem. *Development* **130**, 4073-83.
**Reinhardt, D., Pesce, E. R., Stieger, P., Mandel, T., Baltensperger, K., Bennett, M., Traas, J., Friml, J. and Kuhlemeier, C.** (2003b). Regulation of phyllotaxis by polar auxin transport. *Nature* **426**, 255-60.
**Ruzicka, K., Simaskova, M., Duclercq, J., Petrasek, J., Zazimalova, E., Simon, S., Friml, J., Van Montagu, M. C. and Benkova, E.** (2009). Cytokinin regulates root meristem activity via modulation of the polar auxin transport. *Proc Natl Acad Sci U S A* **106**, 4284-9.
**Sablowski, R.** ( 2007). The dynamic plant stem cell niches. *Curr Opin Plant Biol* **Dec;10**, 639-44.
**Schoof, H., Lenhard, M., Haecker, A., Mayer, K. F., Jurgens, G. and Laux, T.** (2000). The stem cell population of Arabidopsis shoot meristems in maintained by a regulatory loop between the CLAVATA and WUSCHEL genes. *Cell* **100**, 635-44.
**Sessions, A., Weigel, D. and Yanofsky, M. F.** (1999). The Arabidopsis thaliana MERISTEM LAYER 1 promoter specifies epidermal expression in meristems and young primordia. *Plant J* **20**, 259-63.
**Sieber, P., Wellmer, F., Gheyselinck, J., Riechmann, J. L. and Meyerowitz, E. M.** (2007). Redundancy and specialization among plant microRNAs: role of the MIR164 family in developmental robustness. *Development* **134**, 1051-60.
**Skoog, F.** (1950). Chemical control of growth and organ formation in plant tissues. *Annee Biol* **54**, 545-62.
**Skoog, F. and Miller, C. O.** (1957). Chemical regulation of growth and organ formation in plant tissues cultured in vitro. *Symp Soc Exp Biol* **54**, 118-30.
**Steward, F. C., Mapes, M. O., Kent, A. E. and Holsten, R. D.** (1964). Growth and Development of Cultured Plant Cells. *Science* **Vol. 143**, 20-27.
**Teale, W. D., Paponov, I. A. and Palme, K.** (2006). Auxin in action: signalling, transport and the control of plant growth and development. *Nat Rev Mol Cell Biol* **7**, 847-59.
**To, J. P., Haberer, G., Ferreira, F. J., Deruere, J., Mason, M. G., Schaller, G. E., Alonso, J. M., Ecker, J. R. and Kieber, J. J.** (2004). Type-A Arabidopsis response regulators are partially redundant negative regulators of cytokinin signaling. *Plant Cell* **16**, 658-71.
**To, J. P. and Kieber, J. J.** (2008). Cytokinin signaling: two-components and more. *Trends Plant Sci* **13**, 85-92.
**To, J. P. C., Deruére, J., Maxwell, B. B., Morris, V. F., Hutchison, C. E., Ferreira, F. J., Schaller, G. E. and Kieber, J. J.** (2007). Cytokinin Regulates Type-A Arabidopsis Response Regulator Activity and Protein Stability via Two-Component Phosphorelay. *Plant Cell*.
**Tucker, M. R. and Laux, T.** (2007). Connecting the paths in plant stem cell regulation. *Trends Cell Biol* **17**, 403-10.
**Ulmasov, T., Murfett, J., Hagen, G. and Guilfoyle, T. J.** (1997). Aux/IAA proteins repress expression of reporter genes containing natural and highly active synthetic auxin response elements. *Plant Cell* **9**, 1963-71.
**Vanneste, S. and Friml, J.** (2009). Auxin: a trigger for change in plant development. *Cell* **136**, 1005-16.

**Vieten, A., Vanneste, S., Wisniewska, J., Benkova, E., Benjamins, R., Beeckman, T., Luschnig, C. and Friml, J.** (2005). Functional redundancy of PIN proteins is accompanied by auxin-dependent cross-regulation of PIN expression. *Development* **132**, 4521-31.
**West, M. and Harada, J. J.** (1993). Embryogenesis in Higher Plants: An Overview. *Plant Cell* **5**, 1361-9.
**White, P. R.** (1939). Potentially unlimited growth of excised plant callus in an artificial nutrient. *American Journal of Botany* **26**, 59-64.
**Wittlieb, J., Khalturin, K., Lohmann, J. U., Anton-Erxleben, F. and Bosch, T. C.** (2006). Transgenic Hydra allow in vivo tracking of individual stem cells during morphogenesis. *Proc Natl Acad Sci U S A* **103**, 6208-11.
**Xu, J., Hofhuis, H., Heidstra, R., Sauer, M., Friml, J. and Scheres, B.** (2006). A molecular framework for plant regeneration. *Science* **311**, 385-8.
**Yadav, R. K., Girke, T., Pasala, S., Xie, M. and Reddy, G. V.** (2009). Gene expression map of the Arabidopsis shoot apical meristem stem cell niche. *Proc Natl Acad Sci U S A* **106**, 4941-6.
**Yanai, O., Shani, E., Dolezal, K., Tarkowski, P., Sablowski, R., Sandberg, G., Samach, A. and Ori, N.** (2005). Arabidopsis KNOXI proteins activate cytokinin biosynthesis. *Curr Biol* **15**, 1566-71.
**Yu, J., Vodyanik, M. A., Smuga-Otto, K., Antosiewicz-Bourget, J., Frane, J. L., Tian, S., Nie, J., Jonsdottir, G. A., Ruotti, V., Stewart, R. et al.** (2007). Induced pluripotent stem cell lines derived from human somatic cells. *Science* **318**, 1917-20.